Master Thesis of Science

Numerical Simulation for Installation of Jacket Foundation of Offshore Wind Turbines

Oliver Stettner

20.06.2014

European Wind Energy Master - EWEM- Offshore Track

Numerical Simulation for Installation of Jacket Foundation of Offshore Wind Turbines

Master of Science Thesis

For obtaining the degree of Master of Science in Offshore Engineering at Delft University of Technology and in Technology-Wind Energy at Norwegian University of Science and Technology.

Oliver Stettner

20.06.2014

European Wind Energy Master - EWEM
DUWIND - Delft University of Technology
CeSOS - Norwegian University of Science and Technology

European Wind Energy Master - EWEM
Of
Offshore Track

The undersigned hereby certify that they have read and recommend to the European Wind Energy Master - EWEM for acceptance a thesis entitled **"Numerical Simulation for Installation of Jacket Foundation of Offshore Wind Turbines"** by **Oliver Stettner** in partial fulfillment of the requirements for the degree of **Master of Science**.

Dated: 20.06.2014

Supervisor: _____
prof.dr.ir. René Huijsmans of Delft University of Technology

Supervisor: _____
Prof. Torgeir Moan of Norwegian University of Science and Technology

Reader: _____
Zhen Gao of Norwegian University of Science and Technology

Reader: _____
Ir. Peter Naaijen of Delft University of Technology

Abstract

A large contribution to the overall project costs of an offshore wind farm originates from the transport and installation of the substructures. A better understanding of the operational limits that apply for the installation helps to improve the project execution and thus reduces costs. It is important to analyze in which sea states the installation can be carried out safely.

A coupled analysis model consisting of a vessel the jacket and couplings is implemented in SIMO. Time domain simulations of the the lowering and landing process of a jacket substructure are carried out for a jack-up and a floating vessel. Based on operational criteria a workability analysis is performed and the limiting sea states are determined. The jacket substructure needs to be lowered into pre-installed foundation piles and the jacket motions are thus limited to a certain threshold in order for the installation to be successful.

The jack-up vessel is fixed and consequently there are no crane tip motions. The jacket is thus only excited by waves and the motions are small enough for the jacket to successfully enter the foundation piles for all investigated sea states. The floating vessel is excited by waves and the vessel motions lead to larger motions in the jacket too. The jacket does therefore not always enter the foundation piles. The success rate depends on the wave period and decreases for larger wave periods, close to the excitation periods of the vessel. While the floating vessel is only suited for operations in small wave periods the jack-up vessel was able to operate in all investigated sea states.

Acknowledgements

I would like to thank the following people that have supported me throughout my master thesis and the whole EWEM master program.

Torgeir Moan, Zhen Gao and Rene Huijsmans for supervising my master thesis. Lin Li for the continuous help and support and all the time she dedicated to me and master thesis. It was very nice of you to welcome me in your office and I sincerely hope that my thesis results and all the discussions we had are beneficial for your PhD work. All students in the Offshore Track of the EWEM program. It was very nice to get to know all of you and to have made friends of all around the world. I enjoyed traveling around with you guys and hope to see some of you in the future. My parents for the continuous moral and financial support.

Contents

List of Figures

List of Tables

Nomenclature

Latin Symbols

a_z	Vertical fluid particle acceleration	$[m/s^2]$
b_0	Top width	$[m]$
b_N	Base width	$[m]$
F_B	Buoyancy	$[N]$
F_G	Weight	$[N]$
F_S	Slamming Force	$[N]$
F_W	Wave Force	$[N]$
F_{Thrust}	Thrust Force	$[N]$
F_{Tot}	Total Force	$[N]$
T_{lim}	Limiting natural period	$[s]$
v_z	Vertical fluid particle velocity	$[m/s]$
a_x	Horizontal fluid particle acceleration	$[m/s^2]$
a_y	Transverse fluid particle acceleration	$[m/s^2]$
v_x	Horizontal fluid particle velocity	$[m/s]$
v_y	Transverse fluid particle velocity	$[m/s]$
p_0	Static pressure	$[N/m^2]$
C_{DS}	Drag coefficient for steady flow	
D	Member diameter	$[m]$
g	Gravitational constant	$[m/s^2]$
L	Member length	$[m]$
L_s	Submerged member length	$[m]$

m	Member mass per unit length	$[kg/m]$
N	Number of bays	
H	Wave height	$[m]$
k	Wave number	
p	Total pressure	$[N/m^2]$
p^+	Dynamic pressure	$[N/m^2]$

Greek Symbols

Δt	Time Step Size	$[s]$
λ	Wave length	$[m]$
λ	Wave length	$[m]$
η	Wave elevation	$[m]$
ω	Wave frequency	$[rad]$
ρ_w	Density of the fluid	$[kg/m^3]$
β	Angle between wave propagation direction and positive x-axis	$[°]$

Abbreviations

DP	Dynamic Positioning
FFT	Fast Fourier Transformation
RAO	Response Amplitude Operator

Chapter 1

Introduction

1.1 Background and Objective

More and more countries worldwide try to minimize their dependency on fossil fuels such as coal, oil and gas by switching to renewable energy resources such as hydro, solar and wind power. The European Union has the ambitious target to increase the share of renewable energies to 20 percent until 2020. An important component of this energy transition is offshore wind energy as it offers more stable power production compared to onshore wind energy due to the better wind regime offshore. Other countries, such as Japan and the U.S. also have ambitious development plans for offshore wind power, however, due to larger water depths, projects in these areas are somewhat more challenging.
A significant share of the total project costs of an offshore wind farm are the installation costs. These amount to approximately 11 percent. One of the key factors that determine the installation costs are the vessels capability to operate under the prevailing environmental conditions. Wind, waves and currents will have an impact on the installation time and thus on the project costs. It is therefore extremely important to know under which conditions the installation offshore can be carried out safely.

The objective of this master thesis is to investigate the operation limits in terms of sea conditions for a floating installation vessel by numerical simulations. The crane operation for lowering a jacket substructure through the wave zone down into the pre-installed foundation piles is studied using numerical models. A coupled model, consisting of the floating installation vessel, the jacket substructure and the connection between them with lift wires, is build and analyzed using the Marintek software SIMO. The dynamic behavior of the system with the floating vessel is compared to the installation with a fixed jack-up vessel. Simulations are carried out for different wave periods and wave directions. Based on installation criteria a workability analysis is performed. Furthermore, emphasis is put on the correct representation of the hydrodynamic forces that act on the jacket substructure.

1.2 Offshore Wind Substructures

Offshore Wind Turbine substructures exist as floating designs and bottom founded designs. Floating designs transfer all loads (permanent and variable aerodynamic and hydrodynamic loads) to the surrounding water body. The floaters are moored to the seabed. Bottom founded substructures transfer all loads and forces to the soil. In the case of a bottom founded design the substructure can be split into two parts, the support structure and the foundation. The support structure is the connection between turbine tower and seabed. The foundation stands on or penetrates the seabed, thus transferring the loads and forces. An overview of current existing substructures is shown in Figure 1.1.

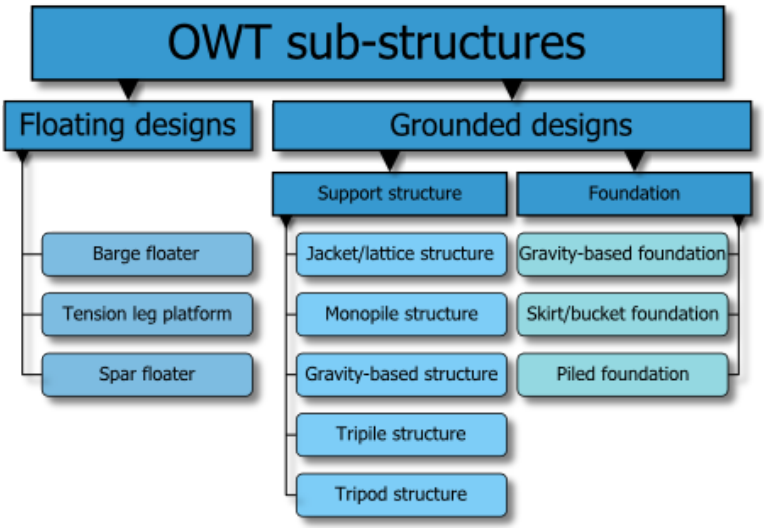

Figure 1.1: *Substructure Types used in Offshore Wind [1]*

At the end of 2012 the monopile had the largest market share among offshore wind support structures with 75 percent, followed by gravity based structures with 21 percent and the tripod and jacket with 2 percent respectively. Less than 1 percent of all offshore wind turbines used a floating foundation [8]. Floating designs, so far, are only installed as prototypes and have not been installed in large scale economic projects. Floating designs are said to be more expensive than bottom founded substructures and are thus only feasible for countries with insufficient shallow water areas such as e.g. Japan. The jacket substructure and floating designs are expected to increase their market share towards 2020, especially with new markets like Asia and the US starting to invest in offshore wind, while the monopile can defend its already high share of the total market [9].

1.2.1 Jacket

The term jacket will be used for a steel frame support structure, which is connected to the ground via piles at the seabed, as commonly done in the offshore wind industry. Normally, the term jacket indicates, that the foundation piles are inserted through the legs. The jacket consists of three or four legs which are connected via tubular bracings. There

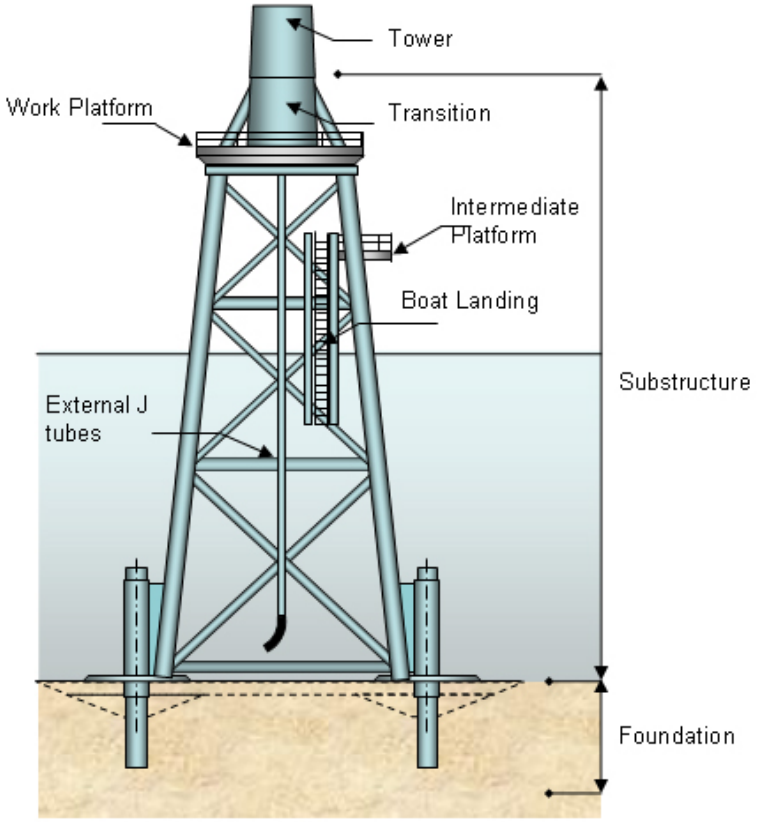

Figure 1.2: *Jacket Substructure [2]*

are different bracing types, such as K, X and diagonal bracings. The point at which the bracing is welded onto the leg is called joint. These joints represent the most crucial part of the steel frame structure due to the increased stresses that occur. There are two options when it comes to installing this type of substructure, namely pre- and post-piling of the foundation piles. Pre-piling is the preferred option, since it allows for a faster installation and a lighter structure. The connection between piles and substructure is achieved by either grouting, swaging or using innovative systems like pile quick coupling. Although the weight is significantly lower than that of a monopile the large number of members and joints that need to be welded make the jacket a labour expensive substructure. Furthermore, the size of the jacket requires larger space, both on land and in regards of the deck capacity of the vessel. Companies aim at automating the complete jacket fabrication, thus elimination the expensive and time consuming labour costs. Furthermore, the automation of the jacket fabrication might ease the complete load out and sea-fastening procedure as standardized equipment can be used.

1.3 Installation Vessels

The expected rise in installed offshore wind capacity leads to an increased demand for installation vessels. The expected growth of 5 GW of offshore wind energy per year is estimated to require 20 vessels to install support structures, 14 vessels to install turbines, 8 vessels to repair turbines and up to 500 maintenance vessels [10]. A variety of options exist when choosing an optimal installation vessel for a project, which can be split in the following four main categories outlined in Table 1.1 below. The term transit indicates whether a vessel moves between the offshore site and the harbour to pick up new substructures itself or if the vessel stays on site and is supplied by smaller feeder vessels. The term station keeping indicates the method a vessel uses to maintain its exact position during installation despite any environmental influences from wind, current and waves. The optimal solution depends on factors like the distance of the windfarm from shore, the water depth and the size and number of substructures that need to be installed.

Table 1.1: *Vessel Types used for Offshore Wind Substructure Installation*

Type	**Transit**	**Station Keeping**	**Example Vessel**
Jack-Up Barge	No	Jack-Up	*Thor*
Jack-Up Vessel	Yes	Jack-Up	*Innovation*
Floating Barge	No	Moored	*Svanen*
Heavy Lift Vessel	Yes	DP System	*Stanislav Yudin*

The four vessel types named above are only valid options for the installation of the substructures. For the tower and wind turbine installation it is normally required by the marine warranty surveyor that the vessel or barge need to be jacked up to prevent any sort of wave impact and thus vessel movement. For the jack-up and floating barges that stay on site and do not pick up the substructures in the harbour themselves (no transit) additional vessels, namely feeder barges and tugs, are required.
A more detailed description of the individual vessel options based on the data sheets of the example vessels mentioned in Table 1.1 is given in the following.

1.3.1 Jack-Up Barge

A jack-up barge is normally brought to site by tug boats since she has no or very limited means of propulsion. Once she arrived at the desired location she can jack-up, using either tugs or a dynamic positioning system to maintain her position. The second generation jack-up barge Thor owned by Hochtief Solutions has a leg length of 82 m and can thus operate in water depths up to 50 m [11]. The legs can be lowered with up to 2.5 m/s per second. Once the barge is jacked-up above the water she can operate without being influenced by waves. Hence, wind is the only limiting factor for operations. Thor has the dimensions of 70x40x6 m and an open deck space of 1850 m^2. She has a cargo load of up to 3300 tons depending on the size of the cargo and the site specific conditions. The maximum lifting capacity is 500 tonnes in a radius of 20 m. The jack-up barge stays at the installation site, only moving between turbine positions. She is supplied with new substructures by either tugged feeder barges or feeder vessels. This means, that the

installation on site is not interrupted by transits of the installation vessel to and from the harbour.

Figure 1.3: *Jack-Up Barge Odin*

1.3.2 Jack-Up Vessel

A jack-up vessel has her own propulsion and sufficient deck space and thus does not require any additional vessels to deliver new substructures. The jack-up vessel Innovation owned by Hochtief InfraSea Solutions has a speed of up to 12 knots [12]. Innovation fulfills DP2 class requirements, being equipped with 4 azimuth and 3 tunnel thrusters to keep her position during jack-up. Safe jacking is possible in wave heights up to 2 meters. When using leg extension she is capable of working in water depths of up o 65 m. The jacking speed is up to 1 m/s. Crane operations can be carried out in wind speeds up to 18 m/s. Innovation has the dimensions of 148x42x11 m and a cargo load of up to 8000 tonnes. The maximum lifting capacity is 1500 tonnes in a radius of 31.5 m. The jack-up vessel transits between offshore site and harbour to pick up new substructures.

Figure 1.4: *Jack-Up Vessel Innovation from HGO IfraSea Solutions*

1.3.3 Floating Barge

The floating barge needs tug assistance to move between turbine locations as it does not come with own propulsion. Monopiles and transition pieces can be delivered by tug boats, for jackets a floating barge is needed. Monopiles and transition pieces are made watertight by plugging both ends and then brought to location by tugging. In case the time needed for the loadout at the harbour and the transit to site is larger than the installation time, an additional tug is hired to prevent any waiting time offshore. The floating barge Svanen from Ballast Nedam is 103 m long and 72 m wide [13]. At site the barge is kept in position using 8 anchors. Svanen has a maximum lifting capacity of 8200 tonnes. The lifting point is within the vessels center of gravity, allowing for installation in harsh environments without ballasting. So far no floating barge optimized for the installation of jacket substructures exist but promising designs that can lead to significant cost savings are being developed.

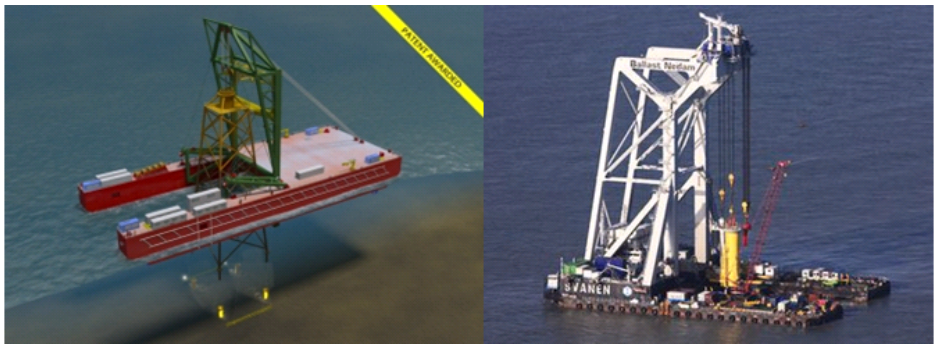

Figure 1.5: *Vessel Concept by Ingenium and Vessel Svanen*

1.3.4 Floating Vessel

A heavy lift vessel has her own propulsion and sufficient deck space and thus does not require any additional vessels to deliver new substructures. The heavy lift vessel is the vessel type which later be used to simulate the installation of substructures. The heavy lift vessel uses a dynamic positioning system to keep its position and is thus affected by waves and current that excite the vessel and lead to motions. The heavy lift vessel Stanislav Yudin from Seaway Heavy Lifting has a transit speed of up to 12 knots [14]. She is equipped with 2 main and 2 bow thrusters. Stanislav Yudin has the dimensions of 180x36x13 m and free deck space of 2560 m^2, allowing for a deck load of more than 5000 tonnes. The maximum revolving capacity is 2500 tonnes. The vessel is equipped with a ballast system to maintain an upright position during lifting operations. To ensure safe operations, lifting height, weight to be lifted and the external forces acting on the ship, such as wave, current and wind, need to be considered. The effect of waves, current and wind will be discussed in the following chapter.

Figure 1.6: *Heavy Lift Vessel Stanislav Yudin*

1.4 Substructure Installation

The installation costs for an offshore wind farm amount to approximately 11 percent of the total lifetime costs, with huge potential for improvement. This section will look at the impact the weather conditions have on the project execution and explain the individual sub-operations that are carried out for the pre-installed jacket concept.

1.4.1 Site Conditions

The environmental conditions at the offshore site, such as water depth, soil, waves, current and wind determine the overall project execution. The wave height and current speed influences the choice of vessels that can be used for installation. If the time required for installation and the vessel restrictions are known, the number of weather windows at site can be determined. Existing long term weather data is used to estimate the number of weather windows and thus installation opportunities during the project planning phase. During the installation phase reliable short term weather forecasts are needed.

Table 1.2 below shows wave data from an offshore wind farm site. The wave conditions for the full year and half year (April to September).

Table 1.2: *Wave Conditions at an Offshore Site*

Condition	**% of time**	
	Full Year	Half Year
Hs $<$ 0.5 m, Tp $\leq$ 6 s	10.25	16.00
Hs $<$ 1.0 m, Tp $\leq$ 6 s	42.75	53.83
Hs $<$ 1.5 m	77.25	86.00
Hs $\geq$ 2.5 m, Tp $>$ 6 s	03.75	01.33

As can be seen in Table 1.2 the prevailing wave height at the installation site can have a large influence on the project execution. The jack-up barge and vessel can operate independently from the wave height once jacked-up. A vessel that can only operate up to wave heights of 1.5 m would at this site already experience a downtime of 14-23 % depending on the season. With charter rates of 250,000 euros per day this can easily have a large impact on the total project costs.

Besides the waves, current also plays an important role. This is especially the case for vessels using dynamic positioning or mooring systems for station keeping, namely the floating barge and the heavy lift vessel. Tunnel thrusters, which are often used for the dynamic positioning of vessels, can lose an considerable amount of thrust due to the flow past the inlet and outlet. A typical thrust reduction of 5 % per knot current speed above the design speed of 2 knots applies [15]. For mooring systems the current forces, together with the wind forces, determine the mean displacement and thus a significant part of the mooring force a system has to withstand.

The wind speed is a significant factor during the loadout and the installation of the substructures. In the harbour the loadout by lifting is restricted by the prevailing wind

speed. The jacket substructures are transported in an upright position on the vessel posing a large lateral area for wind loads attacking at a high point and thus resulting in large overturning moments. Wind loads are especially crucial for rather small vessels with limited stability such as small feeder barges. At site, the wind effects the functionality of dynamic positioning and mooring systems. Furthermore, all lifting operations offshore can only be carried out up to a certain wind speed. For the lifting of the turbine tower and the nacelle a wind speed restrictions of 10 m/s applies, while for the blade the maximum allowed wind speed is 7 m/s [16]. For the substructure installation no value was found in the literature. Although the substructures are somewhat heavier than the tower, nacelle and the blades, the lifting height is lower.

1.4.2 Jacket Installation Sequence

The installation of the jacket substructure follows the following steps:

Placing piling template: The piling template is lifted from the vessel using hydraulic clamps or remotely controlled shackles to avoid the necessity of remotely operated vehicle assistance. The template consists of mudmats for stability and pile sleeves through which the piles are driven. The leveling of the piling template can be achieved using hydraulic jacks.

Placing foundation piles: Once the piling template is leveled on the seabed the foundation pile is picked up from the vessel. Lifting is achieved by means of a hydraulic gripper than goes inside of the pile where it expands. The pile is lowered into the pile sleeve which offers sufficient stability.

Installing hydraulic hammer: Next, the pile gripper is retrieved, placed on the vessel and the hydraulic hammer is connected to the crane. In order to place the hydraulic hammer on the foundation piles ROV assistance might be required.

Driving foundation piles: After the hydraulic hammer is placed on the pile the foundation can be driven to target depth. The pile driving of the remaining piles is done in a similar manner. For the Thornton Bank Offshore Windfarm in Belgium the following pile driving data was found. The windfarm consists of 49 jacket substructures with a pin-pile diameter of 1.8 m. The jackets are mounted with a 6 MW turbine. The pile driving times recorded are between 162-405 min, in average 319 min for the four legs [17].

Retrieving piling template: Once all the foundation piles are driven to target depth, the piling template can be retrieved from the seabed and later be reused for the next turbine location. The piling template is normally adjustable in size, allowing its use for different jacket footprints.

Lifting jacket substructure: The jacket substructures are normally transported in an upright position to reduce the required deck space and avoid complex uprightening operations offshore. The jacket substructures are picked up by the crane using either four hooks, one in each corner or by using a hydraulic gripper that goes inside the transition piece of the jacket.

Placing jacket substructure: The jacket substructure is lowered into the water and the jacket legs are inserted in the already driven foundation piles.

Grouting foundation piles: The connection between foundation piles and jacket is achieved by a grouting connection but other options, as mentioned earlier, are being developed. The grout lines run through the jacket legs and the grout connectors are normally located on the transition deck, hence no subsea operation is required. The grout volume is approximately $10m^3$ per pile.

1.5 Related Work

Offshore lifting operations can be split into different categories. The weight of the lifted object determines whether it is a light or heavy lift. If the weight of the object exceeds 1000 tonnes it is a heavy lift. If the weight of the object is below 100 tonnes it is a light lift [18]. For heavy lifts the coupling between lifted object and vessel needs to be modeled using multibody dynamics. Heave compensation is often not available for heavy lifts as the weight of the object exceeds the capacity of the heave compensator. For light lifts other challenges, e.g. static deformation of lifting wire in current, vertical oscillations of the mass wire system and Mathieu instability need to be investigated [18]. Light lifts are not covered as part of this thesis.

The lifting operation can be divided into 5 phases. The lift off from the vessel, hanging of the lifted object in air, crossing of the splash zone, deep submergence of the lifted object and the landing phase. During the lift off phase on the deck of the vessel attention must be paid to possible snatch loads in the lift wire, impact forces between lifted object and the deck and horizontal sliding of the object across the deck. Minimum requirements for the clearance between lifted object and other structures can be found in applicable guidelines for marine lift operations. The exact clearance that need to be kept also depends on whether other protective measures such as bumpers and guides are used for lift off [19]. When the object is hanging in air large pendulum motions can occur that lead to an increased lift wire tension and possible collision of the lifted object with the vessel. To avoid collision sufficient clearance between vessel hull and lifted object needs to be ensured. Tugger lines can be used to help control and minimize the pendulum motions of the lifted object that are a governing criterion for the lift operation.

1.5.1 Tugger Lines

Tugger lines, sometimes referred to as taglines, are additional wires that are connected to the lifted object and run through winches on the vessel. By applying a certain amount of pretension through the winch the tugger lines counter-act the pendulum motions of the lifted object and help to guide it. In order to gain the largest benefit from the tugger lines, the pretension needs to be chosen carefully. The tugger lines can either be fixed, kept under constant tension or be computer controlled. Heerema Marine Contractors developed a patented solution for a tension controller that greatly reduced the pendulum motions of the lift object [20].

1.5.2 Numerical Simulation of Offshore Lifting Operations

Offshore heavy lift operation involve a number of bodies that need to modeled to get an understanding on how these interact with each other. Computer simulations that are tuned with results from experimental model tests proofed to resemble the motions of the bodies during the actual offshore installation [21]. These bodies include the heavy lift vessel, the object to be lifted and sometimes a transport barge in case that the object is not transported to site on board the heavy lift vessel itself. The heavy lift vessel and the lift object are connected via a lift wire and therefore form a coupled system. This means that the object on the crane will be excited by the motions of the vessel and vice versa. The behavior of the vessel itself can be investigated by looking at the response amplitude operators (RAO). For a ship shaped vessel the RAO will normally show very small motions in short waves, while in long waves these motions increase. If one is interested in the pendulum motions of the jacket hanging from a fixed crane (e.g. in case of a jack-up vessel), the linearized pendulum formula gives a good approximation of the natural period of the pendulum motion [22]. If a floating vessel is used for the installation it is important to investigate the behavior of the coupled system. A good understanding of the coupled system is important for the estimation of limiting parameters such as the relative motions of the lifted object and docking pile loads [23]. The undamped eigenmodes and eigenfrequencies are obtained by solving the equation of motion of the coupled system. For each eigenvalue the corresponding eigenvector defines the contribution of each degree of freedom to the specific resonant mode of motion [18]. Based on the eigenmodes it can be judged how e.g. the roll motions of the vessel will excite the jacket hanging on the crane. Experimental model tests found, that in head seas the vertical motions of the suspended load depend on the motions of the ship and that resonance and coupling effects are of minor importance, while in beam seas coupling effects between roll, yaw and transverse load motions as well as roll resonance effects need to be considered [24]. The limiting oscillations for the vertical motions of the lifted object are the pitch and roll oscillations of the vessel.

1.5.3 Operations involving Transients

Marine operations that involve transient or non-linear effects are challenging to analyze and require a different treatment compared to stationary or linear processes. The limiting sea states of an operation are obtained by analyzing the extreme loads that occur during the most critical phase of on operation, such as the docking of the jacket with the foundation piles. For obtaining extreme loads of parameters that are relevant throughout the whole operation, for example the lift wire tension, when an object is lifted through the wave splash zone down to the sea bed, two methods for investigating the maximum responses exist. The first option is to run steady-state simulation for the critical phases of an operation. If, for example, the lift wire tension is expected to be largest when the object is in the splash zone, simulations can be run with the object staying at that critical vertical level. The second option is to run a large amount of simulations of the actual lowering process until representative results are gained. It was found, that the latter method gives more realistic results, since an unrealistic build-up of oscillations is avoided [25]. The time domain simulations carried out in this thesis are non-stationary processes. The docking of the jacket with the foundation piles represents a highly non-linear phenomenon. Furthermore, it is uncertain which jacket leg enters its corresponding foundation pile first.

Chapter 2

Forces on Slender Elements

2.1 Linear Wave Theory

The first order wave potential, satisfying the Laplace equation as well as the the kinematic boundary conditions, is defined as

$$\phi_0 = \frac{Hg}{2\omega}\frac{\cosh(k(z+h))}{\cosh(kh)}\cos(\omega t - kx\cos(\beta) - ky\sin(\beta) + \phi_\zeta) \tag{2.1}$$

where ωs the wave frequency, Hhe wave height, $k$he wave number and βhe angle between wave propagation direction and positive x-axis.

The wave elevation ηs calculated as

$$\eta = \frac{H}{2}\sin(\omega t - kx\cos(\beta) - ky\sin(\beta) + \phi_\zeta) \tag{2.2}$$

The wave elevation is another important parameter, since the particle velocities and accelerations will be different underneath a crest and trough.

2.1.1 Particle Motions

The horizontal, transverse and vertical particle velocity (v_x v_y v_z) and acceleration (a_x a_y a_z can be found by taking the first and second derivative of the wave potential in respect to x,y,z respectively. The particle velocities and accelerations are later needed to determine the wave forces acting on the jacket. The wave direction is defined in the

global coordinate system.

$$v_x = \omega \frac{H}{2} \frac{\cosh(k(z+h))}{\sinh(kh)} \sin(\omega t - kx\cos(\beta) - ky\sin(\beta) + \phi_\zeta)\cos(\beta) \tag{2.3}$$

$$v_y = \omega \frac{H}{2} \frac{\cosh(k(z+h))}{\sinh(kh)} \sin(\omega t - kx\cos(\beta) - ky\sin(\beta) + \phi_\zeta)\sin(\beta) \tag{2.4}$$

$$v_z = \omega \frac{H}{2} \frac{\sinh(k(z+h))}{\sinh(kh)} \cos(\omega t - kx\cos(\beta) - ky\sin(\beta) + \phi_\zeta) \tag{2.5}$$

$$a_x = \omega^2 \frac{H}{2} \frac{\cosh(k(z+h))}{\sinh(kh)} \cos(\omega t - kx\cos(\beta) - ky\sin(\beta) + \phi_\zeta)\cos(\beta) \tag{2.6}$$

$$a_y = \omega^2 \frac{H}{2} \frac{\cosh(k(z+h))}{\sinh(kh)} \cos(\omega t - kx\cos(\beta) - ky\sin(\beta) + \phi_\zeta)\sin(\beta) \tag{2.7}$$

$$a_z = -\omega^2 \frac{H}{2} \frac{\sinh(k(z+h))}{\sinh(kh)} \sin(\omega t - kx\cos(\beta) - ky\sin(\beta) + \phi_\zeta) \tag{2.8}$$

Linear theory is only valid up to the free surface. Thus linear stretching is applied and the particle velocities and accelerations in the crest are taken as constant equal to the value at the free surface, as outlined in Figure 2.1.

2.1.2 Pressure

The pressure in the fluid is an important parameter determining the hydrodynamic forces acting on a submerged object. The forces are obtained by integration the pressure from Bernoulli, static and dynamic pressure, over the mean wetted surface of the body.
In a fluid at rest, the total pressure $p$ill be equal to the static pressure $p_0$enoted as

$$p = p_0 = \rho_w g(h - z) \tag{2.9}$$

where ρ_ws the density of the fluid, g is the acceleration of gravity, h is the water depth and z is the distance from the seabed. The atmospheric pressure is very small and can be neglected.
If waves are present, the total pressure will be extended by a dynamic pressure term to take into account the change of surface elevation. The dynamic pressure p^+ill be positive under the wave crest and negative under the wave trough, as outlined in Figure 2.2.

$$p = p_0 + p^+ = \rho g h + \rho g \eta \frac{\cosh(k(z+h))}{\cosh(kh)} \tag{2.10}$$

where η is the surface elevation and k is the wave number. An object under a wave crest will experience a lower buoyancy than under a wave trough, compared to the static pressure alone. Under a wave crest, the total pressure will be larger than the static pressure corresponding to the still water level but less than the static pressure corresponding to the still water surface.

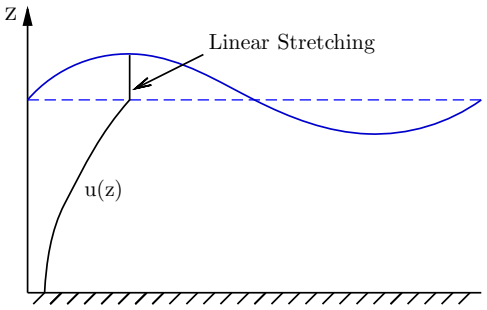

Figure 2.1: *Linear Stretching*

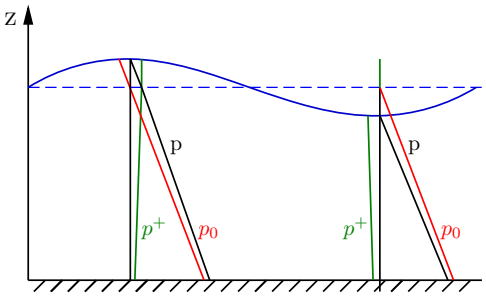

Figure 2.2: *Pressure Distribution*

2.1.3 Irregular Waves

The installation of the jacket is carried out in irregular seas. A simplified 2 parameter Jonswap spectrum is used to describe the unidirectional, irregular waves. The two parameters defining the wave spectrum are the peak period and the significant wave height. The JONSWAP spectrum is defined as

$$S_\zeta^+(\omega) = \frac{\alpha g^2}{\omega^5} \exp(-\beta(\frac{\omega_p}{\omega}^4)\gamma^{\exp(-\frac{(\omega/\omega_p-1)^2}{2\sigma^2})} \tag{2.11}$$

The following coefficients are assumed for the simplified 2 parameter spectrum [6].
$\beta = 1.25$, $\sigma_a = 0.7$, $\sigma_b = 0.9$ and

$$\begin{aligned} \gamma &= 1 \text{ for} \quad T_p \geq 5\sqrt{H_s} \\ \gamma &= 5 \text{ for} \quad T_p \leq 3.6\sqrt{H_s} \end{aligned} \tag{2.12}$$

Figure 2.3 shows the wave spectrum of the smallest and largest peak period investigated for this project. The wave spectra are later compared with the natural periods of the eigenmodes of the jacket and the coupled system. If the natural period on an eigenmode falls within the wave spectrum the mode is likely to occur.

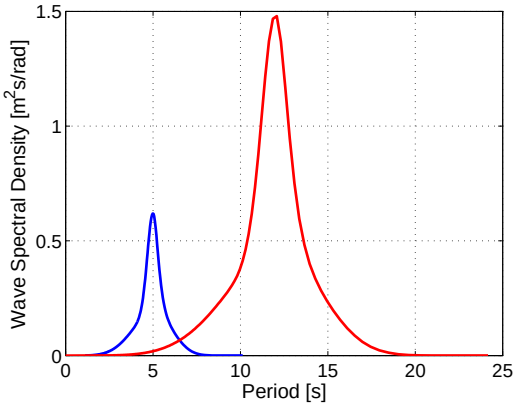

Figure 2.3: *Wave Spectrum for the Smallest and Largest Wave Period Investigated*

2.2 External Forces on the Jacket

The external forces acting on the jacket include weight (F_G), buoyancy (F_B), hydrodynamic wave force (F_W) and slamming force (F_S). For simplicity it is assumed, that there is no wind and no current present at the installation site.
Each slender element is divided into strips of equal length. The weight can be calculated using the full member. The total force (F_{Tot} acting on a member is the sum of the individual strip contributions.

$$F_{Tot} = \sum dF_G + dF_B + dF_W + dF_S \tag{2.13}$$

The following steps must be followed to calculate the hydrodynamic forces on the jacket.

1. Determine the center of the strip in global coordinates
2. Calculate the surface elevation at that point
3. Calculate the wave particle velocities and accelerations based on the surface elevation
4. Calculate the velocities and accelerations normal to the strip, using coordinate transformation. Note, that all three velocity components can contribute to the force.
5. Calculate the buoyancy, wave and slamming force on the strip
6. Express the forces in local coordinates
7. Add all strip contributions to get the force on the whole member
8. Add all member forces to get the force acting on the whole jacket
9. Express the total jacket force in global coordinates

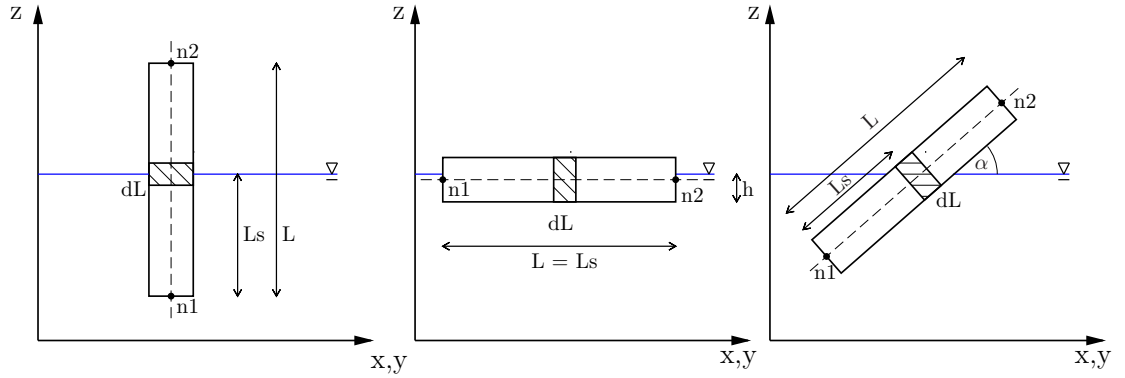

Figure 2.4: *Vertical, Horizontal and Inclined Member*

The formulations for the gravity, buoyancy, wave and slamming force are given in the following. Special features of vertical, horizontal and inclined members as seen in Figure 2.4 partly submerged and fully submerged are discussed.

The horizontal, transverse and vertical water particle velocity and acceleration is decomposed in two components normal to the strip axis ($X_S(2)$ and $X_S(3)$) and one parallel to the strip axis ($X_S(1)$). The force contribution from each component is calculated separately and then added together for each strip.

2.2.1 Gravity Force

The gravity or weight force for all members regardless of their orientation and position can be calculated as

$$F_G = -mgL \tag{2.14}$$

where ms the mass per unit length of the member, gs the acceleration due to gravity and Ls the length of the member. The weight force acts downwards in the earth fixed coordinate system, at the center of gravity of the member.

2.2.2 Buoyancy Force

The buoyancy is determined by integration of the static pressure over the instantaneous body surface. The buoyancy of a strip is equal to the displayed volume of fluid. For the flooded jacket legs, this is equal to the steel volume. Buoyancy is always calculated up to the mean free-surface and is thus, independent of the waves, a constant value. The buoyancy acts in the center of buoyancy and is orientated upwards in the earth fixed coordinate system. For fully submerged members the buoyancy can simply be calculated as

$$F_B = \rho_w g \frac{\pi D^2}{4} L \tag{2.15}$$

where Ds the member diameter, ρ_w the density of water.

For partly submerged members the buoyancy is calculated as follows.

Partly Submerged Vertical Member

For partly submerged vertical members the buoyancy is calculated for the whole member rather than for each individual strip. The instantaneous surface elevation is taken at the longitudinal member axis and assumed constant over the member width. The buoyancy force for a vertical member is calculated as

$$F_B = \frac{\pi D^2}{4} \rho_w L_s \tag{2.16}$$

where L_ss the submerged member length. The only difference to the fully submerged case is the adjustment of the length considered.

Partly Submerged Horizontal Member

For partly submerged horizontal members the buoyancy needs to be calculated for each strip individually, since it cannot be assumed that the instantaneous surface elevation is constant over the member length. The buoyancy of a partly submerged horizontal strip is calculated as

$$dF_B = dL \cdot A_p(h) \cdot \rho_w \tag{2.17}$$

where $A_p(h)$ is the submerged cross sectional area of a cyliner as function of submergence.

$$A_p(h) = \frac{D^2}{4} \arccos(\tfrac{r-h}{h}) - (r-h)\tfrac{\sqrt{2rh-h^2}}{r^2} \quad for \quad h < D \tag{2.18}$$

where r is the member radius and h is the height of submergence (see Figure 2.4). The height of submergence of each strip is based on the instantaneous surface elevation at the center of the strip.

Partly Submerged Inclined Member

For partly submerged inclined members the buoyancy needs to be calculated for each strip individually, since it cannot be assumed that the instantaneous surface elevation is constant over the member length. Furthermore, the lowest point of a strip in global coordinates will not longer be the center point minus the member radius but depend on the actual inclination of the member in respect to the earth fixed coordinate system.

A strip will contribute to the buoyancy if the lowest point (nl indicated by a green star in Figure 2.5) is below the surface. This would require the determination of the point nl for each member strip for every time step of a simulation. A sufficient approximation

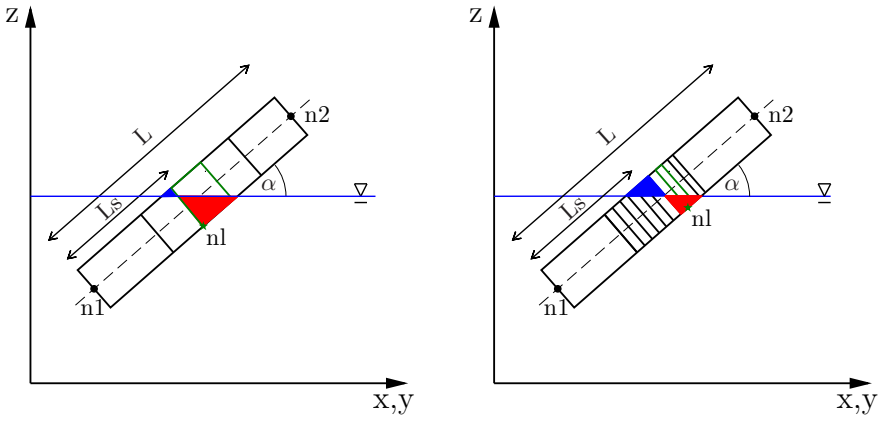

Figure 2.5: *Effect of the Strip Size on Accuracy*

is to assume strips to be either fully buoyant or fully dry. The blue area represents the strip volume that adds to the buoyancy although it is not submerged. The red area does not add to the buoyancy although it is submerged. For large strips this approximation will lead to inaccurate results. For small strips the blue and red area will approximately cancel each other. This means, that although the buoyancy contribution of each strip is not exactly correct, the buoyancy of the whole member will be. Furthermore, it should be noted, that a numerical model of an object will never represent the real object and that usage of long wave approximation and linear wave theory introduces errors too.

2.2.3 Wave Force

Wave forces are calculated using the Morison equation, a semi-empirical formula that uses coefficients to scale the forces in magnitude. The Morison equation is valid as long as the member diameter is small compared to the wave length ($D < 5\lambda$) [26]. This means, that the undisturbed velocity and pressure fields have small variations over the submerged volume of the strip and the excitation loads simplify. Furthermore, by using long wave approximation, the waves generated by the body are very small. This results in very small damping, which can thus be neglected [3].

The total wave force acting on a cylinder can be split into two parts, the inertia force and the drag force. The inertia term includes the Froude-Krylov force and the added mass force. Latter is sometimes also referred to as disturbance force. The inertia force is a function of the fluid particle acceleration, while the quadratic drag term is a function of the fluid particle velocity squared. The inertia and the drag component are thus 90 degrees out of phase.

$$dF_W = \begin{bmatrix} df_{xs(2)} \\ df_{xs(3)} \end{bmatrix} = \left\{ \rho_w \frac{\pi D^2}{4}(1 + C_a) \begin{bmatrix} a_{xs(2)} \\ a_{xs(3)} \end{bmatrix} + \frac{1}{2} C_d D u_n \begin{bmatrix} u_{xs(2)} \\ u_{xs(3)} \end{bmatrix} \right\} dS \tag{2.19}$$

For a moving cylinder, the Morison equation needs to be adjusted, as the relative motions

of the body need to be taken into account. The first term is the Froude-Krylov force and the added mass force due to the fluid acceleration. The additional second term is the added mass force due to the bodies acceleration. The Froude-Krylov force does not depend on the relative acceleration since it is independent of the rigid body motions [22]. The third term is the quadratic drag force. The drag force term can simply be adjusted by using the relative velocities instead of the fluid particle velocities.

$$dF_W = \begin{bmatrix} df_{xs(2)} \\ df_{xs(3)} \end{bmatrix} = \left\{ \rho_w \frac{\pi D^2}{4}(1 + C_a) \begin{bmatrix} a_{xs(2)} \\ a_{xs(3)} \end{bmatrix} - \rho_w C_a \frac{\pi D^2}{4} \begin{bmatrix} \ddot{\eta}_{xs(2)} \\ \ddot{\eta}_{xs(3)} \end{bmatrix} + \frac{1}{2} C_d D u_n \begin{bmatrix} u_{xs(2)} \\ u_{xs(3)} \end{bmatrix} \right\} dS \tag{2.20}$$

with u_r being the relative velocity and u_n being the total relative normal velocity

$$u_r = u_{xs} - \dot{\eta}_{xs} \qquad u_n = \sqrt{u_{r(2)}^2 + u_{r(3)}^2} \tag{2.21}$$

and where u_{xs} and a_{xs} are the water particle velocity and acceleration at the center of the strip; $\dot{\eta}_s$ and $\ddot{\eta}_s$ are the velocity and acceleration in the center of the strip due to the bodies motions; C_a and C_q are the added mass and quadratic drag coefficient respectively.

A more detailed description of the force components is given hereafter. The separation in $X_S(2)$ and $X_S(3)$ direction, however, is neglected. Furthermore, the special case of a partly submerged horizontal cylinder is discussed.

Inertia Force

The inertia force is based on the fact, that accelerations result from forces, according to Newton's second law. These forces come from a pressure gradient in the fluid, which is present regardless of the fact if there is a body in the fluid or not. To calculate the linear hydrodynamic loads on a body, it is possible to split the fluid-body interaction into two problems. This can be done since, due to linearity, the superposition principle is valid. The first problem is called the diffraction problem. It assumes that the body is fixed and interacts with the incident waves. Solving this problem will give the excitation loads. The excitation loads are found by integrating the dynamic pressure over the mean wetted surface of the body.

$$F_{exc} = \int_{S_{0B}} \frac{\partial \phi}{\partial t} n_k \, \mathrm{d}S \tag{2.22}$$

Using the superposition principle, the wave potential can be decomposed in two terms, one for the incident wave and one for diffraction. Integration of the incident wave potential will give the Froude-Krylov force, while integration of the diffraction potential will give the diffraction force. Using long wave approximation, a body can be considered permeable and the wave-body interaction must thus generate a flow opposite to the incident waves to ensure impermeability. This fact, lets the diffraction load appear as radiation load, which is associated with added-mass and damping terms. The second term of the inertia force is hence referred to as added mass force or disturbance force. The excitation forces

for a small volume structure can be expressed as

$$F_{exc} = \int_{S_{0B}} p_0 n_k \, \mathrm{d}S + \sum_{j=1}^{3} a_{0j} A_{kj} \qquad k = 1..3 \tag{2.23}$$

The first term is the Froude-Krylov force, which can for fully submerged small bodies be approximated as

$$F_{FK} = a\rho_w V \tag{2.24}$$

In case of the Morison equation the body is a cylinder. The Froude-Krylov Force and the added mass force are equal in magnitude and Equation 2.23 thus becomes

$$F_{in} = 2\rho_w \frac{\pi D^2}{4} a \tag{2.25}$$

which is the first term of the Morison equation. The inertia force in longitudinal member direction ($X_S(1)$) is calculated up to the mean free-surface, while in the transverse directions ($X_S(2)$ and $X_S(3)$) it is calculated up to the instantaneous free-surface. For members piercing the mean free-surface a correction factor needs to be applied. Instead of using the theoretical value of 2 in Equation 2.25, an experimental coefficient c_M is used. c_M is often referred to as inertia coefficient and it is equal to $(1 + c_A)$. The value of 1 is the coefficient of the Froude-Krylov force, while the added mass coefficient c_A for the disturbance force is usually found to be smaller than 1 in experiments [27]. The added mass and the added mass coefficient are further dealt with in Section 2.2.5.

In case of a cylinder moving in the fluid, the second fluid-body interaction problem needs to be solved. The second problem is called radiation problem. It assumes that there are no incident waves and that the body is forced to oscillate in its six degrees of freedom. Solving the radiation problem will give the added mass, damping and restoring terms of the body. The restoring terms are found by integration of the hydrostatic pressure and they are connected with the change of buoyancy due to the bodies motions. They are not of interest for the given problem. The added mass and damping terms are found by integrating the dynamic pressure over the mean wetted surface of the body.

$$F_{rad} = -\int_{S_{0B}} \rho_w \frac{\partial \phi_R}{\partial t} n_k \mathrm{d}S = \sum_{j=1}^{6} -A_{kj}\ddot{\eta}_j - B_{kj}\dot{\eta}_j \qquad k = 1..6 \tag{2.26}$$

The damping term can be neglected and the load is thus proportional to the body acceleration and only associated with the added mass of the body. Expressing the added mass in terms of the cylinder area and the added mass coefficient, the inertia force for an oscillating cylinder in waves is

$$F_{In} = (1 + C_a)\rho_w \frac{\pi D^2}{4} a - C_a \rho_w \frac{\pi D^2}{4} \ddot{\eta}_x s \tag{2.27}$$

Quadratic Drag Force

A circular cylinder placed in a constant, uniform, potential flow will not experience any hydrodynamic forces. This effect is known as the 'D'Alembert's paradox' and it is due to the fact, that the pressure distribution is symmetric about the x- and y-axis. In reality, however, the flow will separate at the back of the cylinder. The flow separation is linked to the friction between water particles and it leads to a pressure smaller than the ambient pressure. This pressure difference will lead to a mean horizontal force on the cylinder, the drag force. The drag force is scaled using a drag coefficient, which indicates the pressure difference due to the flow separation. The drag coefficient will be discussed in more detail in a following section. The drag force is defined as

$$F_d = \frac{1}{2}\rho_w U^2 C_d D \tag{2.28}$$

where ρ_w is the density of water, U is the undisturbed flow velocity, C_d is the drag coefficient and D is the cylinder diameter. The drag coefficientC_d is often denoted as C_q, indicating that it is the coefficient for the quadratic drag force rather than for the linearized drag force. In case of a moving cylinder, the relative velocity between fluid particles and the body is used.

Partly Submerged Horizontal Member

For a partly submerged horizontal cylinder the inertia and drag term in the Morison equation are modified to consider the submerged area and volume of the member. The wave force in x-direction then reads

$$dF_{Wx} = \left\{ \rho_w A_p(h)(1 + C_a)a_x + \frac{1}{2} C_d \sqrt{D \cdot h - h^2} u_x |u_x| \right\} dS \tag{2.29}$$

and in z-direction

$$dF_{Wz} = \left\{ \rho_w A_p(h)(1 + C_a)a_z + \frac{1}{2} C_d h u_z |u_z| \right\} dS \tag{2.30}$$

2.2.4 Slamming Force

Slamming is a nonlinear phenomenon that occurs during structure-liquid impact. The occurrence and severity of slamming depends on factors such as the relative motion between body and liquid and the geometry of the body; e.g. the deadrise angle, the angle between body and liquid, is an important parameter. The slamming force is found by integrating the pressure over the wetted surface of the body. The pressure from Bernoulli, including second order terms, is

$$p = -\rho_w \frac{\partial \phi}{\partial t} - \rho_w g z - \frac{\rho_w}{2}[(\frac{\partial \phi}{\partial x})^2 + (\frac{\partial \phi}{\partial z})^2] \tag{2.31}$$

Assuming that the body submergence and thus the hydrostatic pressure is small along the body ($\rho_w \partial\phi/\partial t >> \rho_w g z$) and that the pressure variations in time are larger than

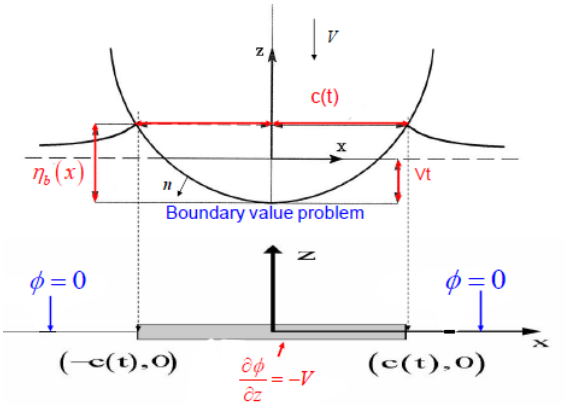

Figure 2.6: *Blunt Body and Equivalent Flat Plate [3]*

those in space ($\rho_w \partial\phi\ \partial t >> 0.5\rho_w[(\partial\phi/\partial x)^2 + (\partial\phi/\partial z)^2]$), the last two terms in Equation 2.31 can be neglected [3]. A blunt rigid body that is symmetric around the z-axis can be modeled by an equivalent flat plate as outlined in Figure 2.6.

Solving the equivalent flat plate problem will yield the velocity potential on the body.

$$\phi = -V\sqrt{c^2 - x^2} \tag{2.32}$$

Inserting Equation 2.32 in the simplified formula for the pressure and integrating it over the wetted length will yield the slamming force for a constant lowering speed of the body. The slamming force is defined in terms of the change of added mass, due to the increase of the wetted length in time, and the relative velocity between fluid particles and body.

$$dF_S = -\frac{A_{33}}{dt}(\frac{d\eta_3}{dt} - w) \tag{2.33}$$

where $\frac{d\eta_3}{dt}$ is the lowering speed of the jacket into the water, w is the incident-wave vertical particle velocity at the center of the strip and A_{33} is the added mass in heave. If a floating vessel is used for the lowering of an object into the water, the vertical crane tip motions need to be considered too.

Slamming on vertical members is not investigated as it will be negligible for the wave conditions present during installation. The slamming force on inclined members depends on the angle between member and instantaneous surface elevation (see angle α in Figure 2.4). The slamming force will be between zero ($\alpha = 90$) and that of a horizontal member of equal length ($\alpha = 0$). Strips of inclined members are submerged to a different extend and thus slamming forces will vary too. The slamming force is only calculated when the member enters the fluid. Water exit forces are not considered. In order to avoid that an additional force is calculated in Matlab when the member exits the water, it is required that the first derivative of the surface elevation is respect to time is positive ($\dot{\eta} > 0$).

2.2.5 Added Mass

Added mass describes the phenomenon of weight that is added to a system due to the fact that an accelerating or decelerating body must move some volume of surrounding fluid with it as it moves [28]. The added mass coefficient is defined as the added mass divided by the displaced fluid mass.

$$C_a = \frac{m_a}{\rho_w \cdot \nabla} \tag{2.34}$$

The added mass coefficient depends on the location of the strip in the fluid domain. The vicinity of the free surface and the seabed will have an influence on C_a. For elements far from the free surface and the seabed the added mass coefficient C_a is a function of the KC number and the roughness (δ). For elements in the vicinity of a fixed boundary, like the seabed, C_a depends on the gap ratio defined as the element diameter divided by the distance to the fixed boundary from the element center point. The added mass m_a of a horizontal circular cylinder piercing the free surface can be obtained from Figure 2.7.

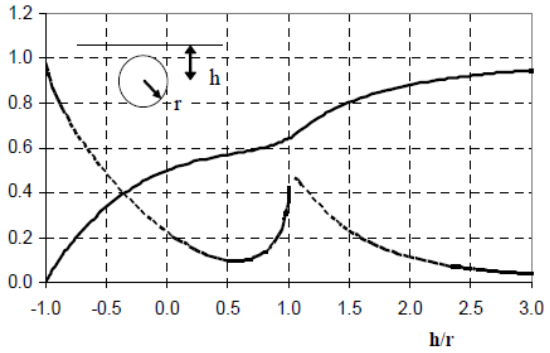

Figure 2.7: *High frequency limit of added mass and its derivative close to a free surface. Solid line: $m_a/\rho\pi r^2$. Dotted line: $(dm_a/dh)/\rho\pi r$ [4]*

To enable the use of Figure 2.7 in the calculations, the curves are digitalized using the freeware *Engauge Digitizer*. Then curve fitting is applied to avoid the need for resource expensive interpolation. The solid line was approximated with two 4th-order polynomials. The curve fitting coefficients as well as the coefficients of determination ($R^2 values$) can be found in Appendix C. The resulting curves are displayed in Figure 2.8.

The use of Figure 2.7 is, however, not adequate for the calculation of slamming forces that occur during the lowering of the jacket at small wave heights. It is thus also possible to use theoretical expressions for the added mass and change of added mass as function of submergence. Assuming a constant added mass coefficient of one, the added mass for a horizontal member can be expressed similar to the buoyancy. In SIMA, the user is not able to input any data for the change of added mass with submergence but only for the depth dependent added mass. The change of added mass and thus the submergence are then automatically based on the input given for the depth depended added mass. The change of added mass is the first derivative of the added mass with respect to submergence h. The added mass and its derivative will reach a constant value once the member is fully submerged. The resulting curves for the added mass as well as for the change of added mass as function of submergence are shown in Figure 2.9.

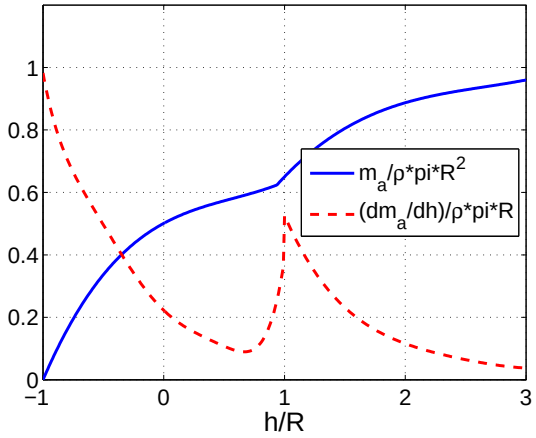

Figure 2.8: *Digitalized high frequency limit of added mass and its derivative close to a free surface*

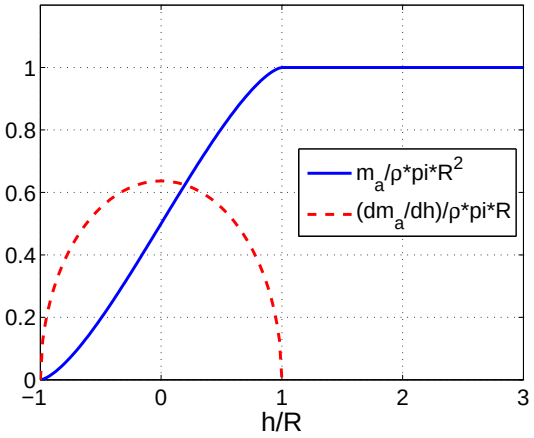

Figure 2.9: *Theoretical added mass and its derivative*

2.2.6 Drag Coefficient

The drag coefficient mainly depends on the Reynolds number and the roughness of the cylinder surface. The Reynolds number indicates the flow regime, whether a flow is laminar or turbulent. Both parameters influence the location of the separation point on the cylinder surface and hence the difference in pressure. The orientation of the cylinder in the fluid, whether the member axis is parallel or normal to the flow, also affects the drag coefficient [26]. The highest listed drag coefficient for steady flow C_{DS}s 1. "For long slender elements a drag coefficient equal to twice the steady state C_{DS} may be applied provided that hydrodynamic interaction effects are not present" [26]. The drag coefficient for all jacket members can therefore be taken as 2. For partly submerged members the drag coefficient is known to vary with the degree of immersion but can be taken as 1 [4]. The fact that the drag coefficient should be equal to twice the steady state value was discovered at a later state in the thesis, when many simulations were already run. All simulations are thus based on a drag coefficient of 1.

2.3 Forces on a Single Member

The equations for the external hydrodynamic forces that act on a jacket were implemented in a Matlab code. This code is validated by comparing the results for fully and for partly submerged horizontal, vertical and inclined members respectively. Writing of an own code allowed for an in depth understanding of the hydrodynamic forces that act on the jacket and a proper set-up of the simulation in SIMO. For the rather small diameter of the member and the small wave height present during installation of the jacket the inertia force is expected to be the dominating wave force component. This observation is in agreement with Figure 2.10, showing the relevant importance of drag and inertia forces. For typical wave heights present during offshore wind substructure installations ($\leq 2.5m$) and jacket member diameters ($\leq 2m$), inertia force will always be dominant.

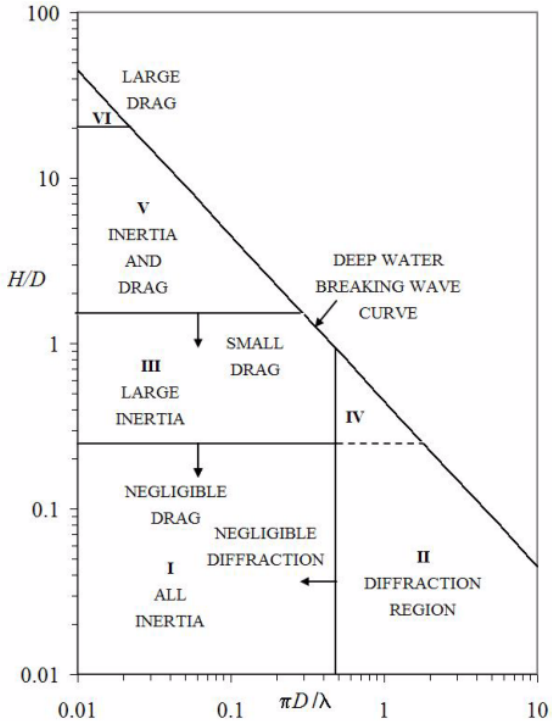

Figure 2.10: *Different wave force regimes [5]. D = characteristic dimension, H = wave height, λ = wave length.*

The results of the codes were found to be matching very accurately. The member dimensions and simulation parameter are outlined in Table 2.1. The prevailing conditions are matched with a realistic environment that will be present during jacket installation, however, regular waves coming from the x-direction are used. The member dimensions equal those of a jacket brace.

Table 2.1: *Member Force Comparison*

Water Depth	40 m
Wave Height	2 m
Wave Period	6 s
Member Diameter	1 m
Member Wall Thickness	0.025 m
Strip Size	0.2 m
Time Step	0.01 s

Fully Submerged Inclined Cylinder

The inclined cylinder is defined by the two nodes shown in Table 2.2. The cylinder has a length of 34.64 m. Figure 2.11 shows the force components acting on the fully submerged inclined cylinder.

Table 2.2: *Member Node Coordinates*

Node	x	y	z
1	10	10	-10
2	-10	-10	-20

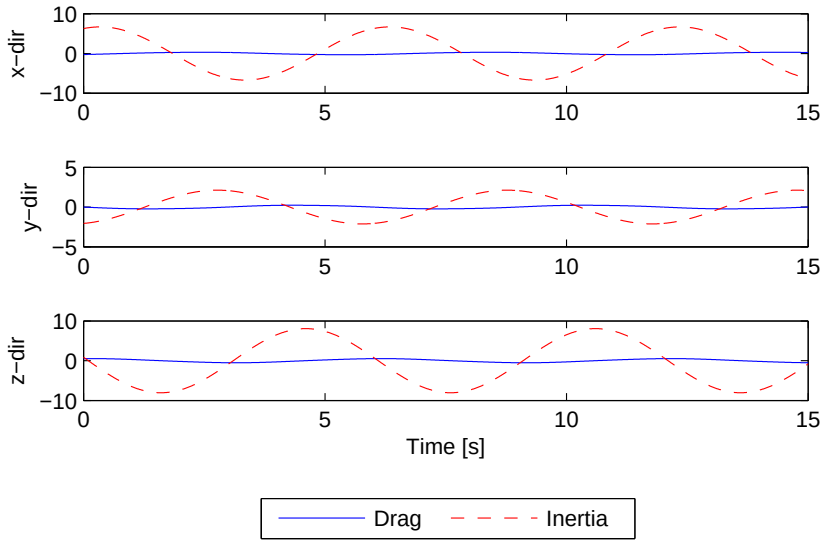

Figure 2.11: *Force Components of a Fully Submerged Inclined Cylinder in [kN]*

The maximum and minimum force components of a fully submerged member will always have the same magnitude. Figure 2.12 shows the total force acting on a fully submerged inclined cylinder.

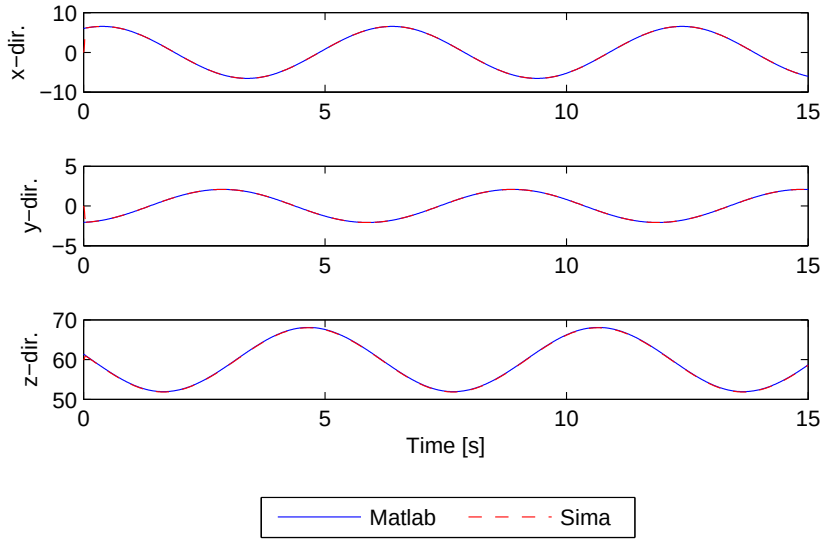

Figure 2.12: *Total Force on a Fully Submerged Inclined Cylinder in [kN]*

Partly Submerged Inclined Cylinder

The inclined cylinder is defined by the two nodes shown in Table 2.3

Table 2.3: *Member Node Coordinates*

Node	x	y	z
1	10	10	-10
2	-10	-10	-20

Slamming Forces are not calculated for this cylinder. Figure B.1 shows the force components acting on the fully submerged inclined cylinder. It can be seen, that the maximum and minimum drag and inertia force are no longer equal in magnitude.

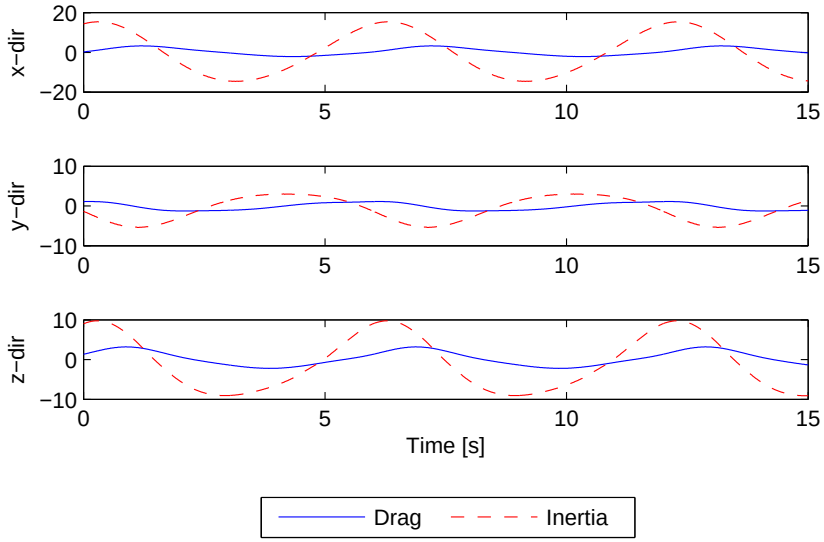

Figure 2.13: *Force Components of a Partly Submerged Inclined Cylinder in [kN]*

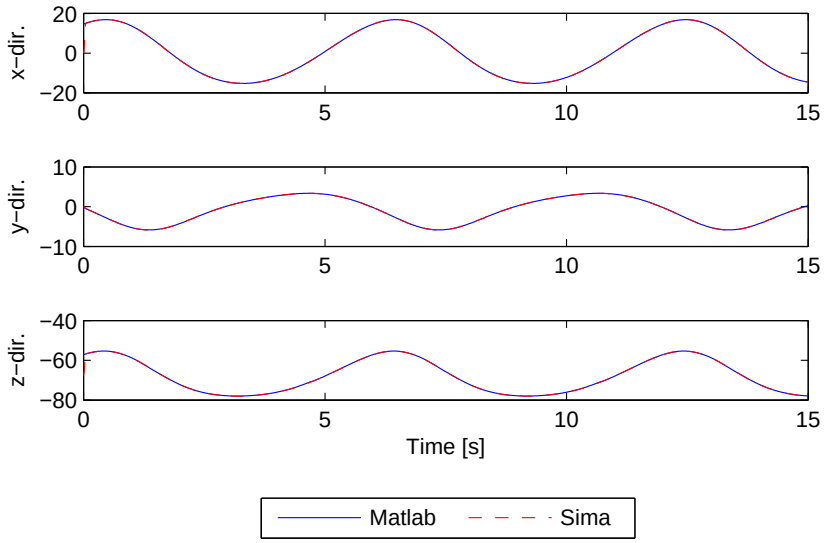

Figure 2.14: *Total Force on a Partly Submerged Inclined Cylinder in [kN]*

Partly Submerged Horizontal Cylinder

The horizontal cylinder is defined by the two nodes shown in Table 2.4. The slamming force is included in the total force for the z-direction. The maximum slamming force in z-direction is 10.79 kN. It occurs when the cylinder enters the water.

The cylinder changes from being fully dry to being fully submerged. The different conditions become visible in the following Figures. The drag and inertia force go to zero when the cylinder leaves the water. When the cylinder enters the water the drag and inertia force increase smoothly. Without depth dependent formulation for the area in the drag term and the volume in the inertia term, the time series for the forces will not be a

Table 2.4: *Member Node Coordinates*

Node	x	y	z
1	0	-10	0
2	0	10	0

smooth curve.

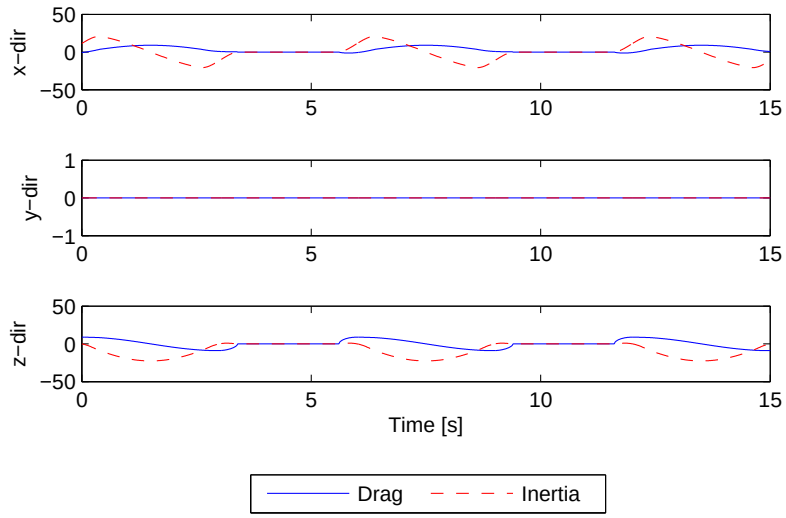

Figure 2.15: *Force Components of a Partly Submerged Horizontal Cylinder in [kN]*

When looking at the total force in z-direction it can be seen that buoyancy and weight are the dominating forces. When the member is dry the total force in z-direction is equal to the weight.

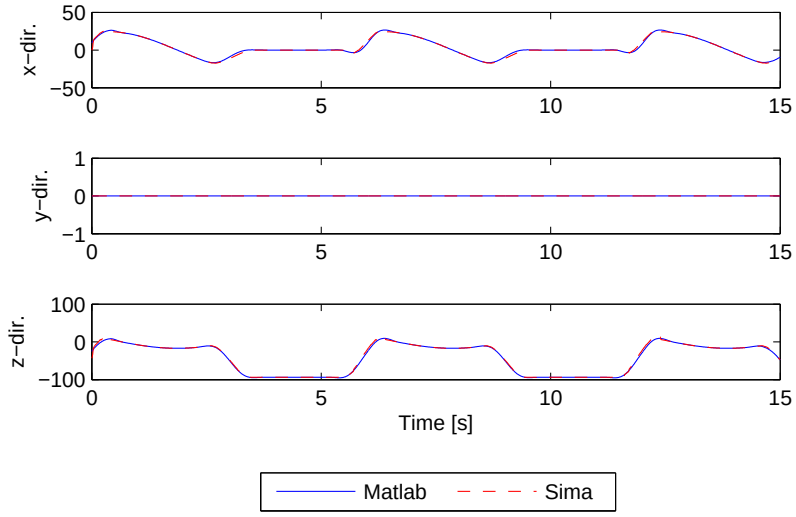

Figure 2.16: *Total Force on a Partly Submerged Horizontal Cylinder in [kN]*

Chapter 3

Numerical Model

3.1 Coordinate Systems

Several coordinate system are required to calculate the forces and motions of the jacket substructure. These systems are right-handed Cartesian coordinate systems with positive direction counter-clockwise. The three coordinate systems required are the global (earth-fixed), the local (body-fixed) and the local strip coordinate system. In the following sections the importance of the individual coordinate systems will be described. Furthermore, coordinate transformation from one system to another will be explained and the transformation equations, giving the relation between two coordinate systems, be stated.

The global (earth-fixed) coordinate system is used to describe the propagation direction of the waves. The X_G, Y_G plane coincides with the still water surface. The Z_G-axis is pointing upwards.

The local (body-fixed) coordinate system moves with the jacket. It is used to define the nodes for the jacket members. The X_B, Y_B plane coincides with the jacket leg tips. The Z_B-axis is pointing upwards. For the given jacket the local coordinates of one jacket leg are given in Table 3.1. A coordinate list of all members can be found in Appendix B. The coordinates are based on the substructure height of 64.75 m, the top width of 14.67 m and the bottom width of 22 m.

Table 3.1: *Local Coordinates of a Jacket Leg*

Node	**x**	**y**	**z**
Node 1	-10.400	-10.400	0.000
Node 2	-6.735	-6.735	64.750

The strip coordinate system is used to calculate the forces on the jacket members. Every member is divided into smaller strips. Unlike the global and the local coordinate system, the strip coordinate system cannot be chosen freely. It is required, that the $X_S(1)$-axis is directed along the longitudinal axis of the member as shown in Figure 3.1. External forces, such as wave and slamming forces need to be calculated normal to the strip coordinate system and later transformed back to the global coordinate system.

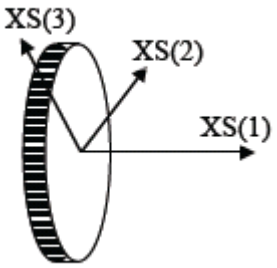

Figure 3.1: *Strip Coordinate System [6]*

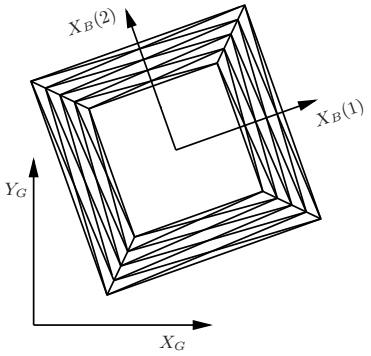

Figure 3.2: *Global and Body C.S.*

The change from one coordinate system to another can be described by translation and rotation of the base vectors [7].

Global to Local Coordinates

For an installed jacket, fixed on the seabed, the correlation between local and global coordinate system does not change in time. A jacket that is lowered into the water, however, will be in motion. Both, the rotation matrix and the translation vector must thus be determined for every time step of the simulation. The transformation from global to local coordinate system is achieved by three rotations in succession [6]. First, the body is rotated by an angle ψ around the common z-axis (yaw). Second, the body is rotated by an angle θ around the common y-axis (pitch). Third, the body is rotated by an angle θ around the common x-axis (roll). The rotation matrix for a transformation from local to global coordinate system is

$$\Lambda = \begin{pmatrix} \cos\psi\cos\theta & -\sin\psi\cos\varphi + \cos\psi\sin\theta\sin\varphi & \sin\psi\sin\varphi + \cos\psi\sin\theta\cos\varphi \\ \sin\psi\cos\theta & \cos\psi\cos\varphi + \sin\psi\sin\theta\sin\varphi & -\cos\psi\sin\varphi + \sin\psi\sin\theta\cos\varphi \\ -\sin\theta & \cos\theta\sin\varphi & \cos\theta\cos\psi \end{pmatrix} \tag{3.1}$$

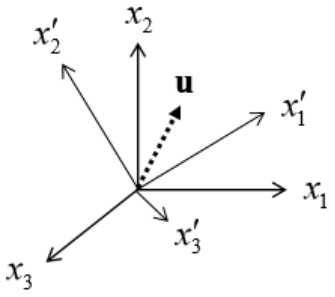

Figure 3.3: *Coordinate Transformation [7]*

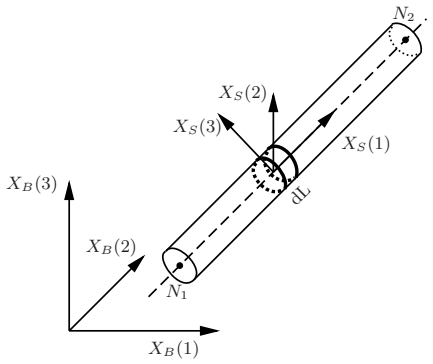

Figure 3.4: *Body and Strip Coordinate System*

Local to Strip Coordinates

As mentioned before, the strip coordinate system cannot be chosen freely. It must thus be determined first. The $X_S(1)$-axis is directed along the longitudinal axis of the member, thus it can be found in the local coordinate system as

$$X_S(1) = \begin{pmatrix} n1_x - n2_x \\ n1_y - n2_y \\ n1_z - n2_z \end{pmatrix} \tag{3.2}$$

$X_S(2)$ must the orthogonal to $X_S(1)$. The scalar product of the two vectors must thus equal zero. There are an infinite number of solutions for this problem.

$$X_S(1) \cdot X_S(2) = 0 \tag{3.3}$$

$X_S(3)$ must be orthogonal to both $X_S(1)$ and $X_S(2)$ and is found as the cross product of the two vectors.

$$X_S(3) = X_S(1) \times X_S(2) \tag{3.4}$$

The strip coordinate system is now determined and the rotation matrix for a transformation from local to strip coordinate system can be set up. The rotation matrix for all strips of a member will be the same, only the translation will differ. The angles between the axis of the strip coordinate and the local coordinate system can be calculated as

$$\alpha = \frac{X_S \cdot b}{|X_S| \cdot |b|} \tag{3.5}$$

where X_S are the base vectors of the strip coordinate system in local coordinates and b are the base vectors of the local coordinate system. The jacket is assumed to be rigid, members do not deform. This means, that the correlation between local and strip coordinate system does not change in time. If members deform the correlation between local and

strip coordinate system would change. The rotation matrix for a transformation between local and strip coordinate system is

$$\Upsilon = \begin{pmatrix} \cos(x_1, x_1') & \cos(x_1, x_2') & \cos(x_1, x_3') \\ \cos(x_2, x_1') & \cos(x_2, x_2') & \cos(x_2, x_3') \\ \cos(x_3, x_1') & \cos(x_3, x_2') & \cos(x_3, x_3') \end{pmatrix} \tag{3.6}$$

The rotation matrix consists of nine direction cosines, where $\cos(x_i, x_j')$ is the cosine of the angle between the x_i and x_j axis as shown in Figure 3.2. The transpose of the matrix is also its inverse, meaning that the matrix is orthogonal.

3.2 Model Overview

Before the installation of the jacket can be modeled the numerical simulation needs to be set up. This chapter describes all bodies and couplings that are part of the installation. The simulation consists of two bodies, namely the installation vessel and the jacket. The couplings that are modeled are the lift wire that connects the jacket to the crane of the vessel, as well as docking cones and fender plates that represent the foundation piles the jacket will be lowered into. Figures 3.5 and 3.6 provide an overview of the two bodies and the lift wire. The dimensions of the bodies are true to scale. The connection between foundation pile and jacket at the seabed is shown in Chapter 3.5 later on. The four legs of the jacket and the corresponding docking cones and fender plates are numbered. Those numbers are later referred to, when the results for each individual location are presented. The origin of the jacket's body coordinate system is chosen to be at the bottom of the jacket in the center between the four piles as indicated by a cross hair in Figure 3.5. The origin and orientation of the vessel's coordinate system is equal to the global coordinate system. Table 3.2 shows the most important coordinates of the system.

Table 3.2: *Key Points in Body Coordinates*

Point	**Body**	**x [m]**	**y [m]**	**z [m]**
Jacket CoG	Jacket	0.00	0.00	39.66
TP Point Mass	Jacket	0.00	0.00	65.25
Hook Point	Jacket	0.00	0.00	66.00
Vessel CoG	Vessel	−7.25	−0.90	2.17
Winch	Vessel	−74.20	0.00	10.00
Crane Tip	Vessel	−15.00	45.00	80.00

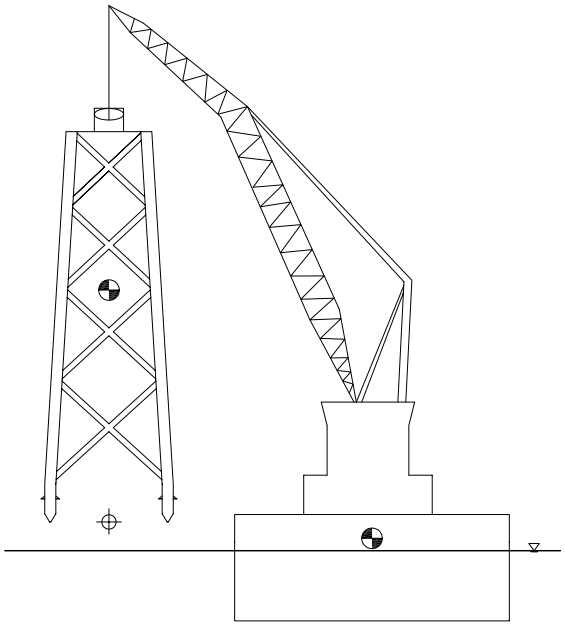

Figure 3.5: *Side View of the Initial Position. Vessel not Heeled*

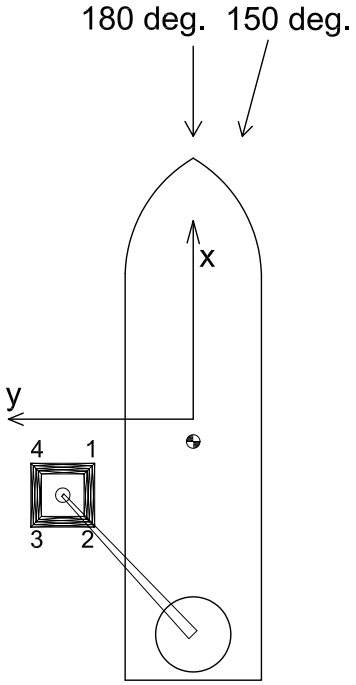

Figure 3.6: *Top View of the Initial Position. Numbering of Leg Positions*

3.3 Jacket

The 10 MW wind turbines are to be build on jacket substructures in 40 m water depth. So far, the EU Mermaid project partners have agreed on the basic dimensions of the jacket, without coming up with a detailed design. The jacket has a height of 64.75 meters and a footprint of 22 times 22 meters. The mass of the jacket is 1000 tonnes excluding the transition piece. It is vital to have realistic dimensions for the jacket substructure. Since the aim of the thesis is not the design of a substructure, existing jacket designs, namely the 5 and 20 MW UpWind turbines, are chosen as reference to come up with a simplified, yet realistic jacket [29]. Common wind turbine scaling laws are applied and for parameters that cannot be upscaled easily linear interpolation between the 5 MW and 20 MW Upwind turbine is applied. The dimensions and levels of the 5 MW and 20 MW UpWind turbines are shown in Table 3.3 below.

The basic jacket geometry is adopted from the 5 MW reference jacket. The jacket consists of four bays with x-bracings. The horizontal mud brace at the bottom of the jacket is not adopted, as the jacket legs enter the foundation piles and therefore cannot have any horizontal connections. The four bays are geometrically equal meaning that the angles for the braces and the angle between leg and braces are always the same. To achieve and geometrically equal design the following equations are utilized [30]. First the scaling coefficient m needs to be determined as

$$m = \frac{b_N}{b_0}^{\frac{1}{N}} \tag{3.7}$$

Table 3.3: *Dimensions of the 5 MW and 20 MW UpWind Turbine*

Dimension	**5 MW Turbine**	**20 MW Turbine**
Rated Power [MW]	5	20
Rotor Diameter [m]	126	258
Rotor Assembly Mass [t]	110	1203
Nacelle Mass [t]	240	2362
Tower Mass [t]	216	4024
Jacket Mass [t]	545	2736
Hub Height [m above MSL]	83	159

where b_N is the base width, b_0 is the top width and Ns the number of bays of the jacket. The height of the top bay is then found as

$$h_1 = h\frac{m-1}{m^N-1} \tag{3.8}$$

and the height of each subsequent bay is found as

$$h_{i+1} = m \cdot h_i \tag{3.9}$$

For the dimensioning of the jacket members it is assumed, that wind loads are dominating and that the jacket design is mainly governed by the fatigue design. The turbine thrust force is balanced by axial forces in the jacket braces, while the overturning moment at the seabed is balanced by axial forces in the legs. If the stress in the members should stay constant, the larger loads from the 10 MW turbine must be balanced by a larger member cross section. A larger diameter of submerged members would normally lead to larger hydrodynamic loads, however, this effect is disregarded for this design.
The thrust force (F_{Thrust}) for the larger turbine can be calculated as

$$F_{Thrust} = \frac{D_R^2}{D_{R,Ref}^2} \cdot F_{Thrust,Ref} \tag{3.10}$$

To obtain the overturning moment, this value is multiplied with the distance between rotor hub and interface level. The new cross sectional area of each member is then found by multiplying the thrust force ratio with the member area from the reference turbine.

$$A = \frac{F_{Thrust}}{F_{Thrust,Ref}} \cdot A_{Ref} \tag{3.11}$$

The diameter and wall thickness of each member is found by assuming the same ratio for diameter over wall thickness then for the reference jacket. The resulting dimensions of the individual members are modified to fit a target mass of 1000 tonnes for the jacket. Furthermore, the following simplifications are made. All jacket braces have the same dimensions and the diameter and wall thickness of all members does not change along its length, as changing dimensions can only be achieved by defining each constant section as individual slender element in SIMO. The transition piece consists of a can, a large

steel tubular to which the tower is bolted on and four diagonal struts acting as additional support between can and deck. In the numerical model the transition piece is represented by a point mass. The transition piece will stay above water and there are no wind forces considered in the simulations. The exact geometry of the transition piece is thus not relevant for the accuracy of the numerical model. The mass of the transition piece assumed to be 250 tonnes. Secondary steel items, such as boat landings and j-tubes are disregarded. A 3D model, as well as a 2D technical drawing of the jacket, can be found in Appendix B.

3.3.1 Member Representation

Each member is defined by two nodes. The coordinates of those nodes is based on a wire frame model, where the diameter of each individual member is not represented. This leads to inaccuracies. First, the nodes of the braces will extend up to the center lines of the jacket legs. In reality, the braces would stop at the cylinder wall of the legs. Second, the volume where two braces overlap is considered twice. The numerical jacket model thus has a larger volume than the real jacket and will therefore experience larger forces. The exact model is much more time-consuming and complex to implement and the node coordinates are harder to obtain. These unrealistic overlaps lead to an increase of 25.77 m^3 in volume equal to a mass of 24.50 tonnes. The influence this has on the wave forces depends on the submergence on the jacket but is very small compared to the total force.

3.3.2 Mass Matrix

The mass matrix for the jacket is made up of the contribution from each individual jacket member and point masses. The mass matrix is later used to determine the eigenmodes of the jacket on the crane and the coupled system.

$$\Delta M = \begin{pmatrix} 1 & 0 & 0 & 0 & z & -y \\ 0 & 1 & 0 & -z & 0 & x \\ 0 & 0 & 1 & y & -x & 0 \\ 0 & -z & y & y^2+z^2 & -xy & -zx \\ z & 0 & -x & -xy & z^2+x^2 & -yz \\ -y & x & 0 & -zx & -yz & x^2+y^2 \end{pmatrix} \cdot mL \tag{3.12}$$

where x, y and z are coordinates of the center of gravity of each member, m is the mass per unit length of the member and L is the member length.

3.4 Vessel

The model for the vessel is based on an existing heavy lift vessel. The motion behavior of the vessel was analyzed using the software WADAM. WADAM solves the radiation and diffraction problem occurring during interaction of waves with floating structures. The relevant vessel properties that are relevant for a successful modeling of the jacket installation are explained based on the required input in SIMA. The hydrodynamic analysis was carried out by PhD student Li Lin. Her results were used for this thesis. The vessel is modeled as a large volume structure. The motions for all 6 degrees of freedom are calculated in the time domain. The main vessel dimensions are given in Table 3.4.

Table 3.4: *Vessel Dimensions*

Length overall [m]	183.0
Breadth (molded) [m]	47.0
Depth at Side [m]	18.2
Draft (operational) [m]	13.5
Displacement [t]	52 000

The vessel comes with a class 3 dynamic positioning (DP) system. The crane has a maximum revolving capacity of 5000 tonnes at 32 meters radius.

Structural Mass

The input for the structural mass includes the location of the center of gravity as well as the mass coefficients. The mass coefficients are the structural mass of the vessel and the 6 mass moments of inertia. The structural mass of the vessel, together with its added mass form the mass matrix of the vessel.

Linear Damping

The input for the linear damping of the vessel consists of a 6x6 damping matrix. There is no damping in heave and pitch.

Hydrostatic Stiffness

The input for the linear damping of the vessel consists of a 6x6 stiffness matrix. It includes stiffness for coupled heave and pitch motions.

Radiation Data

The input for the radiation data of the vessel consists of a 6x6 matrix with the constant part of the frequency dependent added mass.

3.4.1 Ballast

The floating vessel is free to move in all 6 degrees of freedom. The jacket hanging on the crane will cause the vessel to heel and trim. The heeling angle is approximately 5.8 degrees in the equilibrium condition. Heeling of the vessel will also affect the crane tip position that subsequently leads to a change in the jacket position. The initial, desired, position of the jacket and the actual position of the jacket affected by the heeled vessel are shown in Table 3.5.

Table 3.5: *Position of the Jacket due to heeled and trimmed Vessel*

Position	**x**	**y**	**z**
Defined	−15.00	45.00	5.00
Actual	−14.89	52.28	0.67

To assure safe operations and to position the jacket directly above the foundation piles it is thus required to ballast the vessel for it to reach even keel. The ballast of the vessel is simplified as a point mass on the vessel. The overturning moment induced by the point mass balances the moment induced by the jacket. When the jacket is completely in air the full jacket weight needs to be balanced. For increasing submergence of the jacket the weight is reduced by the buoyancy. To ensure even keel at all time the point mass would need to be permanently changed throughout the operation. Continuous adjusting of the ballast, meaning the ballast pumps run throughout the whole operation, introduces possible failures and threats that might jeopardize the operation. Furthermore, partly filled tanks act as free surfaces that affect the motion behavior and stability of the vessel. It is thus decided that the ballasting occurs only once before the lowering procedure is started and is kept constant until the jacket has reached its final position. It is most crucial that the vessel is at even keel when the jacket legs are about to enter the foundation piles. The amount of ballast is thus chosen, that the counter moment of the ballast is equal to the weight of the jacket minus the buoyancy when the jacket is 38 m submerged (just above the foundation piles). Figure 3.7 shows the heel angle and the y-offset of the jacket if the initial, dry weight of the jacket is balanced and if the submerged weight of the jacket is balanced. The time step when the jacket leg tips are at the same vertical level than the foundation piles is indicated by the dashed vertical line. If the dry weight of the jacket is balanced with ballast the vessel will not heel as long as the jacket is in air. Once the jacket is lowered into the water the weight decreases and the ballast overcompensates the overturning moment induced the jacket. The vessel will heel and the crane tip position and consequently the jacket position will change. The offset between jacket legs and foundation piles is then too large and installation is not successful. If the weight of the jacket 38 m below the surface is balanced the vessel will heel towards the jacket side and slowly upend until it is at even keel when the jacket is about to enter the foundation piles. The jacket legs and the foundation piles aligned and installation is successful. The roll motions and the y-offset will change if waves are present. The static offset, however, is avoided by proper ballasting.

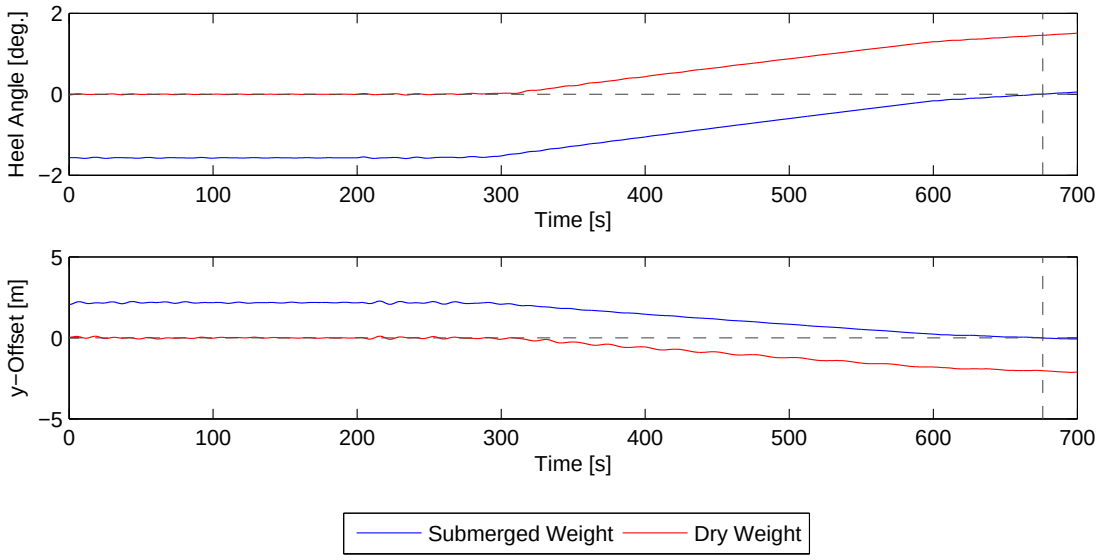

Figure 3.7: *Heel Angle and Jacket Offset for two different ballast conditions*

3.4.2 Response Amplitude Operators

Response amplitude operators (RAOs) give valuable information on how a ship behaves during certain sea states. RAOs are usually obtained by either model tests or by analyzing a panel model of the vessel with an advanced software such as WADAM. To find the RAOs the ship motions are assumed to be linear. By solving the equation of motion that can be set up for the vessel for each degree of freedom the corresponding RAO is obtained.

$$RAO(\omega) = \frac{x}{\zeta_a} = \frac{F_0}{C - (M + A(\omega))\omega^2 + iB(\omega)\omega} \tag{3.13}$$

The amplitude of each rigid body motion, be it translation or rotation, can now be expressed as function of wave height. Knowing these transfer functions, the motions of the vessel can be predicted, which helps to judge the operability of the vessel. The ship motions depend on the direction of the incoming waves. Most ships are symmetric about the longitudinal axis and thus the RAOs will be too. The RAOs of the floating vessel used in this thesis are shown in Figure 3.8. The x- and y-axis are removed due to confidentiality. Only the wave directions that are investigated in this thesis are displayed. For the smallest wave period of 5 seconds investigated in this thesis no large ship responses are to be expected. For increasing wave periods the pitch motion of the vessel is excited, which translates into surge motions of the jacket on the crane. For wave periods larger than 10 seconds the remaining 5 degrees of freedom are increasingly excited by the waves. Surge motions of the vessel will lead to surge motions of the jacket, while roll motions of the vessel translate to sway motions of the jacket. The response amplitudes of the 3 remaining degrees of freedom heave, sway and yaw are relatively small and thus not expected to be an issue.

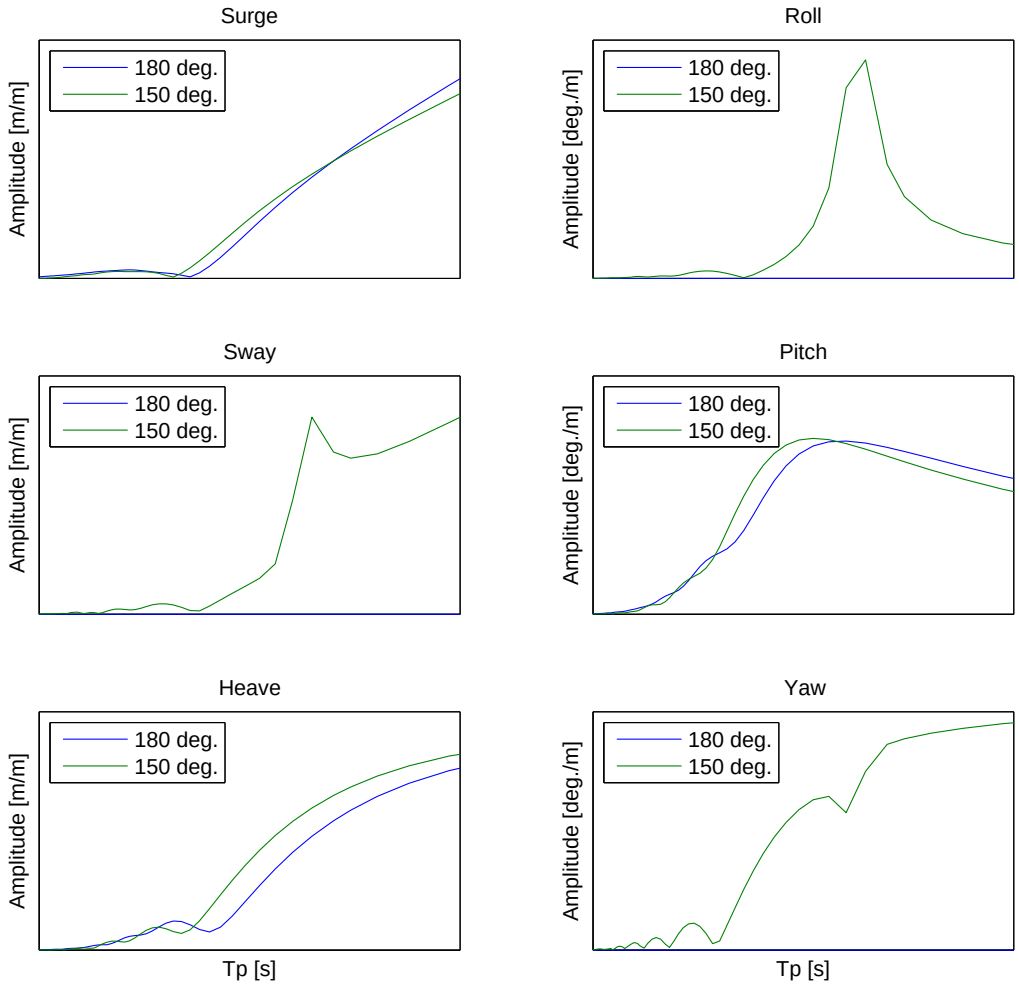

Figure 3.8: *Response Amplitude Operators of the Floating Vessel for the Operational Draft of 13.5 m and a Water Depth of 40 m*

3.5 Coupling Forces

3.5.1 Lift Wire

The lift wire is modeled as a simple wire coupling in SIMO. There is only 1 single lift wire that is attached in the center of the transition piece. It is planned that a hydraulic gripper is used instead of a hook. This gripper can be lowered into the transition piece, where it than expands and pushes against the inner wall of the transition piece. The mass of the wire is not taken into consideration. The characteristics of the lift wire are shown in Table 3.6. The damping of the lift wire can be approximated as 2 percent of the wire cross section stiffness [6].

The length corresponds to the initial, unstretched length of the lift wire from the winch on the vessel to the connection point on the jacket. Flexibility defines the flexibility of the crane. Damping defines the material damping of the lift wire. EA is the product of

Table 3.6: *Lift Wire Properties*

Length	Flexibility	Damping	EA
110 m	2.000e-06 m/kN	1.582e+05 kNs	7.910e+06 kN

the modulus of elasticity and the cross sectional area of the lift wire. The effective axial stiffness of the system is

$$\frac{1}{k} = \frac{l}{EA} + \frac{l}{k_0} \tag{3.14}$$

3.5.2 Landing Devices

The connection between jacket legs and pre-installed foundation piles is modeled with a pin-cone connection. Since the jacket legs are lowered into the foundation piles, the foundation piles are represented by the cone and the jacket legs by the pin. The connection between a jacket leg and foundation pile is shown in Figure 3.9. Once the jacket has reached its final depth the pile stoppers will rest on the foundation piles and act as temporary support until the grouted connection is established.

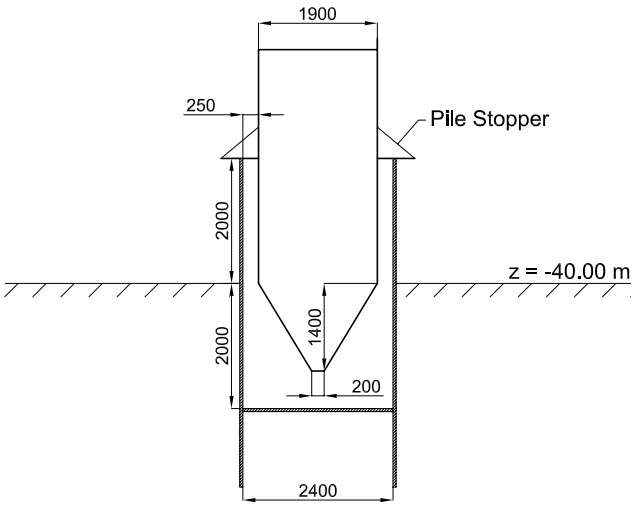

Figure 3.9: *Connection between Jacket Leg ans Foundation Pile*

In SIMO it is not possible to have any object below the seabed. The jacket legs are thus shortened by two meters. Once the lowering of the jacket into the foundation piles is completed, the permanent connection is established by grouting the void. The foundation piles have the dimensions shown in Table 3.7.

The inner diameter of the foundation pile, together with the outer diameter of the jacket leg, determine the maximum allowed offset of the jacket in order to guarantee a successful landing. A larger clearance means that larger offsets during the initial phase of the docking procedure are possible. From an installation point of view, the clearance should thus be

Table 3.7: *Foundation Pile Dimensions*

Length [m]	55.00
Outer Diameter [m]	2.52
Mass [t]	200.00
Wall Thickness [mm]	60.00
Inner Diameter [m]	2.40

as large as possible. The gap between jacket leg and foundation pile is later filled with grout to form a permanent connection. Restrictions apply for the thickness of this grout annulus. The restrictions mentioned in different offshore guidelines are outlined in Table 3.8. The limiting values apply for the ratio of inner foundation pile diameter to annulus thickness.

Table 3.8: *Grout Annulus Thickness*

	Min	**Max**
Norsok N-004	≥ 10	≤ 45
EN ISO 19902	≥ 10	≤ 45
API	≥ 7	≤ 45

The clearance in the used design (250 mm) complies with the API standards and poses only a minor discrepancy to the limits of the Norsok and ISO standards (240 mm). Since the design of the jacket and the foundation piles is not the main purpose of the thesis time domain simulations will be carried out based on the shown jacket-pile connection. The pile stick-up, meaning the distance the piles extend from the seabed, is 2 meters. In reality this pile stick-up can vary between 2-4 meters. Variations in the seabed are leveled by varying the pile stick-up for each individual pile.

Docking Cones

Docking cones are used to represent the foundation piles in the numerical model. A docking pin point, the tip of the jacket leg, and a docking cone point, the top of the foundation pile, are defined with coordinates. The maximum radial distance at entry is defined. If the transverse offset of the pin point from the cone point exceeds this value, the leg will not enter the foundation pile and the installation will not be successful. Next, cross sections are defined, that describe the clearance between the jacket leg and the foundation pile for various axial distances. This allows to represent a certain geometry of the pin and cone, such as the shape of the jacket leg tip shown in Figure 3.9. The foundation pile, restricting the movement of the jacket leg, is represented by a restoring force that is directed towards the center of the foundation pile. The magnitude of this force must be specified by the user. The force increases linearly between the two distances defined. The cross section characteristics of the piles used in the simulations are shown in Table 3.9. The magnitude of the forces and damping used in the simulations are not based on any existing project specifications.

Table 3.9: *Docking Cone - Cross Section Characteristics*

Cross Sec.	Axial Dist.	Vertical Dist.	Force	Damping
		1.00 m	0	0
1	0.00 m	1.20 m	2000 kN	400 kNs/m
		1.40 m	50000 kN	1000 kNs/m
		150	0	0
2	1.40 m	0.25 m	2000 kN	400 kNs/m
		0.35 m	50000 kN	1000 kNs/m
		0.15	0	0
3	2.00 m	0.25 m	2000 kN	400 kNs/m
		0.35 m	50000 kN	1000 kNs/m

Fender Plates

Fender plates are used to represent the pile stoppers in the numerical model. Fenders are contact elements between a moving body (jacket) and a fixed point (foundation pile), that will give a compression force normal to the defined fender plane. For the simulations the fender force is acting upwards, against the lowering direction of the jacket, which will cause the jacket to stop and rest on the fender planes. If the specified force is too small the moving object will simply pierce through the fender plane and the jacket will consequently sink into the seabed. The point on the jacket is located on the leg tip and the fender plate is on the seabed rather than at the top of the foundation piles. This approach was chosen to prevent the jacket from being deflected and possible miss the foundation pile due to the upward force. Fenders are used to keep the jacket at its final position and to prevent the jacket from sinking into the seabed. The representation of the impact forces between pile stoppers and foundation piles with fenders is not accurate and detailed structural analysis should be carried out to determine these forces. These forces can than be used as an input for the design of the jacket legs or to define weather limitations for the operation. Nonetheless, the obtained landing forces will later be presented to give an idea of the order of magnitude that can be expected. The properties for the fenders outlined in Table 3.10 were used in the simulations. The force was chosen to be as small as possible but sufficiently large to prevent failure. Small damping was given for the sake of a stable numerical simulation. Linear interpolation is applied between the two cross sections.

Table 3.10: *Fender Plate - Cross Section Characteristics*

Cross Sec.	Vertical Dist.	Force	Damping
1	0.5 m	0 kN	1 kNs/m
2	0 m	2000 kN	1 kNs/m

Chapter 4

Time Domain Simulation Method

4.1 SIMO

All simulations in this thesis are carried out using Marintek's software SIMO and the corresponding graphical user interface SIMA. SIMO is a non-linear time domain simulation program used for the analysis of rigid-body motions and station keeping of multibody systems. The operation investigated in this thesis consists of two bodies, namely the jacket and the installation vessel. The jacket and the floating vessel are both modeled as 6 DOF bodies that are free to move and rotate in all directions. The jack-up vessel is modeled as a fixed body that is restrained from any translations and rotations. For the system consisting of jacket and floating vessel the following 12 equations of motions need to be solved [6].

$$(m + A(\infty))\ddot{x} + C\dot{x} + D_1\dot{x} + D_2 f(\dot{x}) + K(x)x + \int_0^t h(t-\tau)\dot{x}(\tau)d\tau = q(t, x, \dot{x}) \quad (4.1)$$

where m is the body mass matrix, A is the frequency dependent added mass matrix, D_1 and D_2 are the linear and quadratic damping matrices respectively, K is the hydrostatic stiffness matrix, h is the retardation function of the vessel and q is the external force vector. The external force vector is, in general, comprised of wind, current, first and second order wave excitation and possible other forces. In this thesis, wind and current forces are neglected and a perfect dynamic positioning system is assumed, so that second order wave excitation forces, such as slowly varying wave drift forces, can be neglected too. The stiffness matrix K consists of the hydrostatic stiffness of the vessel and the coupling between the vessel and the jacket via a lift wire. There are no mooring lines in the model. The components of the mass, added mass and stiffness matrices are discussed in a later chapter.

The equations of motions are solved in a stepwise integration method. The integration methods available in SIMO are the modified Euler method, 3^{rd}-order Runge-Kutta-like method and Newmark-β predictor-corrector method, of which the latter one has been used for the simulations. For an explanation of the integration methods it is referred to the theory manual of SIMO (see [6]).

4.1.1 Time Step Size

To assure that all relevant motions of the coupled system are properly represented in the simulations the time step size (Δt) needs to be sufficiently small. The natural periods of the jacket are smaller than that of the vessel. Hence the smallest jacket natural period (T_{lim}) is the governing parameter when choosing a suitable time step size. Typically $\Delta t < 0.1\ T_{lim}$ applies. The natural periods of the jackets rigid body motions are calculated for different jacket positions (see Table 4.1). The positions of the jacket range from being fully in air to just above the foundation piles. The time step size (Δt) is chosen as 0.02 s. This allows for a proper representations of all jacket motions in the response histories.

4.1.2 Wave Methods

For the simulations two different methods are utilized to generate time series. 1^{st} order wave responses for the floating vessel are pre-generated by Fast Fourier Transformation (FFT) for a predefined position and vessel heading. Wave particle dynamics required for the calculation of wave forces on the jacket are calculated by time domain summation of the harmonic components (cosine series). The position of the jacket is changing with each time step, as it is lowered from the air, through the wave splash zone, down to the seabed. Since FFT is only applicable for bodies with predefined position it is not possible to utilize the very high efficiency of FFT for the jacket. For the combination of FFT and cosine series it is ensured, that the same realization of wave components is used for both options for wave response calculation [6].

4.2 Convergence Test

The lowering and landing process of the jacket are subject to nonlinear loads originating from waves. It is insufficient to only run 1 realization of each irregular wave case. To ensure that the obtained results are representative 30 wave realizations (random seed numbers) are run for each sea state (combination of Hs and Tp). It can then be checked how fast the cumulative average (Eq. 4.2) of the results converges to the mean value of all 30 realizations, as has been done in [31].

$$X_i = \frac{1}{i} \sum_{k=1}^{i} X_k \tag{4.2}$$

The convergence of the simulations is checked with the maximum value of the following properties. The horizontal offset of the jacket tip (a), the docking force that occurs during impact of one the jacket legs and the foundation pile (b), the landing force when one of the pile stopper rests on the foundation pile (c) and the lift wire tension (d). Figure 4.1 shows that representative results can be obtained with 30 seeds. The floating vessel with large wave period and oblique waves was chosen for the convergence study as this will results in the largest motions. The large difference that occurs from seed to seed will be discussed later on.

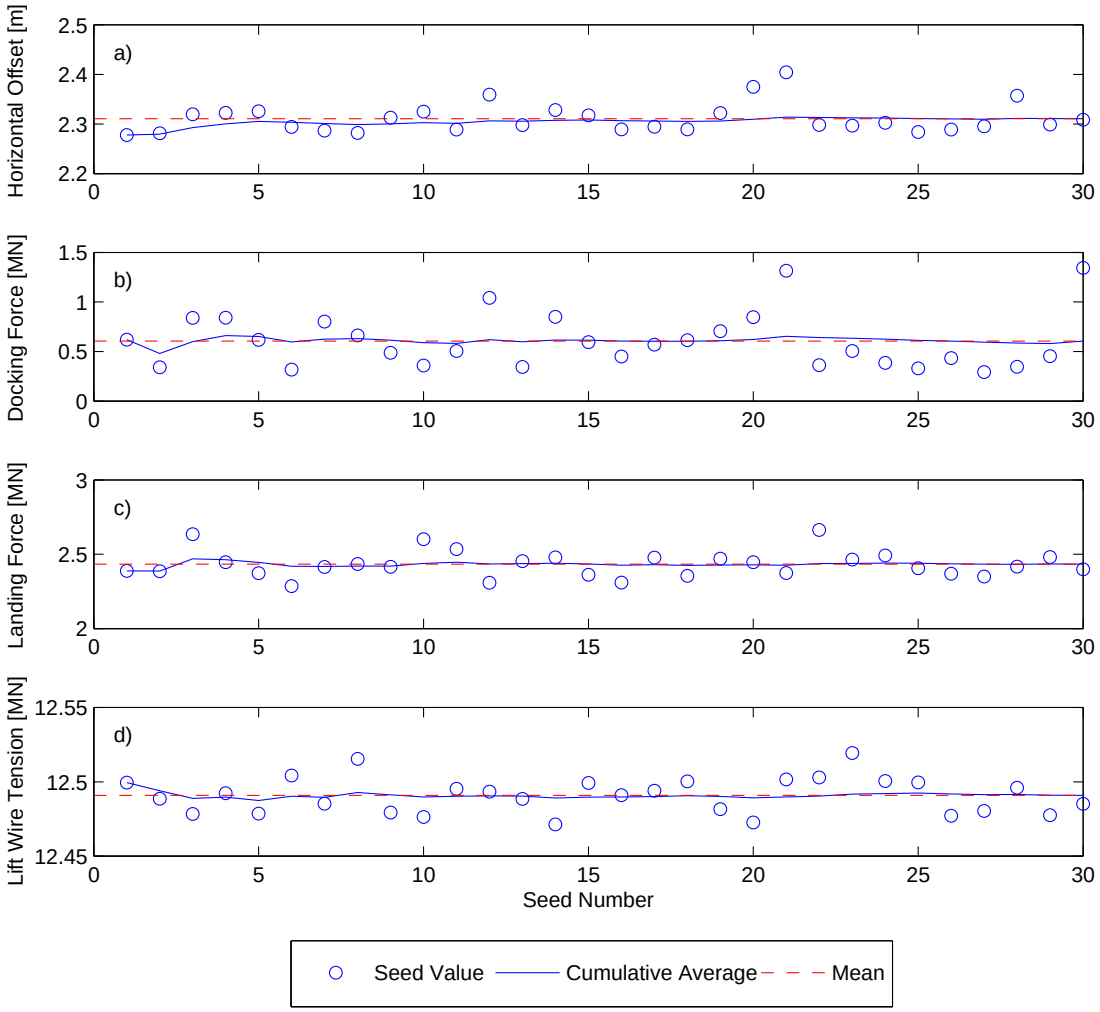

Figure 4.1: *Seed Values, Cumulative Average and Mean Value of Maximum Responses for a Floating Vessel at Hs = 2 m, Tp = 6 s, Dir = 150 deg.*

4.3 Eigenmodes and -values

It is important to analyze at which frequencies a system is excited in its motions. The eigenfrequencies can then be compared with the spectra from the excitation forces such as waves and if applicable wind to see which weather conditions are critical for the marine operation. The undamped eigenfrequencies and eigenmodes of the coupled system can be determined by solving the eigenvalue problem

$$(-\omega^2(M+A)+C)x = 0 \tag{4.3}$$

For a coupled system each eigenmode will have contributions from several degrees of freedom. The magnitude of the corresponding eigenvectors help to identify the modes of motions that give the largest contribution.

4.3.1 Fixed Vessel

The jack-up vessel is restrained from any movements and thus acts as a bottom-fixed structure. The jacket is not affected by the vessel, since no motions transfer from the vessel through the lift wire. The jacket is only excited by the wave forces that act against it. If the lifted objected is restrained from any rotational movements, e.g. through the use of tugger wires, the 6 degrees of freedom become uncoupled. The natural period of the pendulum motion (surge and sway) in air can then be approximated as

$$T_{N1,2} = 2\pi\sqrt{\frac{L}{g}} \tag{4.4}$$

This formula is known as the linear pendulum equation and is strictly speaking, only valid for a point mass suspended from a rod, rather than a wire. The natural period of the heave motion can be approximated using the following equation of a spring pendulum.

$$T_{N3} = 2\pi\sqrt{\frac{k}{m}} \tag{4.5}$$

In the simulations carried out the jacket was not restrained from any rotational movements and was hence modeled as a 6 DOF body. Surge and pitch, as well as sway and roll motions of the jacket are now coupled. The exact eigenmodes and the corresponding eigenvectors are then obtained by solving the eigenvalue problem. M only consists of the mass matrix of the jacket, calculated according to Equation 3.12 and K is the stiffness matrix of the coupled system. The terms in the stiffness matrix are a function of the weight of the load and the length and stiffness of the lift wire. These values are a function of time and change throughout the lowering operation. Furthermore, it should be kept in mind, that the eigenmodes shown are based on the undamped system and that the eigenperiods will increase with damping. Table 4.1 shows the eigenmodes with the corresponding eigenvectors for a jacket tip position of $z = -37.5\ m$.

Table 4.1: *Eigenmodes with Corresponding Eigenvectors for the Jacket Tip Position z = -37.5 m*

Eigenperiod [s]	**1.03**	**9.31**	**9.32**	**36.99**	**37.09**	**216.49**
Surge	0.05	−0.41	−0.37	1.00	−0.88	0.00
Sway	0.05	−0.37	0.41	0.89	1.00	0.00
Heave	1.00	0.00	0.00	0.00	0.00	0.00
Roll	0.04	−0.92	1.00	0.56	0.64	0.00
Pitch	−0.04	1.00	0.92	−0.64	0.56	0.00
Yaw	0.00	0.00	−0.03	0.00	−0.03	1.00

As can be seen from the eigenvectors the first eigenmode is dominated by heave with only minor contributions from surge, sway, roll and pitch. Based on the wave spectra shown in Figure 2.3, it can be said that the eigenmode is of little importance, since there is little to no wave energy present at this period. Eigenmode 2 and 3 are dominated by pitch and roll with major contributions from surge and sway. Mode 2 and 3 are of high importance for the installation, as there is a lot of wave energy present for this period. Mode 4 and

5 are dominated by surge and sway with major contributions from roll and pitch. For a squared jacket the eigenperiods of mode 2 and 3, as well as, for mode 4 and 5 should be the same and the small contribution from yaw present for mode 3 and 5 should not exist. Mode 6 is the uncoupled eigenperiod of the jacket's yaw motion, which is well outside the wave spectra. Figure 4.2 show how the most relevant eigenmodes which are within the wave spectra change for different jacket positions.

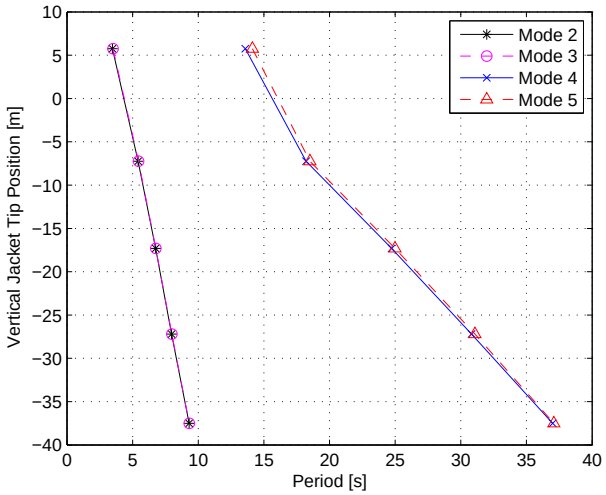

Figure 4.2: *Eigenmodes of the Jacket at Different Vertical Positions*

As can be seen, the eigenperiod of mode 2 and 3 of the jacket increase from approximately 3.5 seconds when the jacket tip is 5 meter above water to 9.3 seconds when the legs are about to enter the foundation piles. Mode 4 and 5 of the jacket have eigenperiods that are represented by wave energy in the spectra. The eigenperiod of those modes increases more rapidly from around 14 seconds in air to approximately 37 seconds before docking. The fact, that the natural periods of the jacket's eigenmodes changes throughout the operation poses another challenge when it comes to evaluating which wave period is critical and which is not.

4.3.2 Floating Vessel

The eigenmodes with the corresponding eigenvectors for the undamped, unballasted vessel are shown in Table 4.2.

The eigenmodes of the vessel together with the RAOs give a good understanding of when and how the vessel is excited by waves. Mode 1 and 2 are dominated by the coupled heave and pitch motions with small contributions from surge. Mode 3 is the dominated by the roll motion of the vessel. Mode 4 and 6 are dominated by the coupled yaw and sway motions of the vessel. Mode 5 is surge motion of the vessel.

The eigenmodes with the corresponding eigenvalues for the coupled system are shown in Table 4.3. The values correspond to a jacket tip position $z = -37.50\ m$, when the

Table 4.2: *Eigenmodes with Corresponding Eigenvectors for the Floating Vessel*

Eigenperiod [s]	**9.87**	**11.19**	**13.93**	**94.53**	**100.01**	**105.51**
Surge	−0.16	−0.07	0.00	0.00	1.00	0.00
Sway	0.00	0.00	0.06	0.85	0.00	0.80
Heave	−0.30	1.00	0.00	0.00	0.00	0.00
Roll	0.00	0.00	1.00	0.02	0.00	−0.03
Pitch	1.00	0.23	0.00	0.00	0.00	0.00
Yaw	0.00	0.00	−0.02	1.00	0.00	−1.00

jacket is just above the foundation piles. The coupled eigenmodes will in the following be compared to the eigenmodes of the jacket and the vessel.

Comparing the eigenmodes of the coupled system with those of the jacket and the vessel the following can be seen. The jacket is easier excited than the vessel and thus most modes are dominated by jacket movements. The eigenperiods of the jacket modes are represented by modes 1, 2, 3, 4, 7, 8 and 12 of the coupled system. The contribution from the vessel for those modes is very small and the eigenperiods of the coupled system only deviate slightly from the jacket alone. There are two modes (2, 4) that are governed by the coupled surge and pitch motions of the jacket, for which the eigenvectors are equal in magnitude but of opposite sign. Mode 5, 6, 9, 10 and 11 get their largest contributions from the jacket, however, with significant contributions from the vessel.Figure 4.3 show how the most relevant eigenmodes of the coupled system which are within the wave spectra change for different jacket positions.

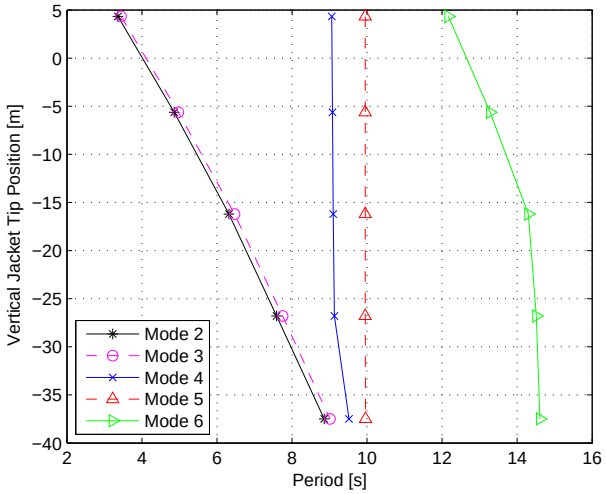

Figure 4.3: *Eigenmodes of the Jacket at Different Vertical Positions for the Coupled System*

The coupled system has 5 modes that have a relevant natural period in regards to the sea states that are investigated in this thesis. Mode 2 and 3 are very similar to those of the jacket. These two modes start with a eigenperiod of 3.4 seconds in air that gradually increases to a period of around 9 seconds before docking.

Table 4.3: *Eigenmodes with Corresponding Eigenvectors for the Coupled System Tip Position z = -37.5 m*

Eigenperiod [s]	**0.99**	**8.86**	**9.01**	**9.52**	**9.96**	**14.61**
Surge (Vessel)	0.00	−0.01	0.00	−0.01	−0.03	0.00
Sway (Vessel)	−0.01	0.00	0.00	0.00	0.00	0.03
Heave (Vessel)	−0.01	−0.03	0.00	−0.02	0.43	0.00
Roll (Vessel)	−0.10	−0.01	−0.06	0.00	−0.01	0.44
Pitch (Vessel)	0.00	0.10	0.00	0.04	0.12	0.00
Yaw (Vessel)	0.00	0.00	0.00	0.00	0.00	0.00
Surge (Jacket)	0.05	0.40	−0.02	−0.41	−0.40	0.02
Sway (Jacket)	0.05	0.05	0.40	0.00	0.01	0.53
Heave (Jacket)	1.00	−0.01	−0.05	−0.01	0.46	0.35
Roll (Jacket)	0.03	0.13	1.00	0.00	−0.01	1.00
Pitch (Jacket)	−0.04	−1.00	0.04	1.00	1.00	0.00
Yaw (Jacket)	0.00	0.01	−0.01	−0.02	−0.02	−0.02
	35.92	**37.77**	**94.28**	**101.10**	**106.62**	**217.29**
Surge (Vessel)	−0.03	0.00	0.17	0.85	0.15	0.00
Sway (Vessel)	0.00	−0.02	0.86	−0.14	0.62	0.00
Heave (Vessel)	0.00	0.00	0.00	0.00	0.00	0.00
Roll (Vessel)	0.00	−0.04	−0.01	0.00	−0.02	0.00
Pitch (Vessel)	0.00	0.00	0.00	0.00	0.00	0.00
Yaw (Vessel)	0.03	0.00	1.00	0.02	−0.81	0.00
Surge (Jacket)	1.00	−0.07	−0.76	1.00	0.91	0.00
Sway (Jacket)	0.06	1.00	0.76	−0.18	1.00	0.00
Heave (Jacket)	0.00	−0.03	−0.01	0.00	−0.02	0.00
Roll (Jacket)	0.04	0.62	0.09	−0.02	0.09	0.00
Pitch (Jacket)	−0.67	0.04	0.09	−0.10	−0.08	0.00
Yaw (Jacket)	0.03	−0.04	0.23	−0.53	−0.73	1.00

Chapter 5

Operational Criteria

To be able to assess under which conditions the safe installation of the jacket substructure is possible, operational criteria need to be defined. These criteria need to be fulfilled in order for the installation to be successful and safe. It can then be checked if all criteria are met for a certain sea state. The criteria that have been established and are considered for installation of the jacket are described in the following. The criteria are (1) the clearance between the jacket in air and the hull of the ship, (2) the successful docking of the jacket leg and the foundation pile, (3) the docking forces that occur during the impact of the jacket leg with the foundation pile and (4) the lift wire tension. The criteria listed below do not necessarily represent a complete list of criteria that need to be met in real life marine operations.

5.1 Clearance

The clearance between the lifted object and the outer hull of the vessel should not fall below 5 m [19]. This operational criteria is crucial for the operation with the floating vessel, when the jacket is still in air and large pendulum motions may occur. The clearance in y-direction will be monitored from the start of the simulation until the jacket legs first enter the water. The pendulum motions of the jacket are reduced once the jacket is partly submerged so that collisions under water are unlikely to occur. The initial distance between the hull of the jack-up vessel and the two jacket legs facing the vessel is 10.5 m. The distance between the hull of the floating vessel and the legs is 12.5 m. This increase in distance is due to the fact, that the submerged weight of the jacket, rather than the dry weight, is counteracted with ballast. When the jacket is in air, the vessel is slightly heeled towards the jacket side. The crane tip and consequently the jacket thus move further out, away from the vessel. The amplitude of the jacket legs y-offset from the initial position caused by both, translation and rotation of the jacket, should therefore not exceed 5.5 m and 7.5 m respectively.

5.2 Successful Docking

The installation can only be successful if the jacket leg (pin) is able to enter the foundation pile (docking cone). Docking is only successful if the horizontal offset between the jacket leg tip and the foundation center is less than 1.1 m, when the jacket leg tip is at the vertical height of the foundation pile entrance. In this case the conical part of the leg tip will hit the foundation pile and the leg will consequently slide into the foundation pile. Once the pile stoppers touch the top of the foundation pile the lowering procedure is finished. In reality, a remotely operated vehicle will be deployed to monitor the jacket motions close to the foundation piles. The winch can be stopped and the substructure left hanging above the foundation piles until a time window opens up, where the vessel and jacket motions are small enough for docking to be successful.

5.3 Docking Forces

Docking forces that occur upon impact of the jacket leg with the foundation pile are restricted by structural limitations. Loads associated with installation operations are variable functional loads that need to be considered in the substructure design [32]. There are, however, no explicit requirements stated in the design guidelines for offshore wind substructures. Instead of giving a strict limitation for the docking force, these will instead be recorded and only be commented if extreme peak values occur.

5.4 Lift Wire Tension

The lift wire tension needs to be carefully monitored and the likelihood of slack and the possibility of snap loads must be assessed. The criteria stated in the DNV guidelines, however, are not applicable for the docking procedure, as they are tailored to the lift-off and landing procedure, rather than uncontrolled slack that can occur during docking of the jacket substructure with the foundation piles. It is therefore only checked if the lift wire tension goes to zero before the jacket rests on the pile stoppers. Furthermore, the maximum lift wire tension that needs to be expected for various sea states is stated.

Chapter 6

Results

6.1 Time Series

Figure 6.1 shows the time series of the jacket motions and the tension in the lift wire for the floating and jack-up vessel. The z-position of the jacket tip shows the different stages and winch speeds of the lowering process. The small difference in the vertical position between the floating and the fixed vessel can be explained with the fact that the floating vessel heels towards the jacket side. The x- and y-position of the jacket tip are given as the offset from the defined, anticipated position that matches the foundation piles. The total offset may not exceed 1.10 meter when the jacket is entering the foundation piles. The time series for the x-offset indicates motions of similar amplitude for the fixed and the floating vessel. The large y-offset of the jacket for the floating vessel can again be explained with the ballasting of the vessel. The y-offset due to waves is small and similar for the fixed and floating vessel. The lift wire tension is dominated by the weigh of the jacket. When the jacket enters the water the lift wire tension is reduced by the buoyancy of the jacket. Once the jacket landed on the foundation piles, the winch is still running and the tension in the wire goes to zero. For the floating vessel small fluctuations in the lift wire tension can be observed due to vertical crane tip motions. The motions of the jacket induced by the waves have a very small effect on the lift wire tension for both, the fixed and the floating vessel.

When a floating vessel is used for the substructure installation the vessel motions will influence the jacket motions. For the smallest investigated wave period of 5 seconds the vessel motions are very small, as indicated by the response amplitude operators of the vessel. For larger wave periods the vessel motions become larger and can have a significant impact on the marine operation. It is thus wise to look at the vessel motions too. Figure 6.2 shows the vessel motions for oblique seas and a significant wave period of 12 seconds. The observed vessel motions are in accordance with the RAOs. The surge, heave and pitch motions are clearly excited by the waves and show a significant amplitude. The sway and roll motions of the vessel are very small, as waves of 12 seconds are just outside the resonance area. Larger periods that would excite the roll and sway motions of the

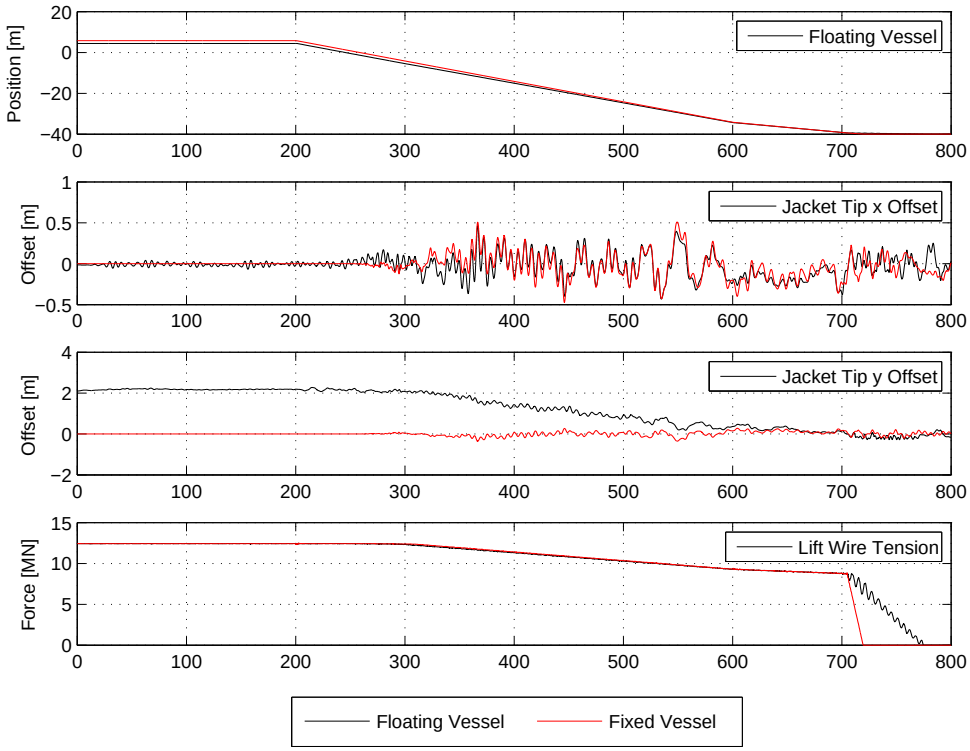

Figure 6.1: *Jacket Motions and Lift Wire Tension for Jack-up Vessel, Hs = 2 m, Tp = 5 s, Dir = 150 deg., Seed No. 1*

vessel are not investigated in this thesis. Once the load of the jacket is taken from the crane small sway motions can be observed. The initial roll angle is due to the ballasting of the vessel, as described in Section 4.3.2. The ballast of the vessel is chosen to allow for an even keel when the jacket is about to enter the foundation piles. The heeling of the vessel during other phases of the installation is tolerated. The pitch motion of the vessel was not balanced with ballast but the vessel position was adjusted so that the jacket is vertically in line with the foundation piles if the vessel is pitched 0.13 degrees.

Figure 6.3 shows the corresponding time series for the floating and jack-up vessel for a larger wave period of 10 seconds. For the jack-up vessel no significant difference to the smaller wave period can be observed. The unsteady lift wire tension is due to the fact that the conical part of the jacket leg hits the foundation pile during docking instead of entering the foundation pile completely centered. Docking is, however, successful. For the floating vessel large pendulum motions of the jacket in air can be observed that are damped out, once the jacket enters the water. These pendulum motions can reach extremely large amplitudes, so that the required clearance between vessel hull and lifted object in some cases cannot be guaranteed. The use of tugger wires is thus strongly recommended and should be part of further work. In water the jacket motions are very small and the amplitude of the motions varies in each simulation depending on the surface elevation. The lift wire tension is again dominated by the weight of the jacket until docking occurs.

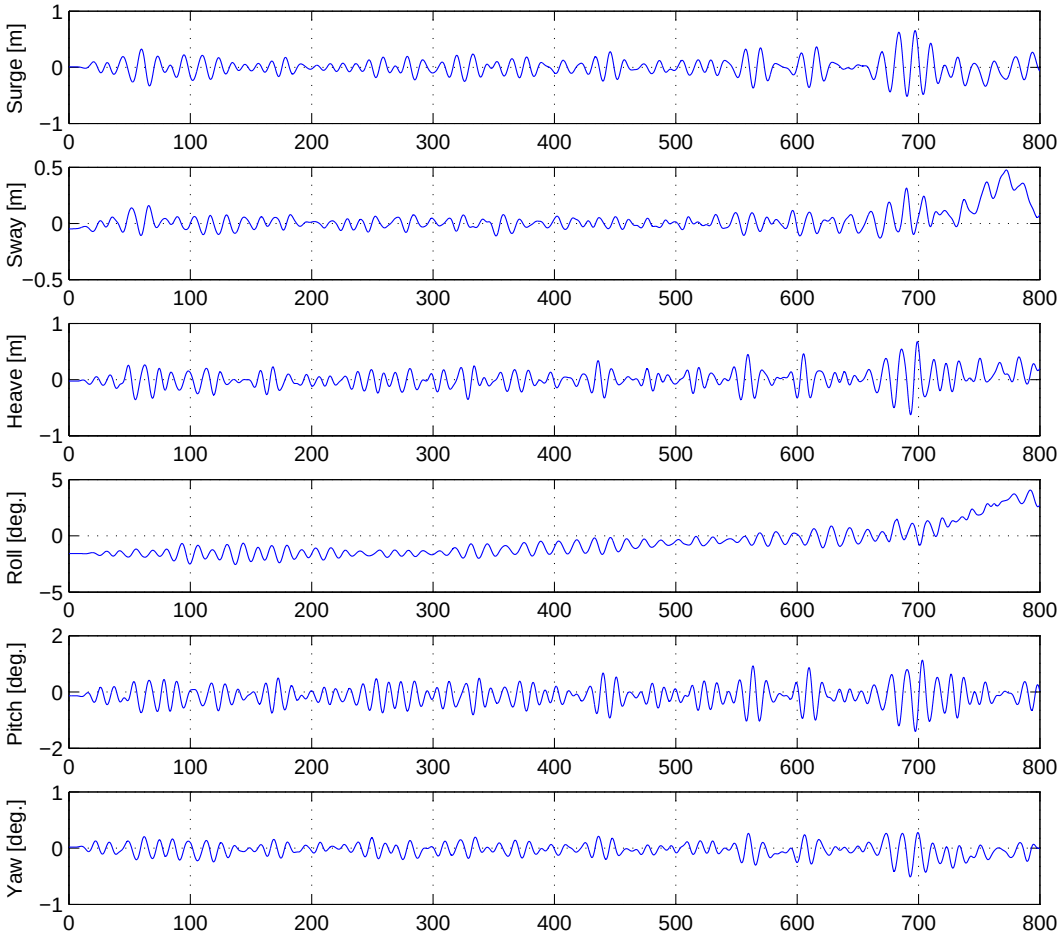

Figure 6.2: *Floating Vessel Motions for Hs = 2 m, Tp = 12 s, Dir = 150 deg., Seed No. 1*

During docking the lift wire tension varies depending on if and how the impact between jacket and foundation pile occurs. After docking the lift wire tension of the jack-up vessel goes to zero once the jacket has landed and the winch payed out enough wire for it to go slack. For the floating vessel the vertical crane tip motions and the fact that the vessel heels to the opposite side once the jacket rests on the pile stoppers, delay the successful completion of the installation.

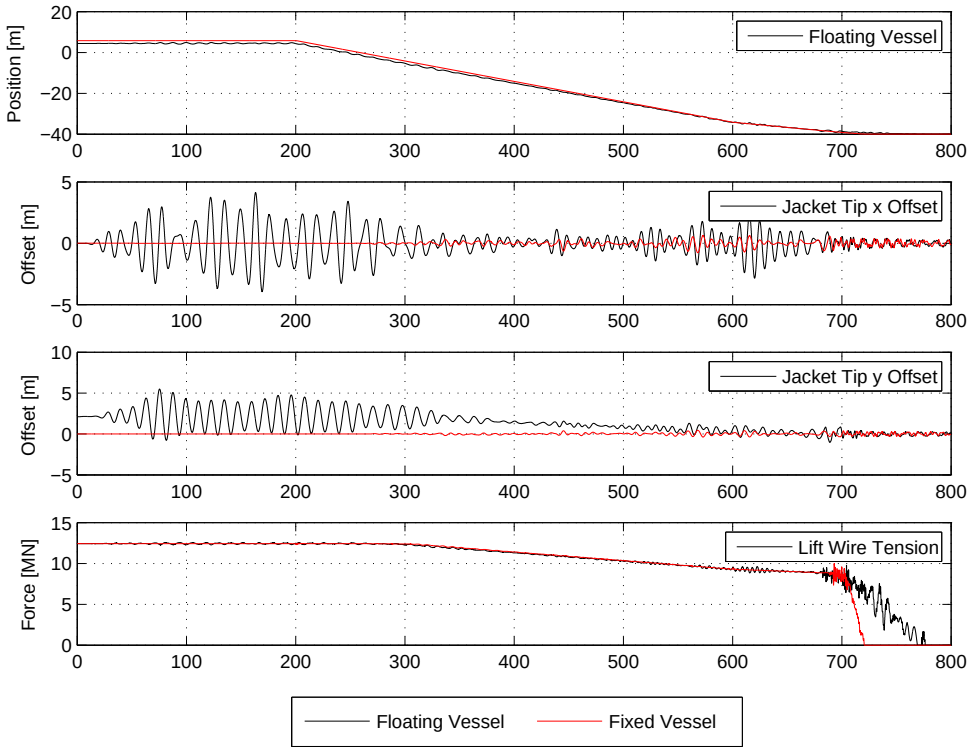

Figure 6.3: *Jacket Motions and Lift Wire Tension for Floating Vessel, Hs = 2 m, Tp = 10 s, Dir = 150 deg., Seed No. 1*

6.2 Clearance

The clearance between the two legs facing the vessel and the ship hull was investigated for all sea states. Figure 6.4 shows the rate of seeds with sufficient clearance. In head seas the pendulum motions of the jacket stay small even for larger wave periods. For oblique waves the pendulum motions are increased significantly and the clearance requirements are not always met for wave periods of 11 and 12 seconds.

In real offshore lifting operations those large pendulum motion cannot occur since control measures such as tugger lines need to be implemented. Common offshore guidelines require that "the lifted object shall be adequately controlled in order to avoid any significant and undesirable yawing and/or pendulum motions" [33].

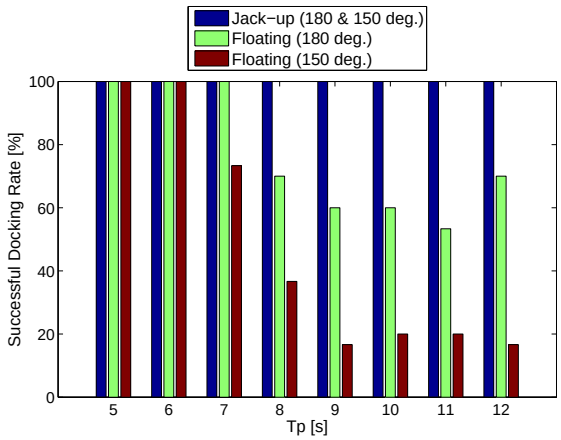

Figure 6.4: *Rate of Sufficient Clearance for the Jack-up and Floating Vessel at Wave Dir. 180 and 150 deg.*

6.3 Successful Docking

The results showed that for all simulations docking forces were calculated for all 4 piles. According to the theory manual for SIMO docking forces are only recorded if the entry into the cylinder opening is successful and that they are zero until this is the case [6]. Upon closer investigation of the individual time series it was found, that for certain sea states large jacket displacements are present even when the jacket is supposed to be already inside the foundation piles. Docking forces were also recorded for this time period. It was therefore found that the model for docking cones in SIMO will indicate a successful docking even when this is not the case. The two failure cases described in the following will give docking forces in SIMO, although in reality, the jackets would not enter the foundation piles.

Failure Case 1 In the first failure case the initial docking, the first time the tip of the jacket leg enters the foundation pile, will be successful (1). SIMO from now on calculates docking forces. Due to the vertical motions from the jacket it can happen that the jacket leaves the foundation piles again (2). If the jacket now lowers again, this time next to

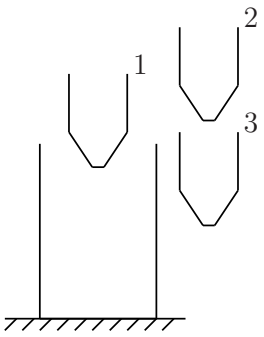

Figure 6.5: *Failure Case 1*

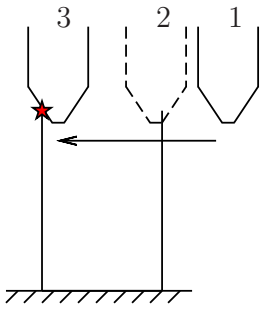

Figure 6.6: *Failure Case 2*

rather than into the foundation pile SIMO will still calculate docking forces (3). Figure 6.7 shows the time series of a simulation where failure case 1 occurs and docking subsequently is not successful. The time series of the vertical jacket leg tip position, its horizontal offset and the docking force are shown. The vertical position of the foundation pile opening and the maximum allowable horizontal offset are indicated by the red horizontal lines. The first docking attempt (around T = 670 s) is successful. The offset is within the limits when the jacket leg enters the foundation piles and docking forces are from now on recorded. Due to the vertical crane tip motions the jacket leaves the foundation pile again. The next times the jacket leg reaches the same vertical level than the foundation pile opening the horizontal offset is too large for docking to be successful, as can be easily seen between T = 690-710 s. Despite the fact that the jacket leg is far beside the foundation pile, peak docking forces occur, when the jacket tip reaches the vertical level of the foundation pile opening.

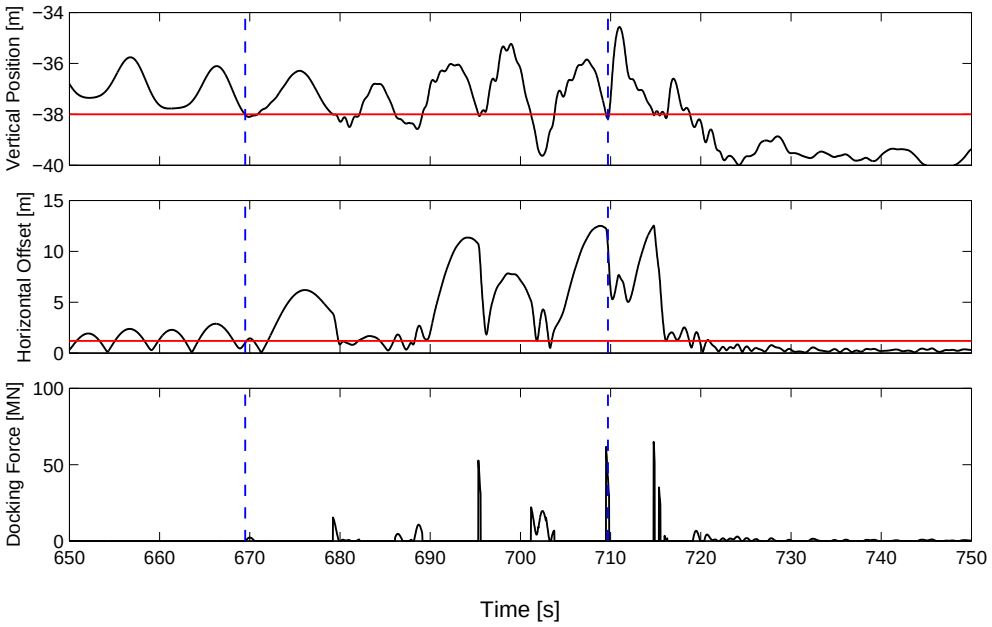

Figure 6.7: *Failure Case 1. Leg Position and Docking Force for Hs = 2 m, Tp = 9 s, Wave Dir. = 150 deg., Seed 12, Leg 1*

Failure Case 2 In the second failure case the first docking attempts are not successful (1). As the foundation piles are only represented by docking cones rather than a physical body, the jacket leg can enter the docking cone from the outside (2). Once the jacket leg penetrated the docking cone and hits the inner wall of the foundation pile, SIMO starts to record docking forces (3). Figure 6.8 shows the time series of a simulation where failure case 2 occurs and docking subsequently is not successful. The time frame where the failure can be seen is contained within vertical lines. The jacket leg is at the same vertical level than the opening of the foundation pile. The offset of the leg, however, is too large for docking to be successful, meaning that the jacket leg is next to rather than in

the foundation pile. No docking force is generated at the beginning. The horizontal offset now decreases and reaches an acceptable limit indicating that the jacket leg is now inside the foundation pile. The jacket leg has penetrated the wall of the foundation pile. After that the offset increases again and once the leg hits the inside wall of the foundation pile docking forces are recorded. After that large vertical and horizontal jacket motions are observed that are governed by peak impact forces whenever the leg tip reaches the vertical level of the pile opening, regardless of whether it is in the boundaries of the foundation pile opening or not.

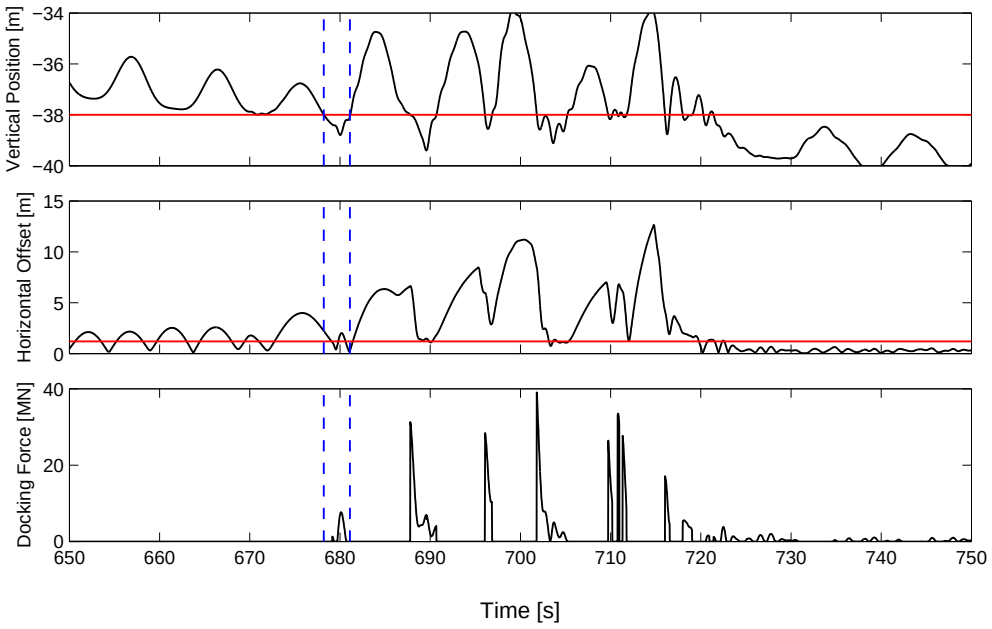

Figure 6.8: *Failure Case 2. Leg Position and Docking Force for Hs = 2 m, Tp = 9 s, Wave Dir. = 150 deg., Seed 12, Leg 4*

To identify the simulations, where the landing of the jacket inside the foundation piles is actually successful the following condition was implemented and checked for.

1. For each leg determine the time steps at which the jacket leg tip enters the foundation piles.
2. Calculate the horizontal offset of the jacket leg tip in respect to the center of the foundation pile.
3. If the horizontal offset during any of the entrance cases, for any of the legs, exceeds the foundation pile radius the installation is not successful.

Seeds for which the installation is not successful are excluded in the further investigation of the docking forces and the lift wire tension during docking. Figure 6.9 shows the number of seeds for which the installation of the jacket succeeds.

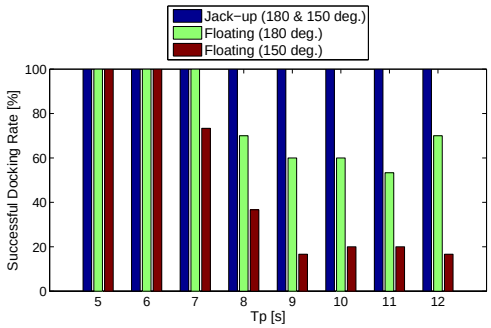

Figure 6.9: *Rate of Successful Docking for the Jack-up and Floating Vessel at Wave Dir. 180 and 150 deg.*

For the jack-up vessel the jacket structure enters the foundation piles at all investigated sea states. For the floating vessel installation is always successful for wave periods 5-7 and 5-6 seconds for 0 deg. and 150 deg. wave direction respectively. For larger investigated wave periods the floating vessel has a success rate of around 60 percent in head seas and less than 20 percent in oblique waves. Successful docking is identified as the most critical operational criteria. To check up to which extend the obtained results from 30 seeds is representative one of the critical sea states, namely a wave period of 9 seconds is run for 120 seeds.

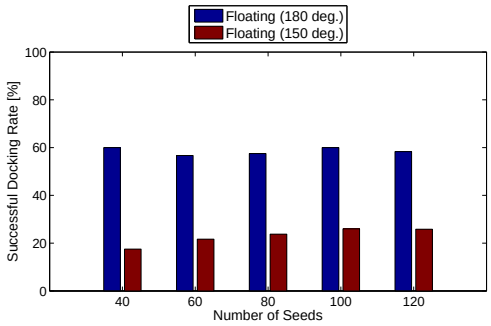

Figure 6.10: *Rate of Successful Docking for the Floating Vessel for Different Number of Seeds*

As can be seen in Figure 6.10 the success rate in head seas stay around 60 percent. For 30 seeds the success rate was 60 percent, while for 120 seeds it reduces to 58 percent. For oblique waves at coming from 150 degrees the success rate based on 30 seeds is 17 percent, while for 120 seeds it is 25 percent. Based on those findings it can be concluded that the number of seeds run in this thesis might be insufficient for representative results.

6.4 Docking Forces

Figure 6.11 shows the mean values of the maximum docking forces from all successful seeds for different wave periods and foundation piles at head seas (wave dir = 180 deg.). In case of the jack-up vessel a steady increase in docking forces at all four pile locations can be observed. The magnitude of the docking force stays very small and does not exceed 1 MN. No peaks in docking forces are observed for wave periods close to the natural period of the jacket's eigenmodes. Furthermore, no significant difference between the individual pile locations can be identified. For the floating vessel the docking forces are slightly above those of the jack-up vessel for wave periods of 5 and 6 seconds. From 6 to 8 seconds the docking forces increase significantly and reach magnitudes twice as large as those of the jack-up vessel.

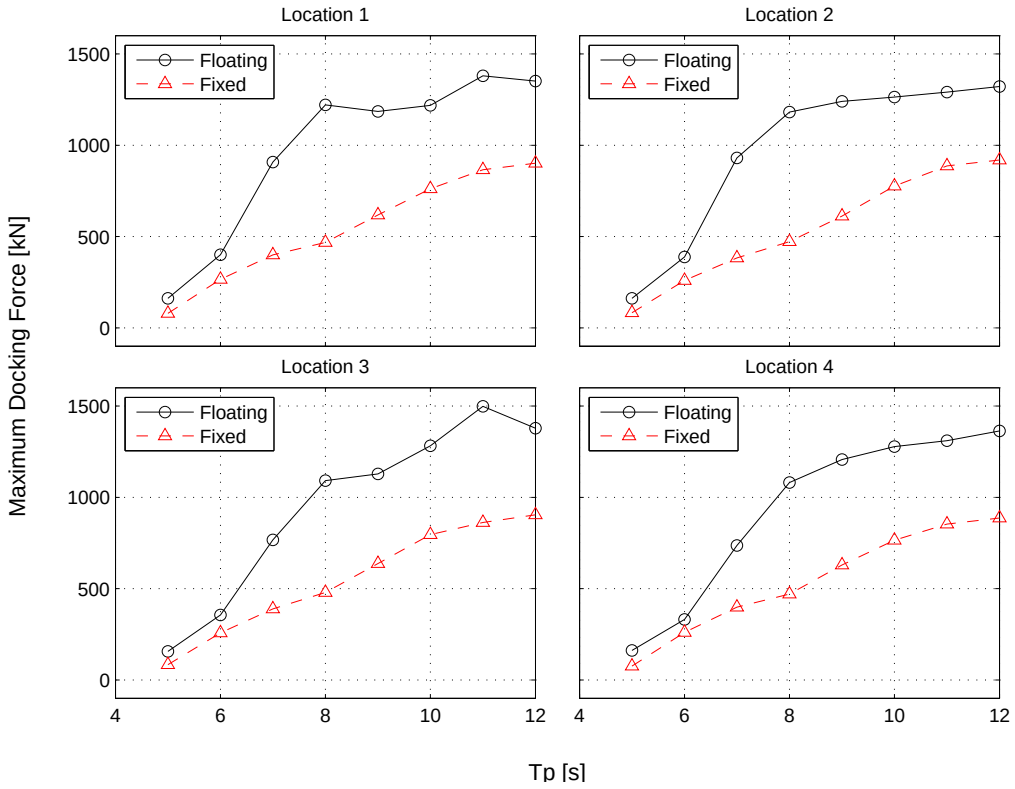

Figure 6.11: *Mean Maximum Docking Forces as Function of Wave Period Tp for Hs = 2 m, Wave Dir. = 180 deg.*

Figure 6.12 shows the mean maximum docking forces based on 30 seeds for different wave periods and foundation piles at oblique seas (wave dir = 150 deg.). For the jack-up vessel a small increase in the docking forces can be observed compared to head seas. This can be explained with the larger lateral area of the jacket that is now exposed to waves. The overall docking force stays small and no peaks indicating resonance are observed. For the floating vessel the docking forces in oblique waves are in a similar magnitude than for head seas. Judging from the mean maximum docking forces it can be concluded that if docking is successful, the magnitude of the docking force is not governed by the wave direction but rather by the wave period.

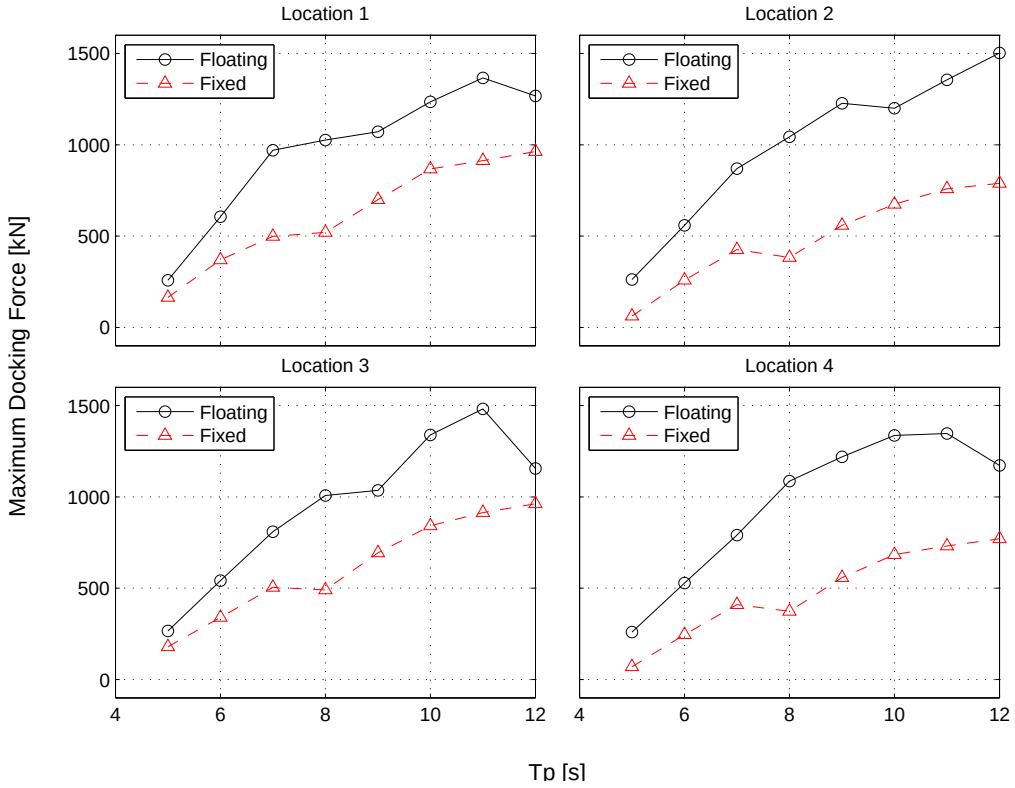

Figure 6.12: *Mean Maximum Docking Forces as Function of Wave Period Tp for Hs = 2 m, Wave Dir. = 150 deg.*

To get a statistical representation of the docking forces it is attempted to fit a cumulative distribution function to the maximum docking forces of each seed. The two extreme value distributions that are fitted are the Gumbel and Weibull distribution, using maximum likelihood fitting. The fits are based on the maximum docking force of each simulation regardless of the leg position it occurred at. The Gumbel distribution is commonly used for short, non stationary processes and forces that are dominated by sudden impact loads. Figures 6.13 and 6.14 show Gumbel distribution for the fixed and floating vessel at a wave period of 5 seconds. It can be seen that the lower and upper end of the distribution does not agree with the data. The Weibull distribution is used for longer, stationary processes with relatively linear force distribution [34]. Figures 6.17 and 6.18 show a Weibull fit for the docking forces occurring at small wave periods for the fixed and floating vessel respectively. For the fixed vessel the Weibull distribution fails to represent the lower end of the docking forces, however, unlike the Gumbel distribution represents the upper end very well. The docking forces of the floating vessel match the Weibull distribution very well, such that it could be used for further statistical treatment of the results. For a larger wave period of 12 seconds the Gumbel distribution seems to be a better match as can be seen in Figures 6.15 and 6.16. The lower end does not fit the distribution, however, the upper and the larger forces seem to be represented well. For larger wave periods the results of both, the fixed ad the floating vessel agree well with the Weibull distribution.

The maximum docking force that has a 10 percent probability of exceedance can now be calculated. Although this probability is not explicitly mentioned in any guidelines it is

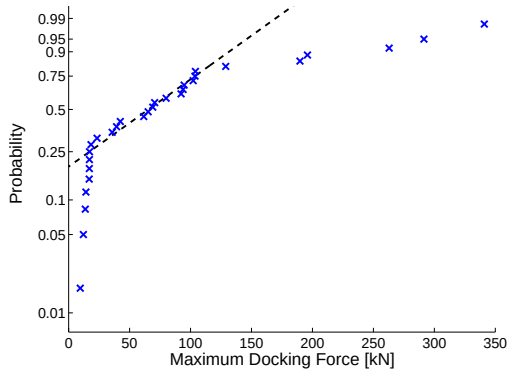

Figure 6.13: *Gumbel Distribution for Fixed Vessel, Tp = 5 s., Wave Dir = 180 deg.*

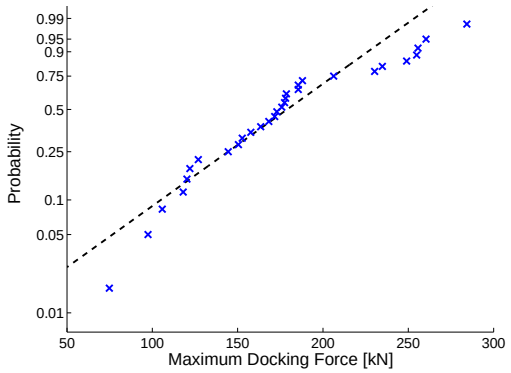

Figure 6.14: *Gumbel Distribution for Floating Vessel, Tp = 5 s., Wave Dir = 180 deg.*

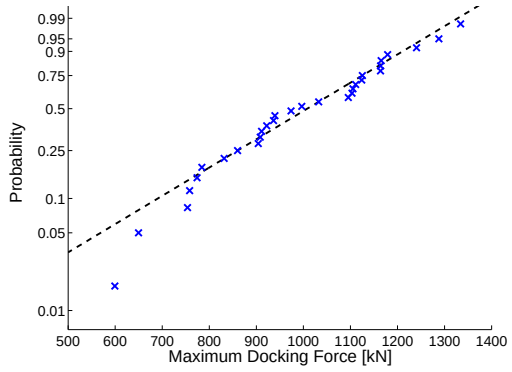

Figure 6.15: *Gumbel Distribution for Fixed Vessel, Tp = 12 s., Wave Dir = 180 deg.*

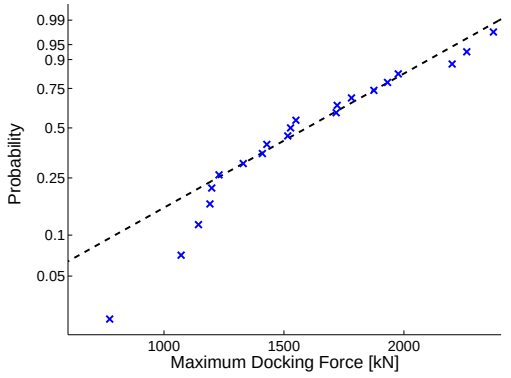

Figure 6.16: *Gumbel Distribution for Floating Vessel, Tp = 12 s., Wave Dir = 180 deg.*

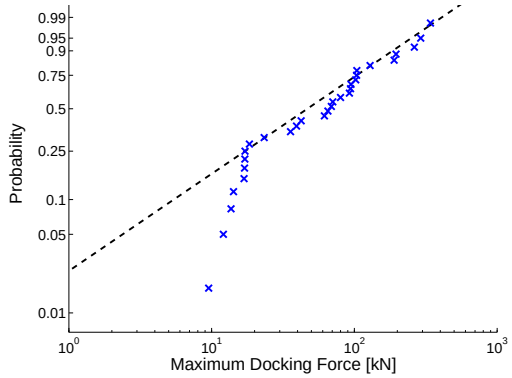

Figure 6.17: *Weibull Distribution for Fixed Vessel, Tp = 5 s., Wave Dir = 180 deg.*

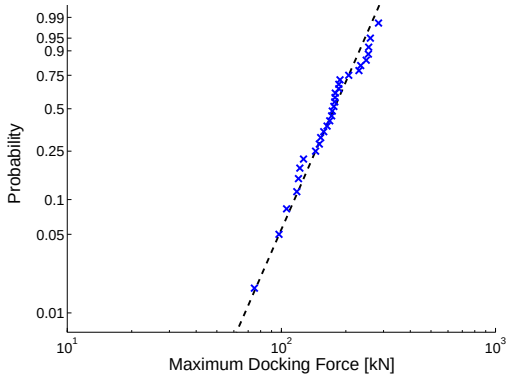

Figure 6.18: *Weibull Distribution for Floating Vessel, Tp = 5 s., Wave Dir = 180 deg.*

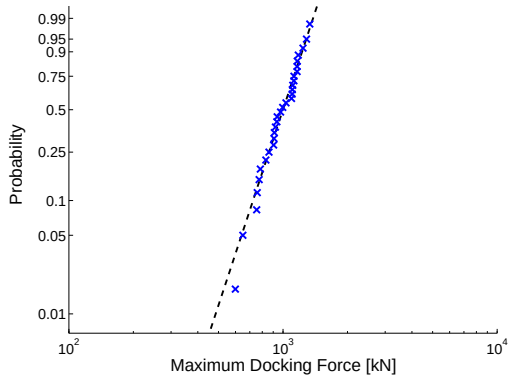

Figure 6.19: *Weibull Distribution for Fixed Vessel, Tp = 12 s., Wave Dir = 180 deg.*

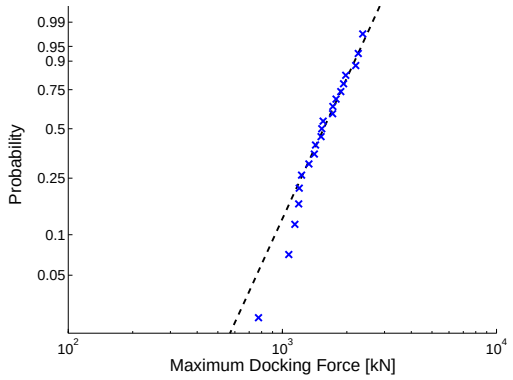

Figure 6.20: *Weibull Distribution for Floating Vessel, Tp = 12 s., Wave Dir = 180 deg.*

often used in the industry as an orientation. Figure 6.21 shows those forces, regardless of the individual pile position. The maximum docking forces with a 10 percent change of exceedance are, as expected, larger than the previously stated mean values. The shape of the curve is similar to that of the mean forces. The largest docking force likely to occur at a wave period of 12 seconds using the floating vessel is approximately twice as large as the one for the jack-up vessel.

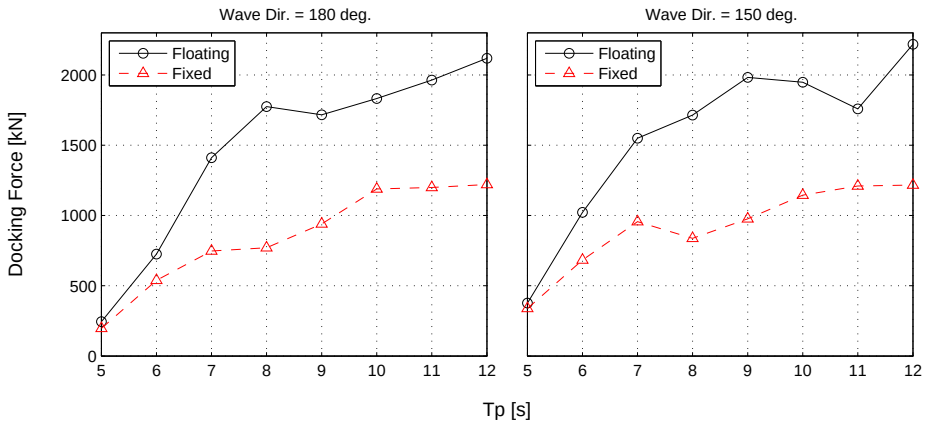

Figure 6.21: *Docking Forces with a 10 Percent Probability of Exceedance*

Regarding the docking forces in general it should be noted, that the forces calculated in SIMO are not suited to derive and structural requirements of the jacket legs or foundation piles. Docking cones are modeled as spring damper systems and the restoring force gradually increases between the cross sections specified. The actual impact is therefore not correctly represented in the model.

6.5 Lift Wire Tension

The lift wire tension will be investigated for 2 phases of the lowering operation. When the jacket is fully in air and during docking of the jacket into the foundation piles. The phase in air is from the first time step until the jacket tip center point reaches MSL ($z = 0$). The docking phase starts from the time step when docking forces first occur at any of the 4 foundation piles until the last time step. The lowering phase of the jacket is not critical for the lift wire tension. The lift wire tension reduces steadily due to increasing buoyancy of the jacket and there are no significant vertical wave excitation forces acting on the jacket. The reduction of the winch speed from 0.1 m/s to 0.05 m/s gives only small additional lift wire tension. Figure 6.22 shows the lift wire tension in air for head and oblique seas. For the fixed vessel the lift wire tension is constant, equal to the dry weight of the jacket. For the floating vessel the lift wire tension increases for larger wave periods. This can be explained with the increased vessel motions and thus pendulum motions of the jacket in air. Compared to the dry weight of the jacket, the increase in lift wire tension is small and accounts for an increase of merely one percent for the largest investigated wave periods.

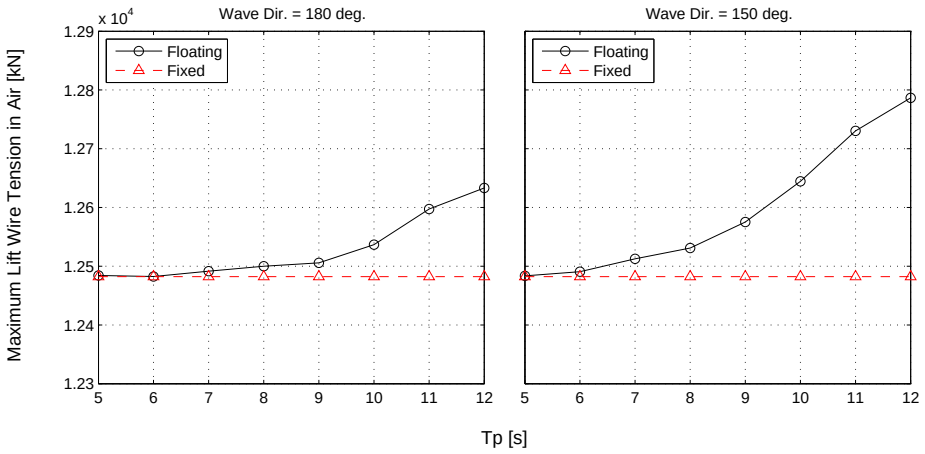

Figure 6.22: *Mean Maximum Lift Wire Tension in Air as Function of Wave Period for Hs = 2 m, Wave Dir. = 180 and 150 deg.*

Figure 6.23 shows the lift wire tension during docking for head and oblique seas. The mass of the jacket at that point has reduced to 960 tonnes and the lift wire tensions without any effects from docking should thus be around 8900 kN. The very small lift wire tension for the fixed vessel in head seas in 5 second waves cannot be explained. The remaining results for the fixed vessel are around the submerged weight of the jacket. This would indicate that the jacket enters the foundation piles without any major docking, where the jacket rests on the foundation piles before it slips in. For the floating vessel the lift wire tension can be larger than the static weight of the submerged jacket. This phenomenon can occur when the jacket already entered all four foundation piles. If the vessel now moves the jacket is restrained from following those motions. The distance between crane tip and hook point increases and thus does the tension in the lift wire. Another possibility

is, that the jacket leg temporarily rests on the foundation pile and the tension in the lift wire is reduced. When the jacket then slides into the foundation pile, the tension increases abruptly. The tension in the lift wire during docking stays below the tension in air and is thus not a critical design factor.

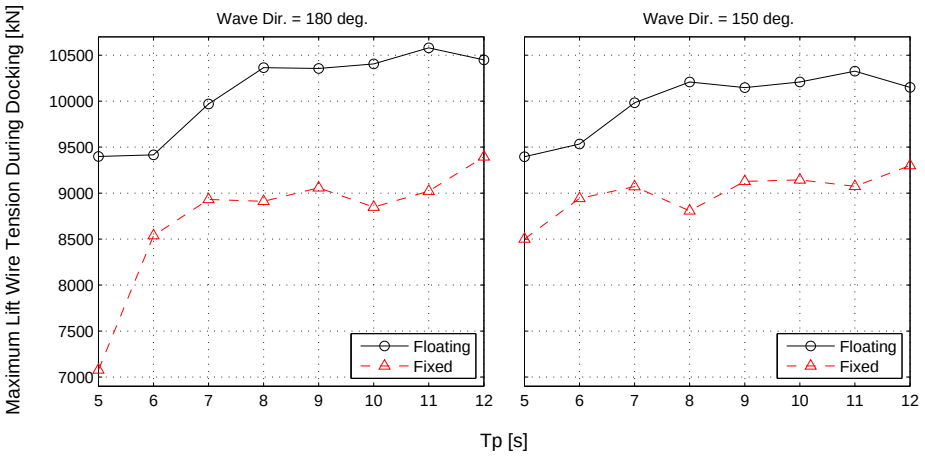

Figure 6.23: *Mean Maximum Lift Wire Tension during Docking as Function of Wave Period for Hs = 2 m, Wave Dir. = 180 and 150 deg.*

Far more interesting is the minimum lift wire tension that occurs during docking, shown in Figure 6.24. It helps to identify the possibility of slack and the margin that is left before the lift wire goes slack. The time period investigated starts when the first leg reaches the opening of the foundation pile until any of the legs is 1.6 m inside the foundation pile. The conical section of the foundation pile is 1.4 m long. It is therefore ensured that the jacket can no longer rest on the foundation pile after that period. Furthermore there is no effect from the fender plates at that point. The previously found results can be confirmed. When a jack-up vessel is used the jacket enters the foundation piles more smoothly and the lift wire tension is less effected by any major docking events. The lift wire tension therefore is close to the weight of the submerged jacket. If a floating vessel is used the average minimum lift wire tension decreases for increasing wave periods. This is due to the fact, that the jacket motions become larger and the jacket legs will therefore slide into the foundation piles on the conical section rather enter the piles directly. The jacket then rests on the conical section of the legs. The foundation pile take up some of the vertical force and the lift wire tension is reduced.

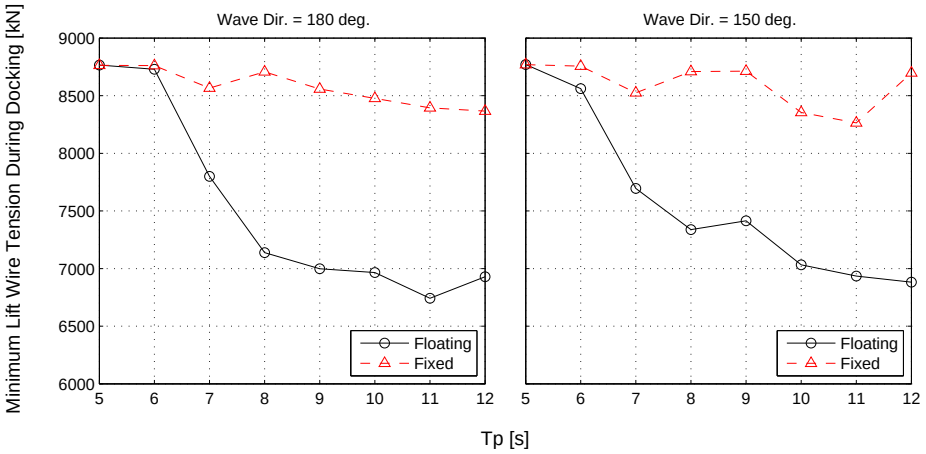

Figure 6.24: *Mean Minimum Lift Wire Tension during Docking as Function of Wave Period for Hs = 2 m, Wave Dir. = 180 and 150 deg.*

6.6 Landing Forces

Although there is no formal operational criteria defined for the landing forces between jacket pile stoppers and foundation piles the forces are presented in the following. The mean maximum landing forces for head sea conditions are shown in Figure 6.25. For the fixed vessel the landing forces increase with increasing wave period. Since the crane tip is fixed and there are not motions from the vessel, the larger motions are solely due to the larger jacket motions. There is no significant difference between the four legs. The landing forces that occur when a floating vessel is used are smaller than those of the fixed vessel for small wave periods of 5 to 7 seconds. This phenomenon needs further investigation, however it could be due to the fact that the vessel is ballasted for the docking condition. After docking the jacket is lowered into the foundation piles and the weight of the jacket thus continues to decrease. The vessel than heels towards the opposite site. This effect partly counteracts the lowering of the jacket with the winch and leads to a softer landing. For wave periods of 8 to 10 seconds the landing forces are larger than those of the fixed vessel. This can be explained with the larger vertical crane tip motions that add to the total vertical impact velocity. The fact that the recorded landing forces for the largest investigated wave periods are larger for the fixed vessel cannot be explained and required further investigation. Furthermore, the landing forces of the floating vessel seem to decrease for wave periods larger than 11 seconds.

The mean maximum landing forces for oblique sea conditions are shown in Figure 6.26. There is a distinct difference between pile location 1 and 3 compared to location 2 and 4. Location 1 and 3 are the diagonal pair of legs that is in the wave direction, whereas location 2 and 4 are almost normal to the wave direction (see Figure 3.6). At small wave periods the landing forces are equally distributed among the four piles. For wave periods larger than 7 seconds pile location 2 and 4 see a steep increase in landing forces, with the fixed vessel showing larger forces for waves periods larger than 10 seconds. Pile location 1 and 3 show a steady increase of the landing forces, with the fixed vessel being below the floating vessel. For both directions and both vessel types in can be observed that the total

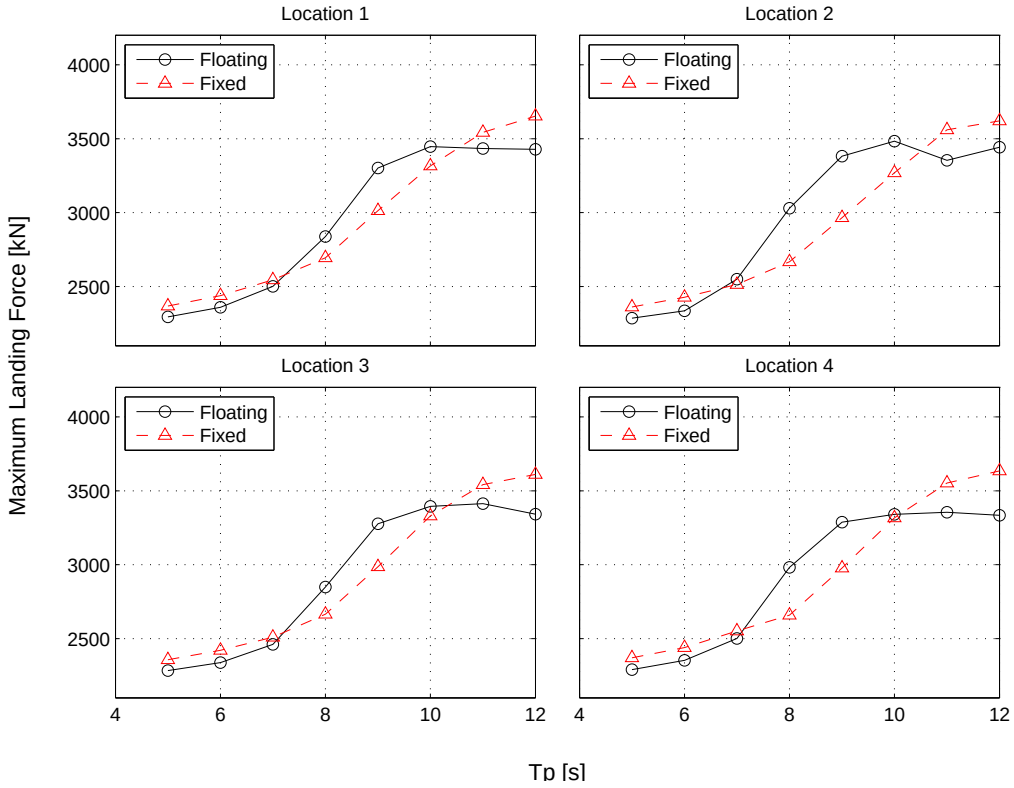

Figure 6.25: *Mean Maximum Landing Forces as Function of Wave Period Tp for Hs = 2 m, Wave Dir. = 180 deg.*

landing force as sum of the 4 individual piles equals the same. The total landing force is around 9.5 MN at a wave period of 5 seconds, approximately equal to the weight of the jacket. It then increases to roughly 14 MN at a wave period of 12 seconds. The landing forces obtained in SIMO should not be used as a guideline for any structural design on the pile stoppers. First, as for the docking cones, the impact between pile stoppers and foundation piles does not represent reality as the stiffness is not as high as it should be. Second, a point fender is used to represent the circular pile stopper. The main purpose of the fender plates is to provide a vertical barrier at the bottom that prevents the jacket from sinking into the seabed.

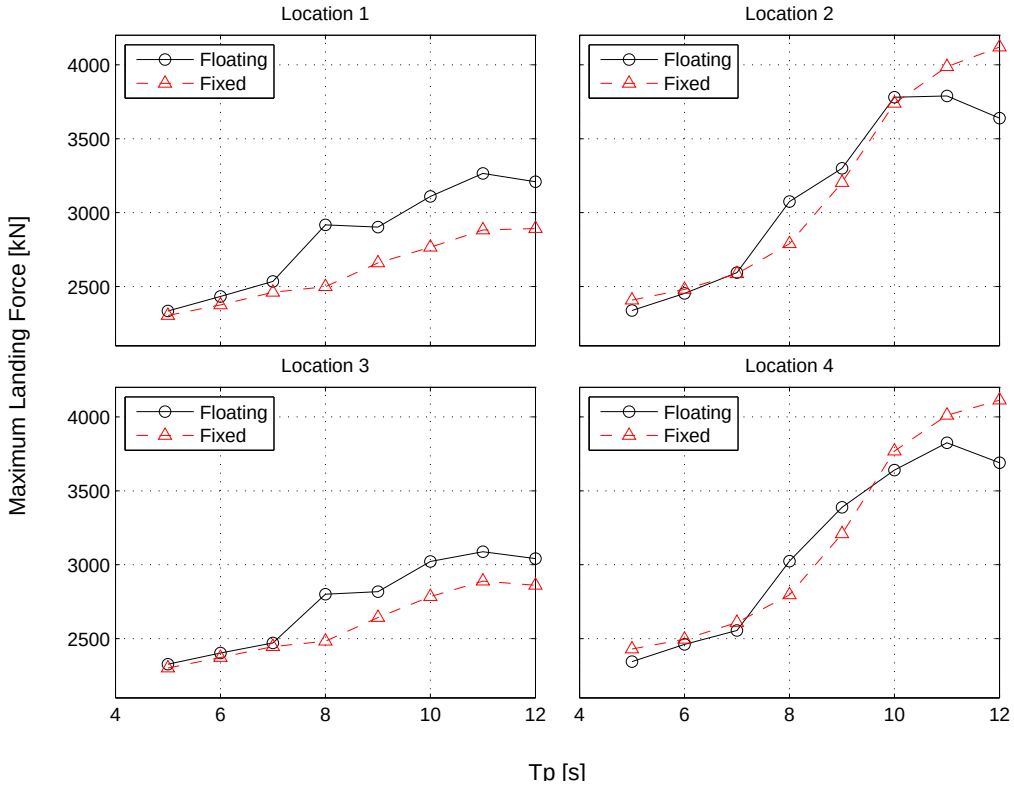

Figure 6.26: *Mean Maximum Landing Forces as Function of Wave Period Tp for Hs = 2 m, Wave Dir. = 150 deg.*

6.7 Workability Analysis

Based on the defined operational criteria and the results that are obtained from the numerical simulations, a workability analysis can be performed to identify the sea states suitable for the installation of the jacket. The operational criteria are listed in chronological order in which they take place during the installation. For the jack-up vessel all simulations resulted in a successful installation of the jacket. The jack-up vessel is therefore not shown in the following tables. If a seed fails a criterion it is not considered for the following conditions as the operation is already considered failed. Table 6.1 shows the overall success rate for the floating vessel in head seas. The pitch motions of the vessel excite a pendulum motion of the jacket in x-direction. Although the pendulum motions can be significant, they are not restricted by any clearance criteria. There is sufficient clearance between the jacket and the vessel hull for all investigated sea states. In order to assure successful docking the tolerance for the jacket motions is considerably less compared to clearance in air. For larger wave periods the vessel's pitch motion and the wave forces acting on the jacket result in too large jacket offset. Subsequently docking is not always successful. When docking is successful the forces that do occur are limited and are not expected to be a limiting factor, provided that the jacket leg is designed accordingly. The lift wire tension does not go to zero before landing of the jacket is completed.

Table 6.2 shows the overall success for the floating vessel in oblique seas. The roll motions of the vessel lead to pendulum motions of the jacket in y-direction that, for large periods,

Table 6.1: *Overall Success Rate in % for Hs = 2 m, Wave Dir. = 180 deg.*

Wave Period [s]	**5**	**6**	**7**	**8**	**9**	**10**	**11**	**12**
Clearance	100	100	100	100	100	100	100	100
Successful Docking	100	100	100	70	60	60	53	70
Docking Force	100	100	100	70	60	60	53	70
Lift Wire Tension	100	100	100	70	60	60	53	70
Total	100	100	100	70	60	60	53	70

do not meet the clearance criterion. Docking becomes increasingly challenging for larger wave periods and can only be guaranteed for wave periods in which the vessel is not noticeably affected by waves. If docking is successful the forces that do occur are assumed to be of minor relevance for the marine operation (not the structural design). The lift wire tension does not go to zero and there is thus no slack in the line before the lowering operation is completed.

Table 6.2: *Overall Success Rate in % for Hs = 2 m, Wave Dir. = 150 deg.*

Wave Period [s]	**5**	**6**	**7**	**8**	**9**	**10**	**11**	**12**
Clearance	100	100	100	100	100	100	87	80
Successful Docking	100	100	73	37	17	20	20	17
Docking Force	100	100	73	37	17	20	20	17
Lift Wire Tension	100	100	73	37	17	20	20	17
Total	100	100	73	37	17	20	20	17

The following can be concluded from the investigation of the suitability of the two vessel types in different sea states. While in head seas the floating vessel proofs to be a good alternative to the jack-up vessel in smaller wave periods, it starts to show its disadvantages for larger wave periods where vessel motions start to be an important factor. With overall success rates of just above 50 percent the floating vessel is no longer an alternative to the jack-up vessel and the time that is saved by the fact that the vessel does not need to jack-up at each turbine location does not make up for the greatly reduced weather window. If the waves start to hit the vessel from an angle the vessel motions get larger and hence does the disadvantages compared to the jack-up vessel. The overall success rate drops below 20 percent for the most critical sea states that are in range of the eigenperiods of the coupled system and the excitation period of the vessel motions.

Chapter 7

Conclusion and Further Work

7.1 Conclusion

This master thesis examined the installation of an offshore wind jacket substructure designed for a 10 MW turbine and the relative importance of the different wave force components that act on the jacket members. The suitability of both, a jack-up vessel and a floating vessel were investigated for different irregular sea states. A numerical model was set-up in SIMO consisting of the vessel, the jacket, the connection between them with a lift wire and the foundation piles comprised of docking cones and fender plates. Time domain simulations of lowering and landing processes were carried out for a total of 8 different wave periods and 2 different wave directions. Operational criteria for the clearance between jacket and ship hull in air, successful docking and resulting docking forces and lift wire tension were defined and compared with the results. Based on the simulation results and the operational criteria a workability analysis was performed and recommendation for the usage of the vessel types given.
When a floating installation vessel is utilized, the pendulum motions of the jacket in air can be significant at large wave periods due to the vessel's motions. The usage of tugger wires to control the jacket is therefore highly recommended and required by classification societies. For a fixed jack-up vessel there are no jacket motions and thus the clearance between jacket and vessel hull is not an issue. The docking of the jacket legs into the foundation piles was identified as the most critical part of the operation. Only a small tolerance exists for the jacket motions in order for the legs to enter the foundation piles. The jack-up vessel was capable of installing the jacket at all investigated sea states. A possible error was found in SIMO, that indicates successful docking of the jacket into the foundation piles, although, upon closer investigation of the time series, this does not seem to be the case. This issue was discovered at a very late stage of the thesis and required programming of an own post-processor that judges whether or not the jacket enters. The wave forces acting on the substructure only cause minor jacket motions that do not compromise the operation. Using a floating installation vessel for the installation proofed to be challenging. The coupled motions between vessel and jacket led to large

jacket motions and the success rate for the docking was very small for wave periods that fall in the range of the eigenmodes of the coupled system. If docking is successful the impact forces that occur are predictable. This is due to the fact, that docking only occurs if the jacket motions are not too large and consequently the velocity of the jacket too. The vertical velocity of the jacket during impact did not give any significant problems. The minimum and maximum lift wire tension during docking was measured but no significant restrictions could be identified that arise from the tension in the lift wire. The maximum lift wire tension during docking with the submerged jacket suspended from the crane is less than the wire tension in air that is approximately equal to the dry weight of the jacket. During docking the jacket can hit the foundation piles. The jacket then rests on the foundation piles that take up some weight of the jacket and the tension in the lift wire is reduced. There does, however, remain enough tension to prevent the lift wire from going slack.

The overall installation procedure proofed to be very difficult to analyze. The fact, that the foundation piles are at the same vertical level adds additional uncertainties since it cannot be clearly determined, which jacket leg enters its corresponding foundation pile first. According to DNV guidelines, "a passive docking system should be designed with a primary and a secondary docking pile, i.e. engaging one docking pile at a time" [35]. A passive docking system is a system that does not require outside intervention from people or hydraulics. In this thesis, however, the planned design anticipated for the EU Mermaid project was used. The docking forces were matched with Weibull distributions and a satisfactory result was achieved. The master thesis gave a good understanding of the challenges that need to be addressed during the numerical modeling of marine operations. The lack of project data resulted in a variety of assumptions that affect the results. Especially the numerical model of the docking cones and fender plates is mainly based on assumptions. A detailed review of a number of guidelines was required to get an understanding of what factors and parameters matter for the installation. A close supervision of a company that deals with offshore installations would have been beneficial to the outcome of this thesis.

7.2 Further Work

A variety of simplifications were made in this master thesis, partly due to a lack of information. To correct modeling of the foundation piles proofed to be the most challenging part of this thesis and as the time series of the docking suggest there seem to be some issues with SIMO. There are a lot of potential improvements to the numerical model and also to the extend of the simulation in general. Below is a list of improvements to the model, as well as possible verification and sensitivity studies that could be performed.

- Implement tugger wires to control the pendulum motions of the jacket in air.
- Perform a sensitivity analysis for the docking cone stiffness and the shape of the jacket leg tip. A more tapered leg tip might decrease the docking forces.
- Implement motion control devices, such as a heave compensator for the crane and roll damping tanks for the vessel.

- Investigate if having the foundation pile openings at different vertical levels and thus a controlled successive docking benefits the installation.
- Investigate to what extend point fenders are a good representation of the pile stoppers and evaluate possible alternatives.
- Investigate the mean offset of the jacket before docking and check whether adjusting the crane tip position accordingly increases the rate of successful docking.

References

[1] LORC Knowledge. Support Structure Concepts for Offshore Wind Turbines, 2011. URL http://www.lorc.dk/offshore-wind/foundations. Retrieved 30.10.2013.

[2] Wind Energy The Facts. Offshore Support Structures, 2013. URL http://www.wind-energy-the-facts.org/offshore-support-structures.html. Retrieved 12.12.2013.

[3] Marilena Greco. TMR 4215: Sea Loads - Lecture Notes. Technical report, Norwegian University of Science and Technology, 2012.

[4] Det Norske Veritas. *DNV-RP-C205, Environmental Conditions and Environmental Loads*. Det Norske Veritas, 2010.

[5] S.K. Chakrabarti. *Hydrodynamics of Offshore Structures*. Springer Verlag, 1987.

[6] SIMO project team. *SIMO - Theory Manual Version 3.6, rev: 2*, 2009.

[7] University of Auckland. Solid Mechanics - Lecture Notes, 2013. URL http://homepages.engineering.auckland.ac.nz/~pkel015/SolidMechanicsBooks. Retrieved 20.11.2013.

[8] Athanasia Arapogianni. The European Offshore Wind Industry - Key Trends and Statistics 2012. Technical report, European Wind Energy Association, 2013.

[9] Roland Berger Strategy Consultants. Offshore Wind Toward 2020 - On the Pathway to Cost Competitiveness. Technical report, Roland Berger Strategy Consultants, 2013.

[10] Germanischer Lloyd. Mapping the Future in Offshore Wind - Wind Turbine Installation Ships and Wind Farm Service Vessels. Technical report, GL, 2012.

[11] Hochtief Contruction AG. Jack-up platform Thor. Technical report, Hochtief Contruction AG, 2009.

[12] HGO InfraSea Solutions. Heavy-lift Jack-up Vessel INNOVATION Power of Performance. Technical report, HGO InfraSea Solutions, 2013.

[13] Ballast Nedam. Data Sheet - Svanen. Technical report, Ballast Nedam, (no year indicated).

[14] Subsea 7. Data Sheet - Stanislav Yudin. Technical report, Stanislav Yudin, 2012.

[15] Jeroen Lusthof. Floating Structures - Lecture Slides. TU Delft, 2013.

[16] Arne Flodrus. Experiences from the Construction and Installation of Lillgrund Wind Farm. Technical report, The Swedish Energy Agency ,Vattenfall Vindkraft AB, 2008.

[17] Alain Michel Jules Norro, Bob Rumes, and Steven Johan Degraer. Differentiating between Underwater Construction Noise of Monopile and Jacket Foundations for Offshore Windmills: A Case Study from the Belgian Part of the North Sea. *The Scientific World Journal*, 2013:7, 2013.

[18] Finn Gunnar Nielsen. *Lecture Notes in Marine Operations*. Department of Marine Hydrodynamics, Norwegian University of Science and Technology, 2007.

[19] Technical Policy Board. *0027/ND - Guidelines for Marine Lifting and Lowering Operations*. GL Noble Denton, 22 June 2013.

[20] Geert Meskers and Radboud van Dijk. A Damping Tugger System for Offshore Heavy Lifts. In *OMAE2012 - Proceedings of the ASME 2012 31st International Conference on Ocean, Offshore and Arctic Engineering*, Rio de Janeiro, Brazil, 1-6 July 2012.

[21] J.L. Cozijn, R.J. van der Wal, and C. Dunlop. Model Testing and Complex Numerical Simulations for Offshore Installation. In *ISOPE - Proceedings of the 18th International Offshore and Polar Engineering Conference*, Vancouver, Canada, 6-11 July 2008.

[22] O. M. Faltinsen. *Sea Loads on Ships and Offshore Structures*. Cambridge University Press, 1990.

[23] H.J.J. van den Boom, J.N. Dekker, and R.P. Dallinga. Computer Analysis of Heavy Lift Operations. In *OTC 5819 - 20th Annual Offshore Technology Conference*, Houston, Texas, 2-5 May 1988.

[24] G.F. Clauss and T. Riekert. Operational Limitations of Offshore Crane Vessels. In *OTC 6217 - 22nd Annual Offshore Technology Conference*, Houston, Texas, 7-10 May 1990.

[25] Peter Chr. Sandvik. Estimation of Extreme Response from Operations Involving Transients. In *MOSS 2012 - 2nd Marine Operations Speciality Symposium*, 2012.

[26] Det Norske Veritas. *DNV-RP-H103, Modelling and Analysis of Marine Operations*. Det Norske Veritas, 2012.

[27] Massie Journe. Offshore Hydromechanics - Lecture Notes. Technical report, Delft University of Technology, 2001.

[28] Prof. A.H. Techet. 2.016 Hydrodynamics: Added Mass - Lecture Notes. Technical report, Massachusetts Institute of Technology, 2013.

[29] Wybren de Vries. Support Structure Concepts for Deep Water Sites. Technical report, Delft University of Technology, 2011.

[30] Jeroen Hoving. Bottom Founded Structures - Lecture Slides. TU Delft, 2013.

[31] Lin Li, Zhen Gao, and Torgeir Moan. Numerical Simulations for Installation of Offshore Wind Turbine Monopiles using Floating Vessels. In *OMAE2013-11200 - Proceedings of the ASME 2013 32nd International Conference on Ocean, Offshore and Arctic Engineering*, Nantes, France, 9-14 June 2013.

[32] Det Norske Veritas. *DNV-OS-J101, Design of Offshore Wind Turbine Structures.* Det Norske Veritas, 2013.

[33] Det Norske Veritas. *DNV-OS-H205, Lifting Operations - (VMO Standard - Part 2-5).* Det Norske Veritas, 2014.

[34] Martin Nore. Extreme Response Analysis Project Considerations and Use. In *9 Loefteseminar - KranTeknisk Forening*, Norway, 05 December 2012.

[35] Det Norske Veritas. *DNV-OS-H205, Offshore Installation Operations - (VMO Standard - Part 2-4).* Det Norske Veritas, 2013.

Appendices

Appendix A

Assignment

The following tasks should be addressed in the thesis work:

1. A literature review should be carried out, covering wind turbine installation using floating vessels, hydrodynamic loads on slender elements with partial or full submergence in wave splash zone, dynamics related to crane operations, statistical treatment of transient response signals.

2. Considering one typical member in jacket foundation, study the relative importance of various forces that acts on that member. Surface-piecing member or fully submerged member could be considered. These forces may include buoyancy, F-K force, diffraction and radiation forces, drag force and wave slamming force.

3. Implement the hydrodynamic load formulation in the Matlab code and validate it by comparing the basic cases with the results from the tool Simo.

4. Based on the installation vessel data provided by Lin Li, establish a coupled analysis model in Simo which includes the floating vessel, a jacket foundation model and their coupling, and carry out time-domain simulations of lowering and landing processes.

5. Perform systematic simulations considering various environmental conditions, identify and quantify the critical response parameters that may define the operation limits, and perform a workability study of the vessel based on the analysis results.

6. Conclude the work and give recommendations for future work.

7. Report and conclude this study.

The work scope could be larger than anticipated. Subject to approval from the supervisor, topics may be deleted from the list above or reduced in extent.

In the project, the candidate shall present his personal contribution to the resolution of problem within the scope of the project work.

Theories and conclusions should be based on mathematical derivations and/or logic reasoning identifying the various steps in the deduction.

The candidate should utilize the existing possibilities for obtaining relevant literature.

The project report should be organized in a rational manner to give a clear exposition of results, assessments, and conclusions. The text should be brief and to the point, with a clear language. Telegraphic language should be avoided.

The project report shall contain the following elements: A text defining the scope, preface, list of contents, main body of the project report, conclusions with recommendations for further work, list of symbols and acronyms, reference and (optional) appendices. All figures, tables and equations shall be numerated.

The supervisor may require that the candidate, in an early stage of the work, present a written plan for the completion of the work. The plan should include a budget for the use of computer and laboratory resources that will be charged to the department. Overruns shall be reported to the supervisor.

The original contribution of the candidate and material taken from other sources shall be clearly defined. Work from other sources shall be properly referenced using an acknowledged referencing system.

Appendix B

Jacket Model Details

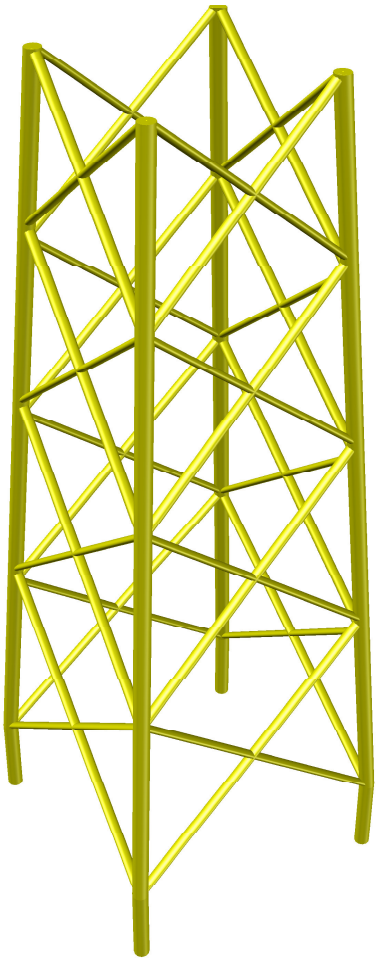

Figure B.1: *3D Jacket Model*

Table B.1: *Jacket Member Coordinates*

Member Type	Node 1			Node 2		
	x	y	z	x	y	z
Leg	−10.050	−10.050	4.500	−6.385	−6.385	64.750
Top X-Brace	−7.167	7.167	52.000	−6.385	−6.385	64.750
Top X-Brace	−7.167	−7.167	52.000	−6.385	6.385	64.750
Upper X-Brace	−8.032	8.032	37.891	−7.167	−7.167	52.000
Upper X-Brace	−8.032	−8.032	37.891	−7.167	7.167	52.000
Lower X-Brace	−8.990	8.990	22.278	−8.032	−8.032	37.891
Lower X-Brace	−8.990	−8.990	22.278	−8.032	8.032	37.891
Bottom X-Brace	−10.050	10.050	5.000	−8.990	−8.990	22.278
Bottom X-Brace	−10.050	−10.050	5.000	−8.990	8.990	22.278
Leg Bottom	−10.050	−10.050	0.000	−10.050	−10.050	4.500
Leg	10.050	−10.050	4.500	6.385	−6.385	64.750
Top X-Brace	−7.167	−7.167	52.000	6.385	−6.385	64.750
Top X-Brace	7.167	−7.167	52.000	−6.385	−6.385	64.750
Upper X-Brace	−8.032	−8.032	37.891	7.167	−7.167	52.000
Upper X-Brace	8.032	−8.032	37.891	−7.167	−7.167	52.000
Lower X-Brace	−8.990	−8.990	22.278	8.032	−8.032	37.891
Lower X-Brace	8.990	−8.990	22.278	−8.032	−8.032	37.891
Bottom X-Brace	−10.050	−10.050	5.000	8.990	−8.990	22.278
Bottom X-Brace	10.050	−10.050	5.000	−8.990	−8.990	22.278
Leg Bottom	10.050	−10.050	0.000	10.050	−10.050	4.500
Leg	10.050	10.050	4.500	6.385	6.385	64.750
Top X-Brace	7.167	−7.167	52.000	6.385	6.385	64.750
Top X-Brace	7.167	7.167	52.000	6.385	−6.385	64.750
Upper X-Brace	8.032	−8.032	37.891	7.167	7.167	52.000
Upper X-Brace	8.032	8.032	37.891	7.167	−7.167	52.000
Lower X-Brace	8.990	−8.990	22.278	8.032	8.032	37.891
Lower X-Brace	8.990	8.990	22.278	8.032	−8.032	37.891
Bottom X-Brace	10.050	−10.050	5.000	8.990	8.990	22.278
Bottom X-Brace	10.050	10.050	5.000	8.990	−8.990	22.278
Leg Bottom	10.050	10.050	0.000	10.050	10.050	4.500
Leg	−10.050	10.050	4.500	−6.385	6.385	64.750
Top X-Brace	7.167	7.167	52.000	−6.385	6.385	64.750
Top X-Brace	−7.167	7.167	52.000	6.385	6.385	64.750
Upper X-Brace	8.032	8.032	37.891	−7.167	7.167	52.000
Upper X-Brace	−8.032	8.032	37.891	7.167	7.167	52.000
Lower X-Brace	8.990	8.990	22.278	−8.032	8.032	37.891
Lower X-Brace	−8.990	8.990	22.278	8.032	8.032	37.891
Bottom X-Brace	10.050	10.050	5.000	−8.990	8.990	22.278
Bottom X-Brace	−10.050	10.050	5.000	8.990	8.990	22.278
Leg Bottom	−10.050	10.050	0.000	−10.050	10.050	4.500

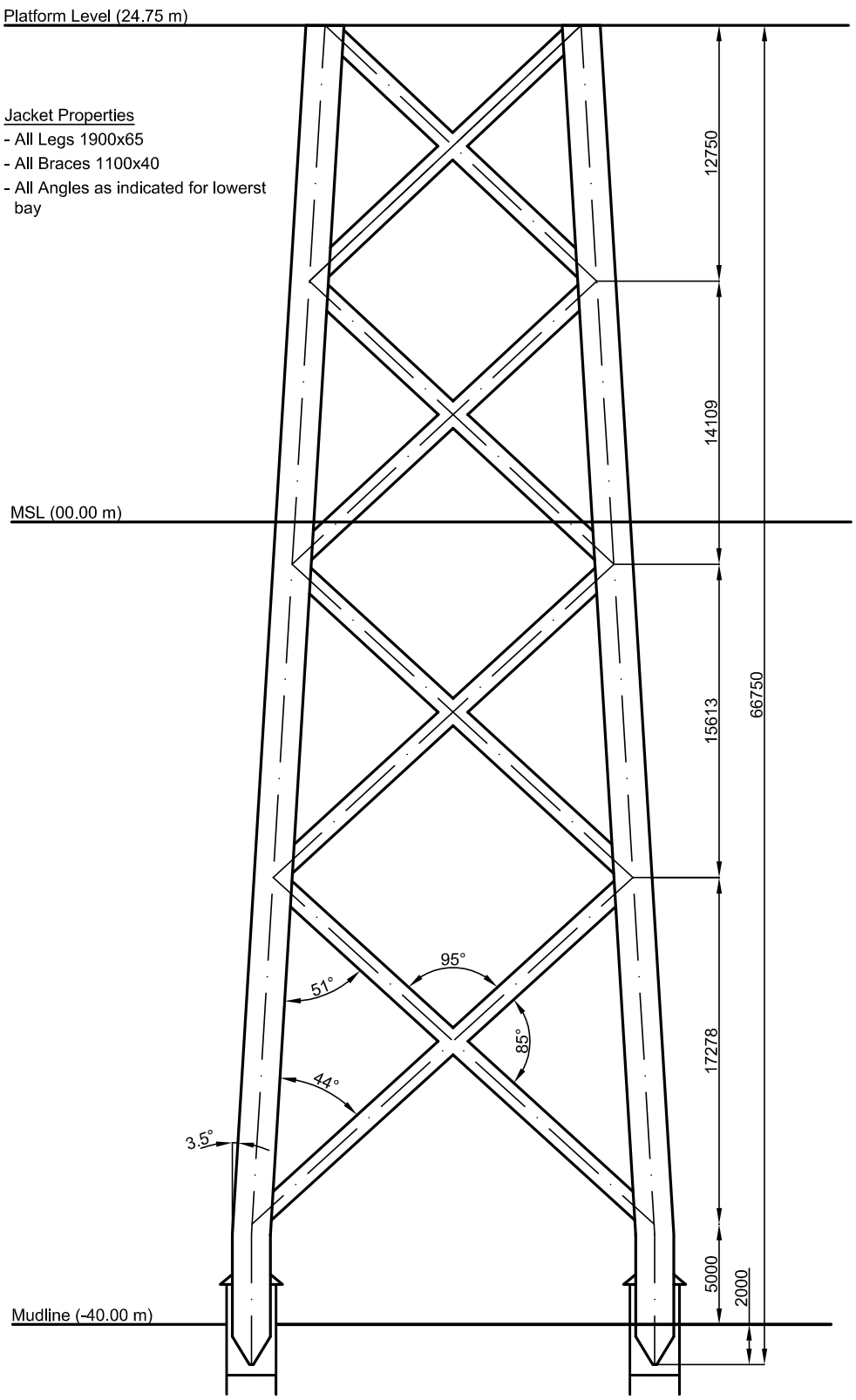

Figure B.2: *Side View of the Jacket*

Appendix C

Curve Fitting Coefficients

Below are the coefficients for the polynomial functions that are used to represent the non-dimensional added mass and change of added mass from Figure 2.8. The coefficient of determination (R^2), as well as the number of points the interpolated curve is based on, are stated as well. The curve representing the non-dimensional added mass is represented by two 4^{th} order polynomials. The curve representing the non-dimensional change of added mass is represented by one 7^{th} and one 5^{th} order polynomial.

Table C.1: *Curve Fitting Coefficients for $m_a/\rho\pi r^2$ and $(dm_a/dh)/\rho\pi r$*

Curve	$m_a/\rho\pi r^2$		$(dm_a/dh)/\rho\pi r$	
h/r Range	$0 \leq 0.93$	$> 1 \leq 3.94$	$0 \leq 1$	$> 1 \leq 5.13$
Data Points	50	46	56	30
R^2	0.9977	0.9994	0.9997	0.9991
c1	0.1071	0.0418	0.6896	0.0506
c2	-0.1844	-0.3330	0.1939	-0.5083
c3	0.2098	0.9434	-0.6689	1.9500
c4	0.5009	-0.0022	-0.1208	-3.4620
c5	-	-	0.4412	2.4960
c6	-	-	-0.3710	-
c7	-	-	0.2226	-

Appendix D

Docking Force Results

The maximum docking of each seed for the different sea states are shown in the following. The **solid black line** corresponds to the **floating vessel**. The **dashed red line** corresponds to the **jack-up vessel**. Only seeds where docking is successful are shown. Weibull distributions are shown for sea states where at least 50 percent of the seeds (15) docked successful.

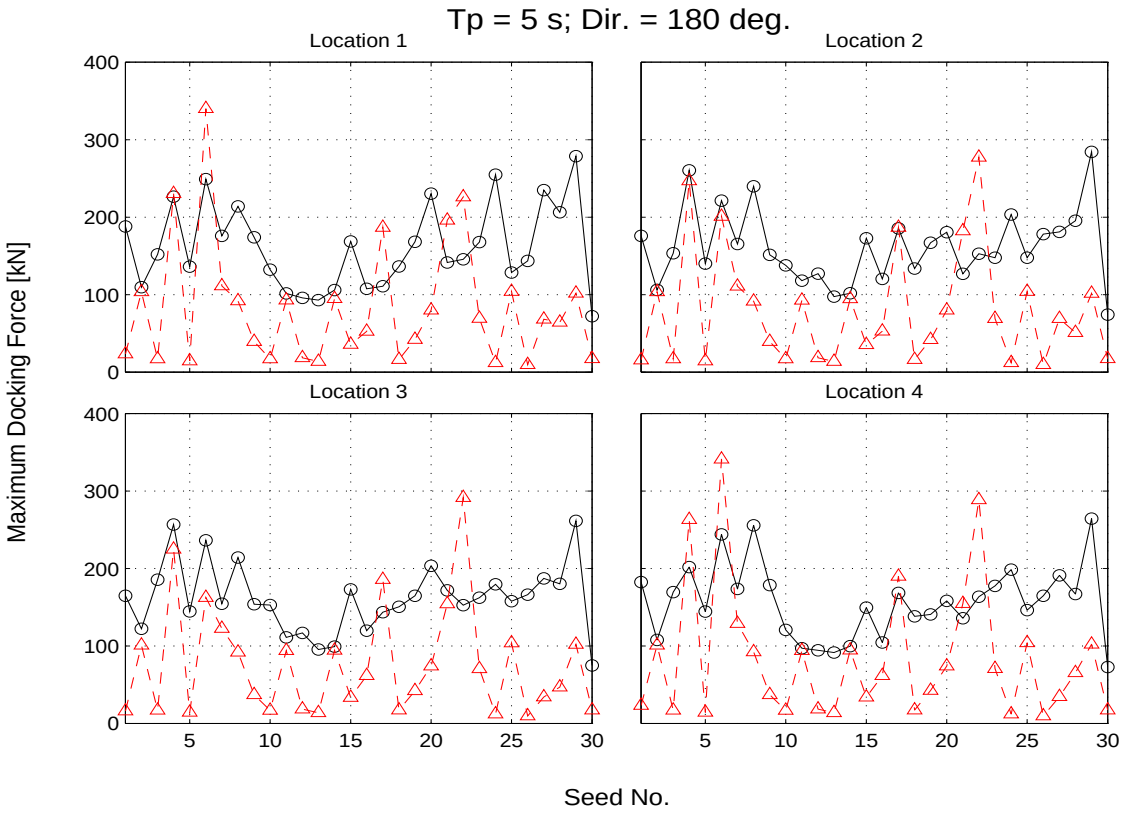

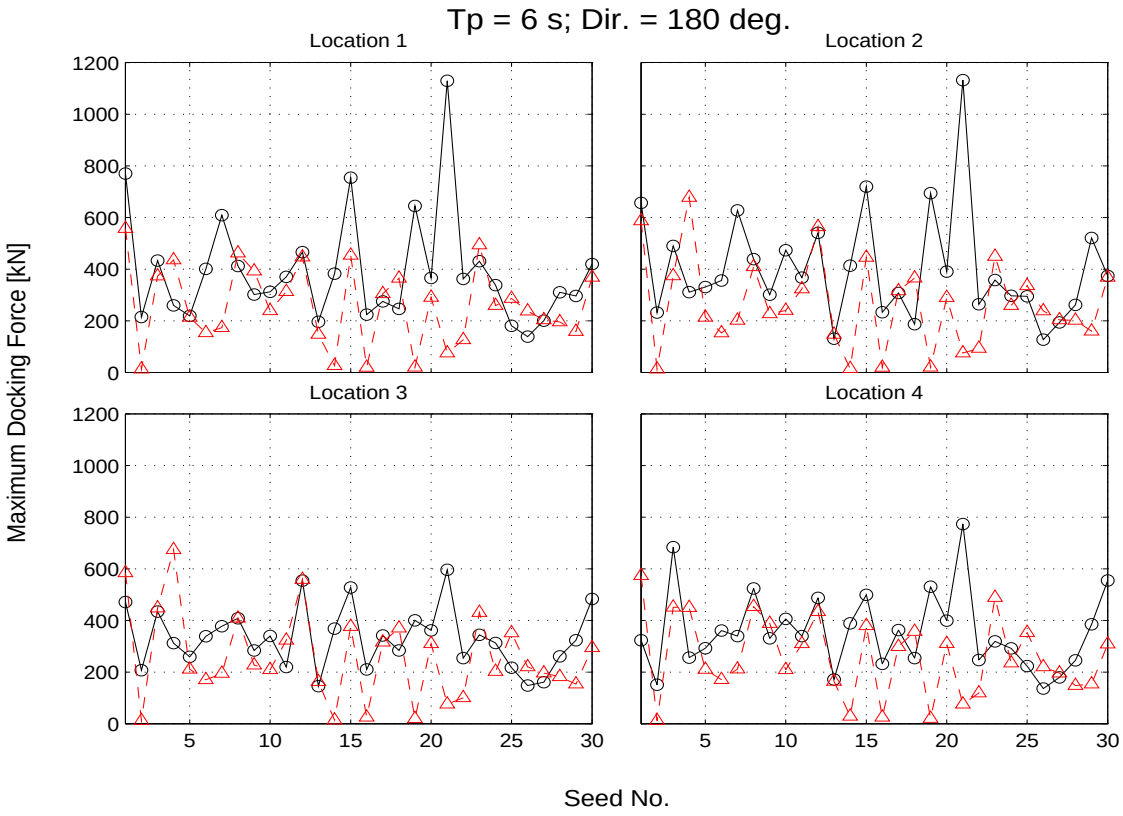
Tp = 6 s; Dir. = 180 deg.
Location 1
Location 2
Location 3
Location 4
Maximum Docking Force [kN]
Seed No.

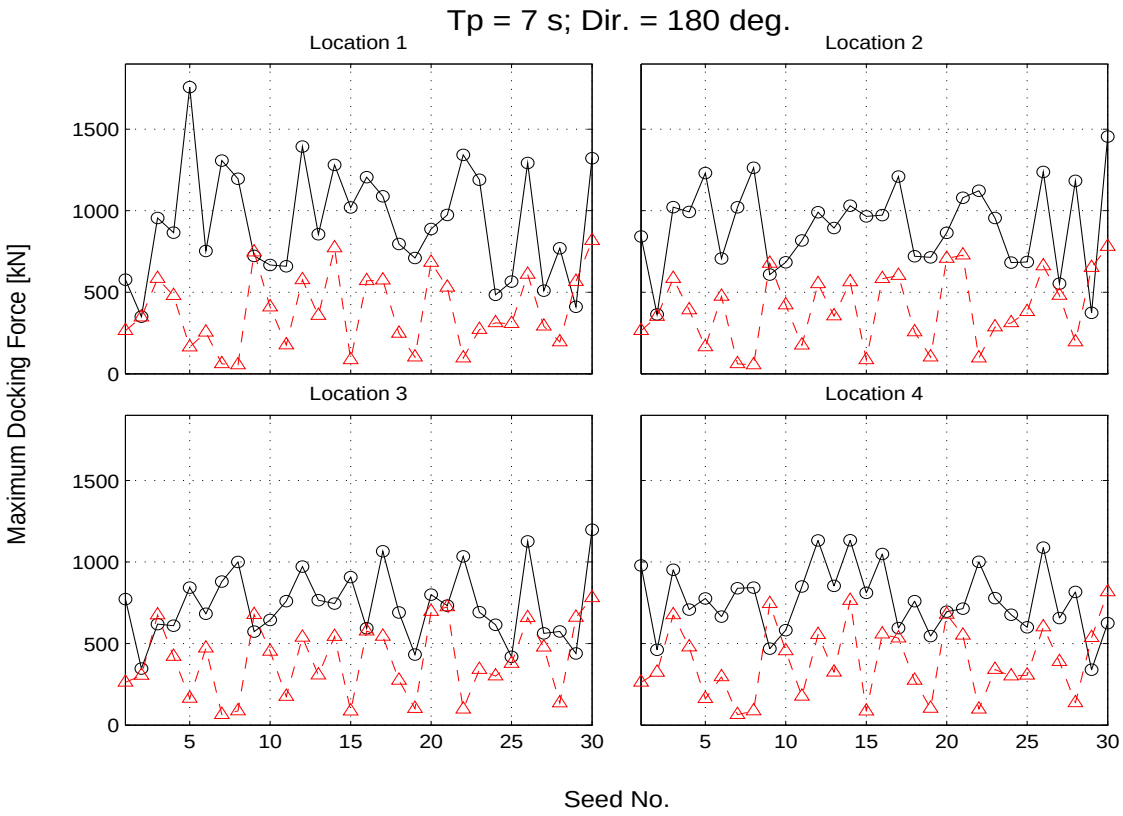
Tp = 7 s; Dir. = 180 deg.
Location 1
Location 2
Location 3
Location 4
Maximum Docking Force [kN]
Seed No.

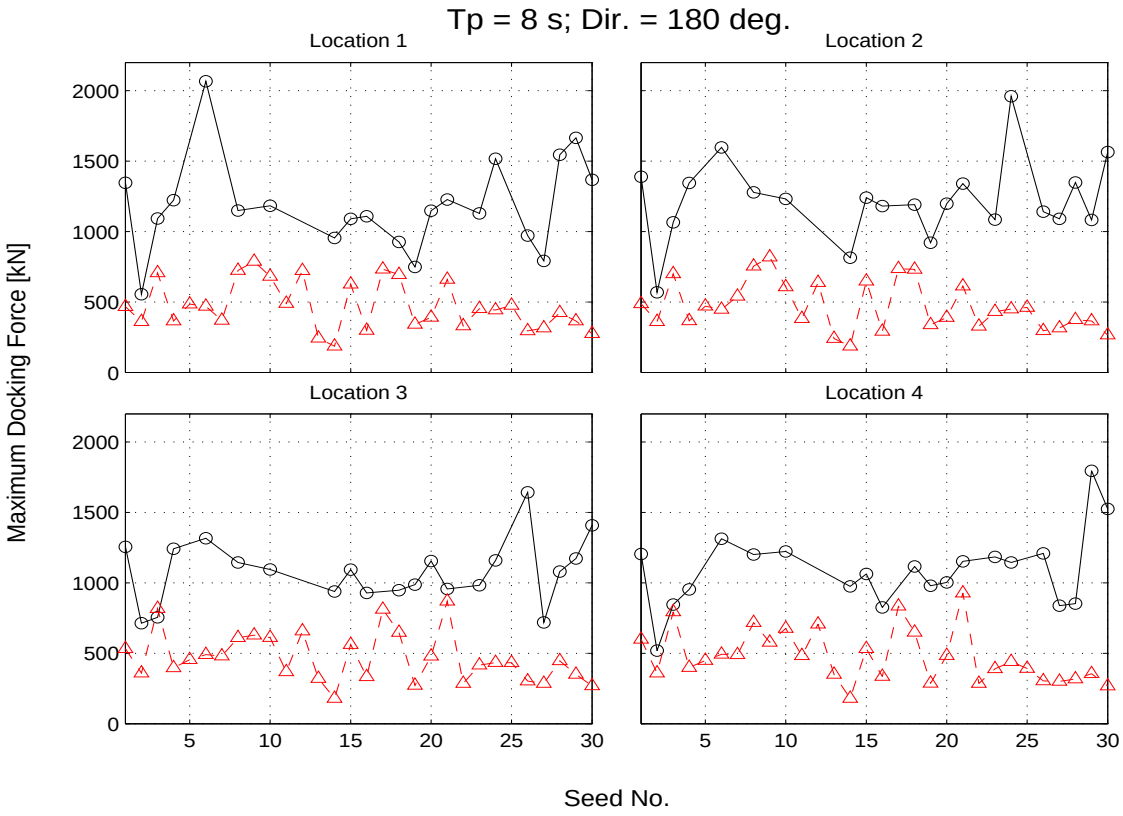
Tp = 8 s; Dir. = 180 deg.
Location 1
Location 2
Location 3
Location 4
Maximum Docking Force [kN]
Seed No.

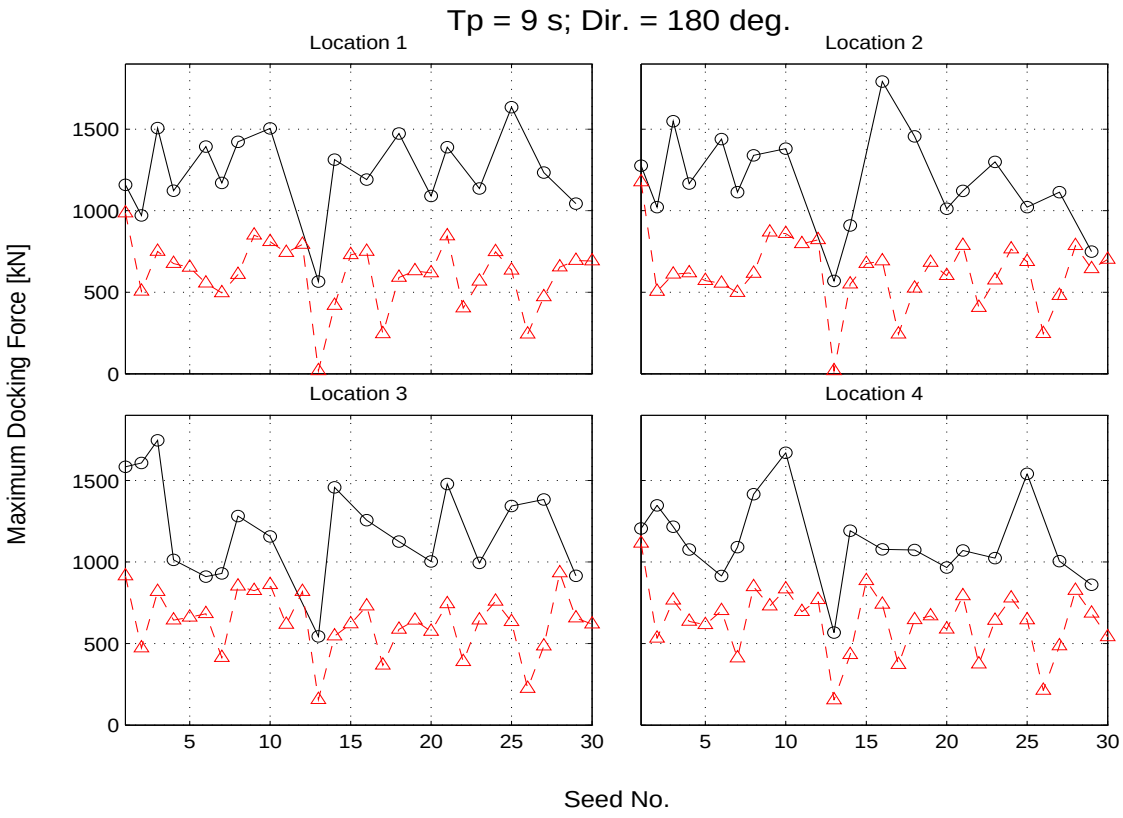
Tp = 9 s; Dir. = 180 deg.
Location 1
Location 2
Location 3
Location 4
Maximum Docking Force [kN]
Seed No.

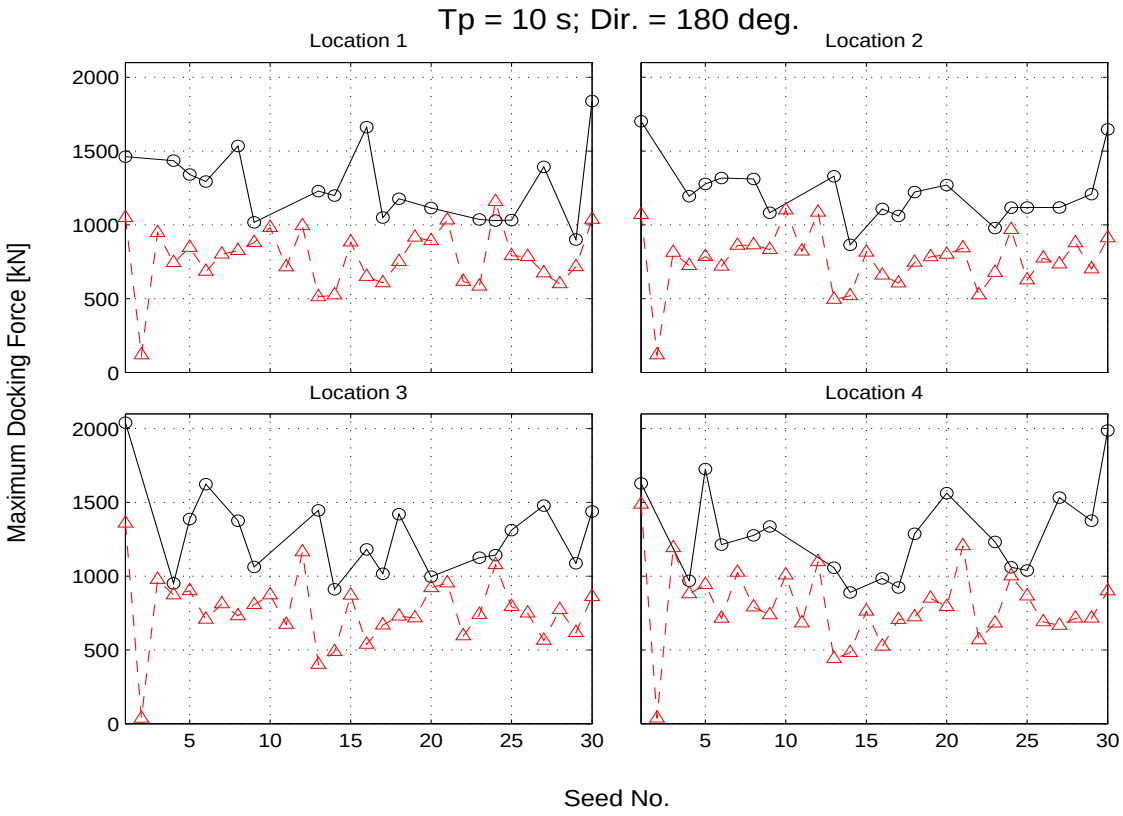
Tp = 10 s; Dir. = 180 deg.
Location 1
Location 2
Location 3
Location 4
Maximum Docking Force [kN]
Seed No.

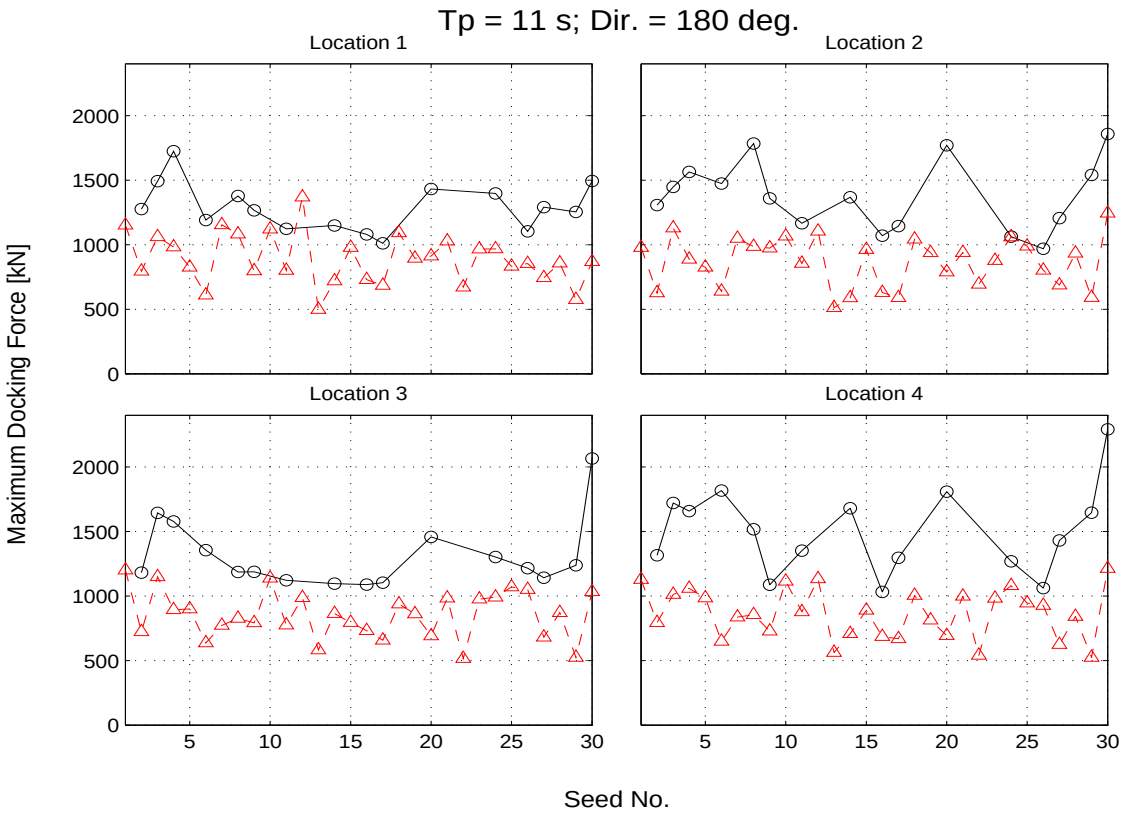
Tp = 11 s; Dir. = 180 deg.
Location 1
Location 2
Location 3
Location 4
Maximum Docking Force [kN]
Seed No.

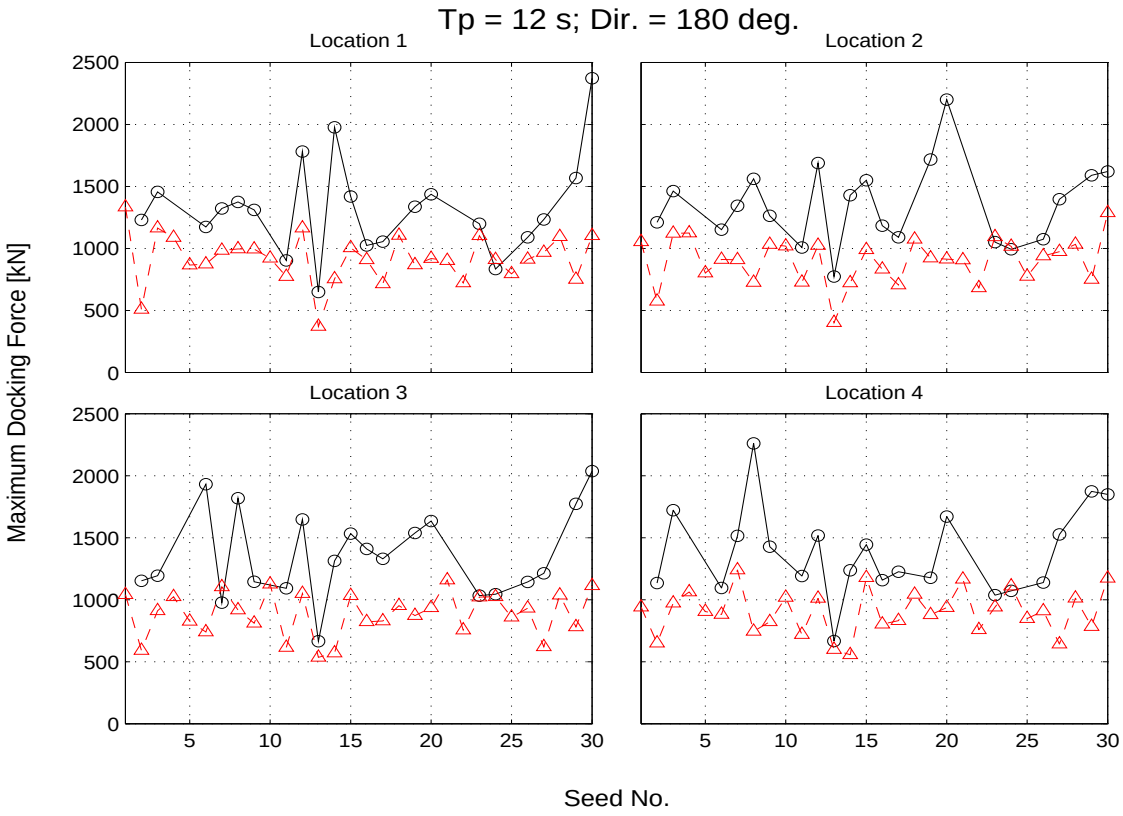
Tp = 12 s; Dir. = 180 deg.
Location 1
Location 2
Location 3
Location 4
Maximum Docking Force [kN]
Seed No.

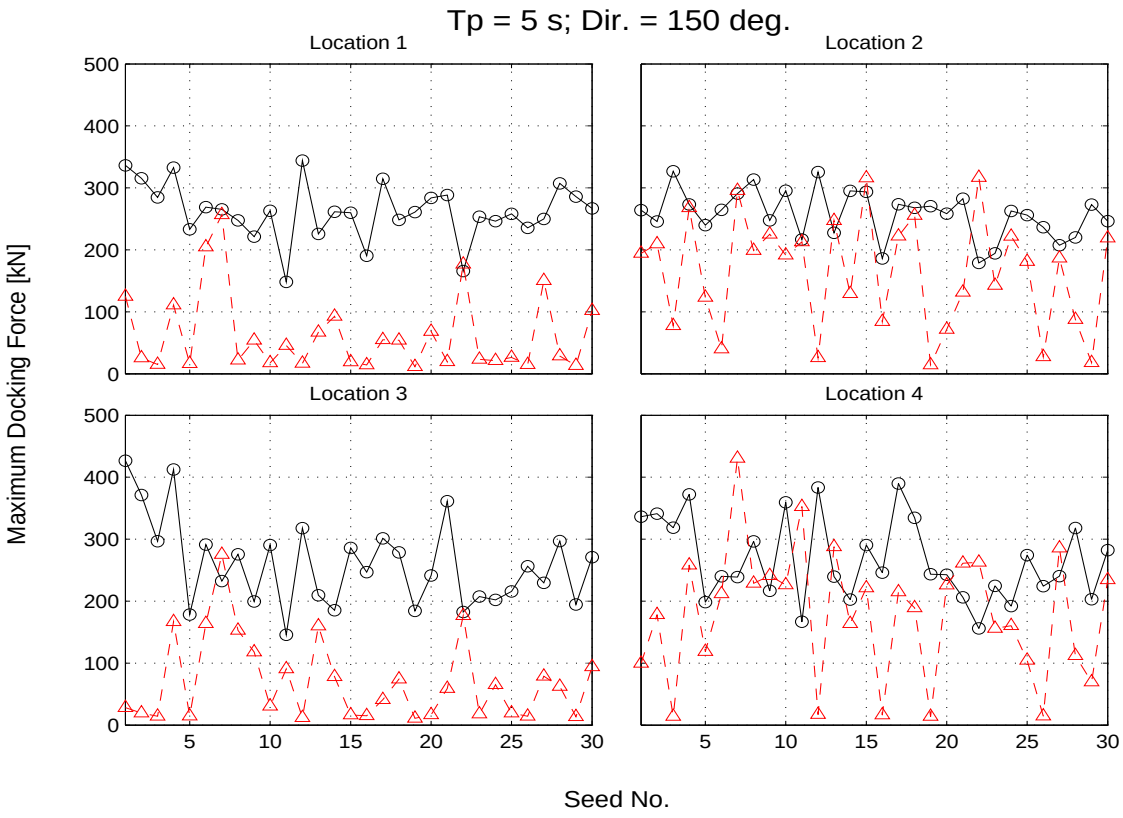
Tp = 5 s; Dir. = 150 deg.
Location 1
Location 2
Location 3
Location 4
Maximum Docking Force [kN]
Seed No.

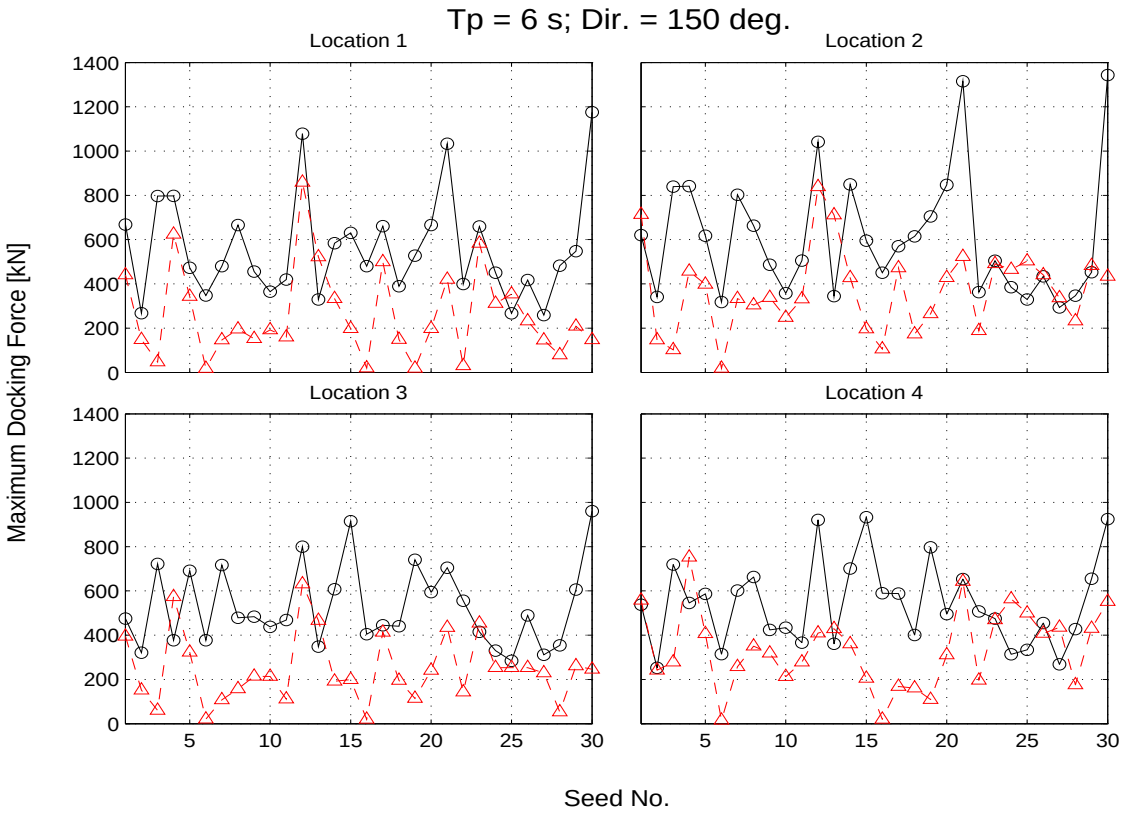
Tp = 6 s; Dir. = 150 deg.
Location 1
Location 2
Location 3
Location 4
Maximum Docking Force [kN]
Seed No.

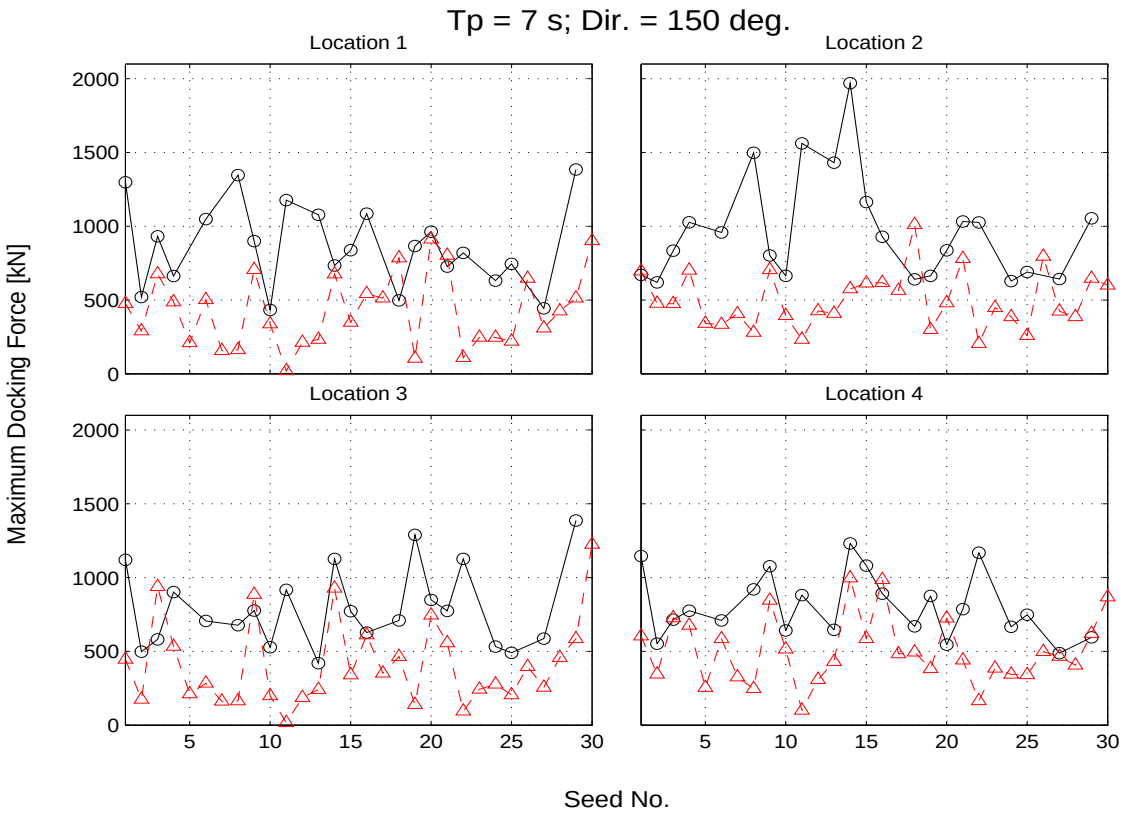
Tp = 7 s; Dir. = 150 deg.
Location 1
Location 2
Location 3
Location 4
Maximum Docking Force [kN]
Seed No.

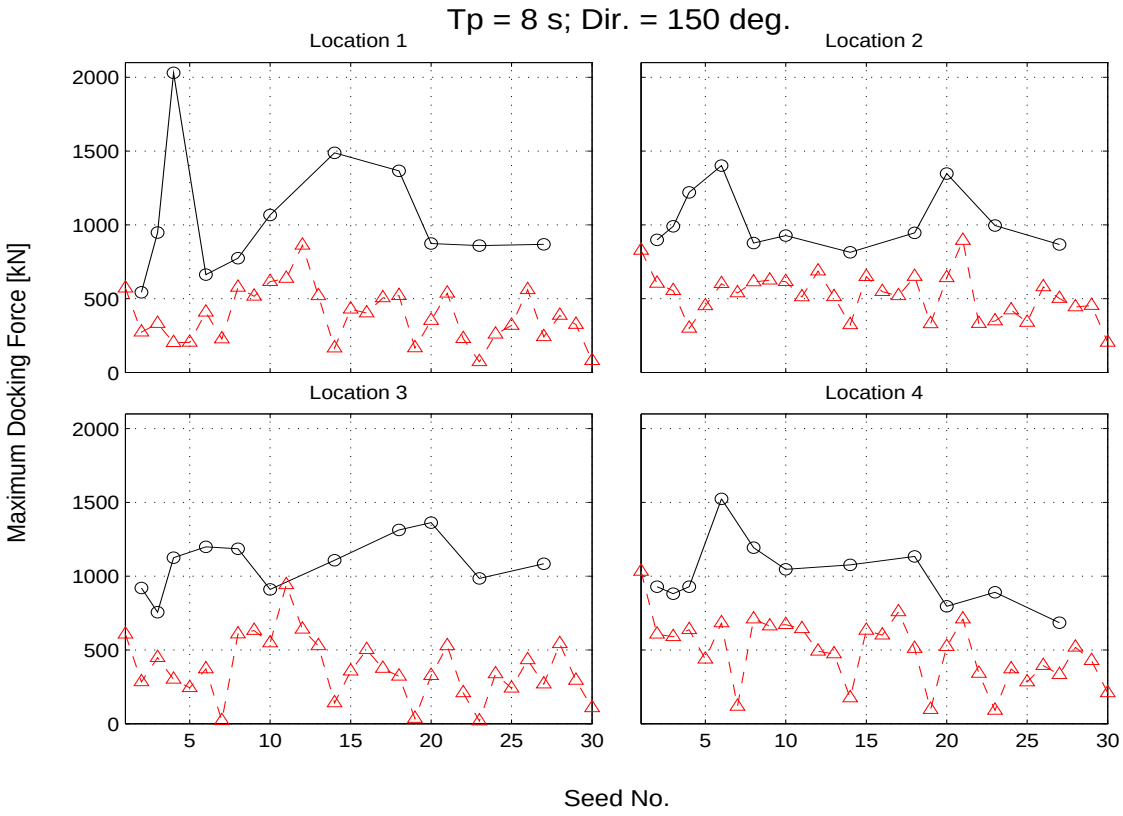
Tp = 8 s; Dir. = 150 deg.
Location 1
Location 2
Location 3
Location 4
Maximum Docking Force [kN]
Seed No.

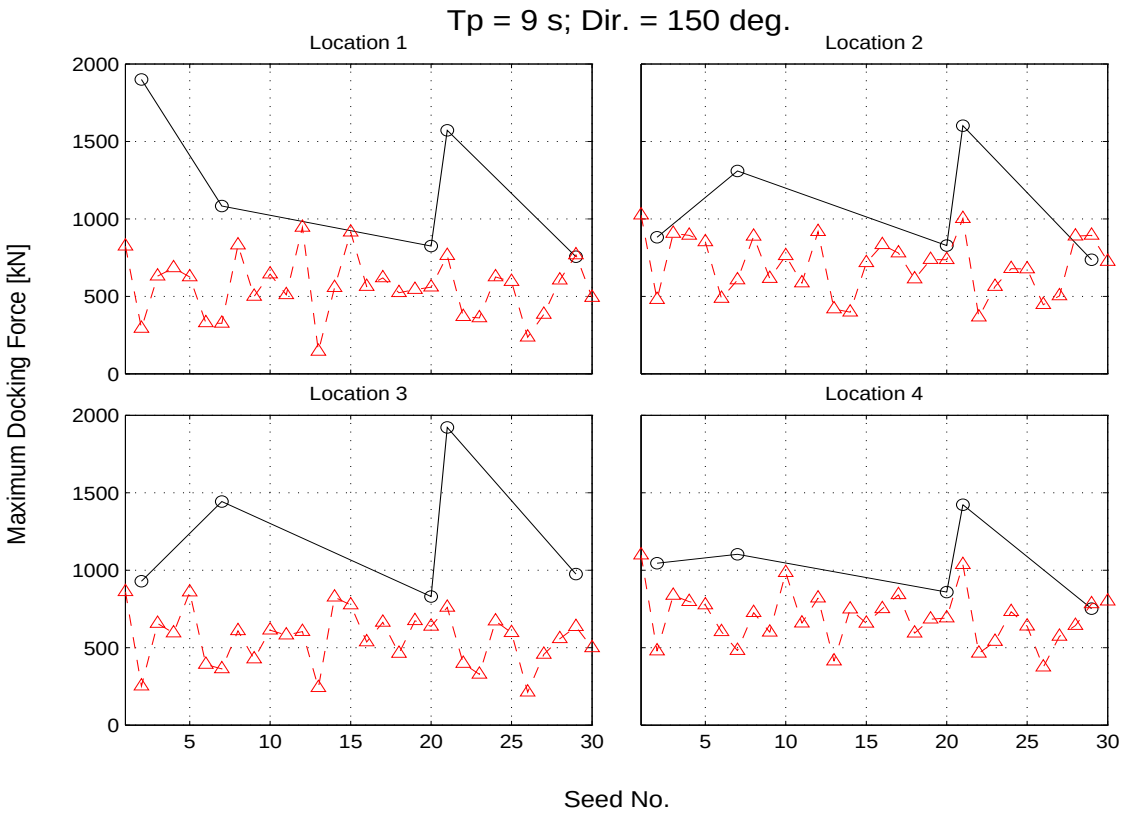
Tp = 9 s; Dir. = 150 deg.
Location 1
Location 2
Location 3
Location 4
Maximum Docking Force [kN]
Seed No.

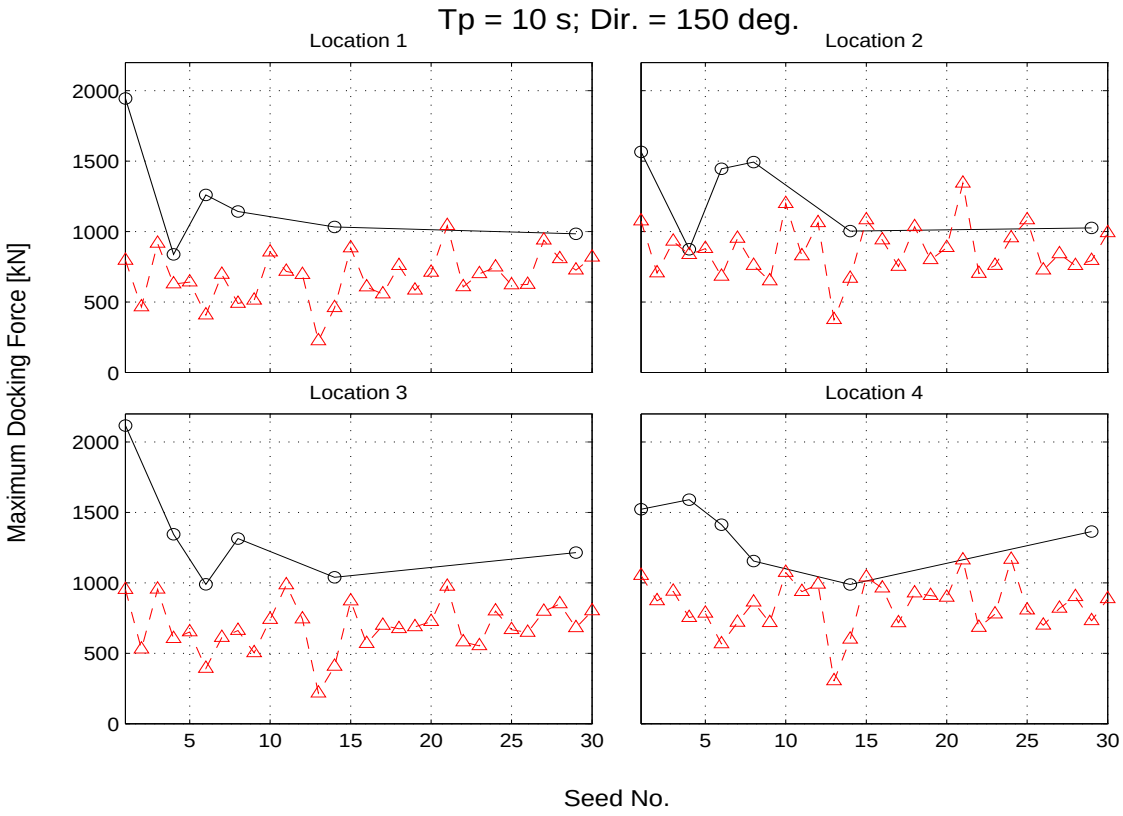
Tp = 10 s; Dir. = 150 deg.
Location 1
Location 2
Location 3
Location 4
Maximum Docking Force [kN]
0
500
1000
1500
2000
5
10
15
20
25
30
Seed No.

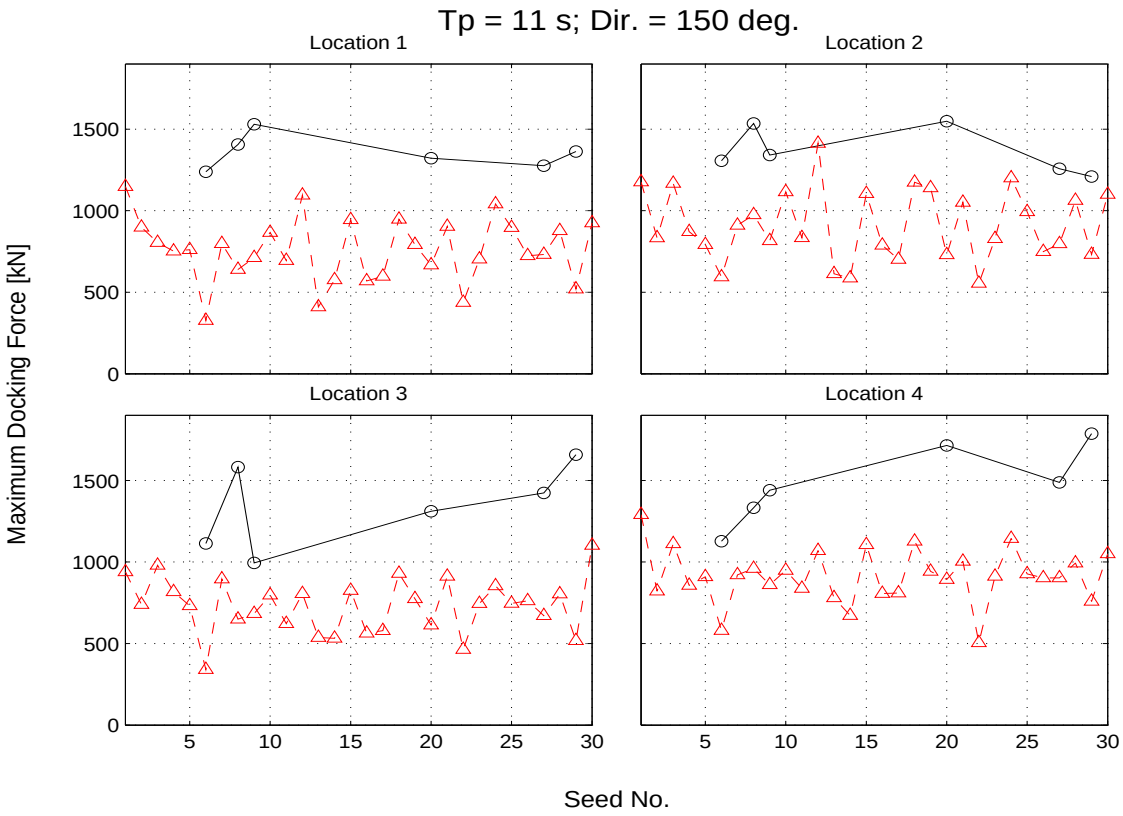
Tp = 11 s; Dir. = 150 deg.
Location 1
Location 2
Location 3
Location 4
Maximum Docking Force [kN]
0
500
1000
1500
5
10
15
20
25
30
Seed No.

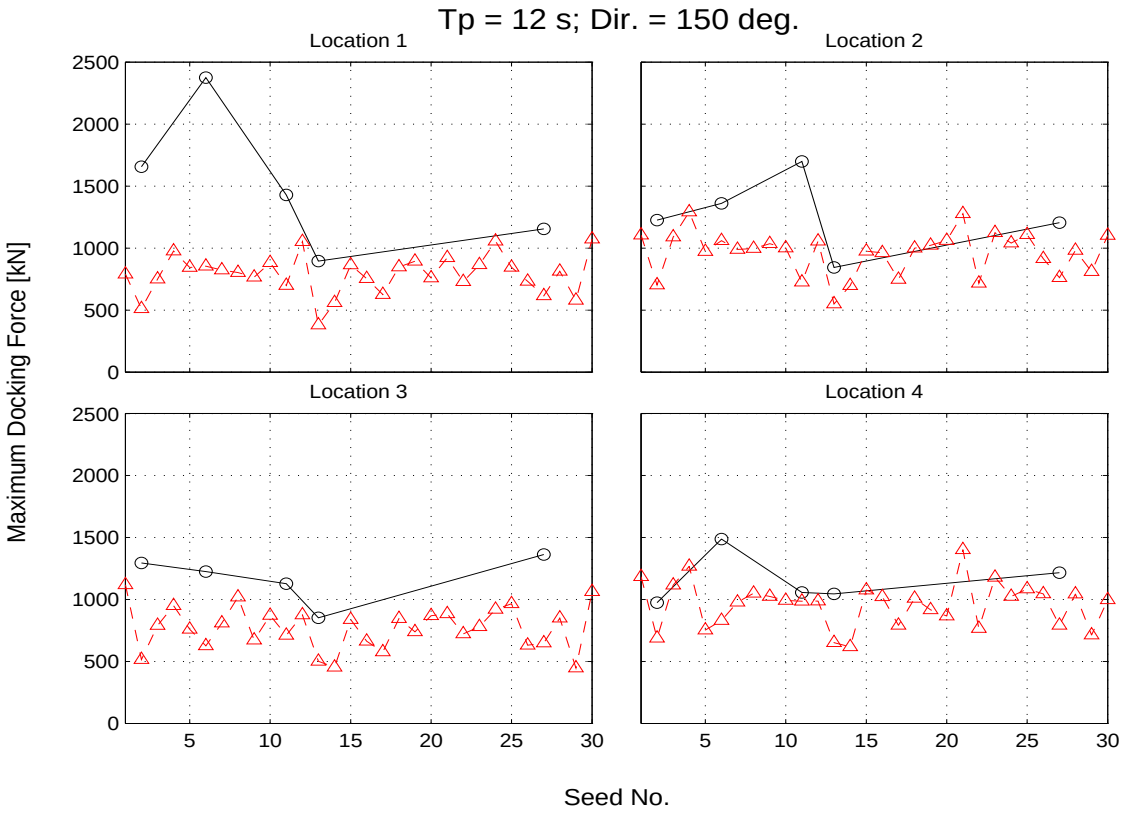
Tp = 12 s; Dir. = 150 deg.
Location 1
Location 2
Location 3
Location 4
Maximum Docking Force [kN]
Seed No.
0
500
1000
1500
2000
2500
5
10
15
20
25
30

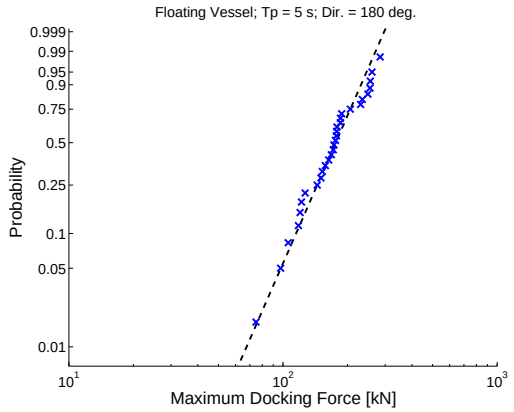
Floating Vessel; Tp = 5 s; Dir. = 180 deg.
Probability
Maximum Docking Force [kN]

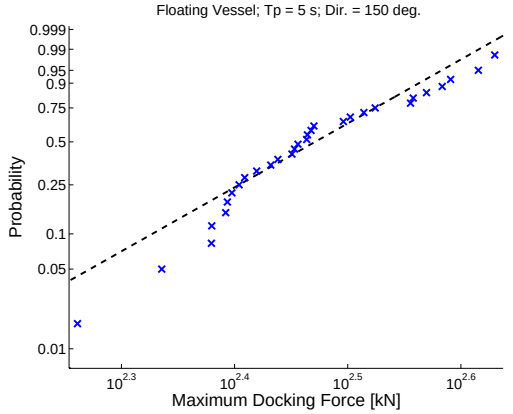
Floating Vessel; Tp = 5 s; Dir. = 150 deg.
Probability
Maximum Docking Force [kN]

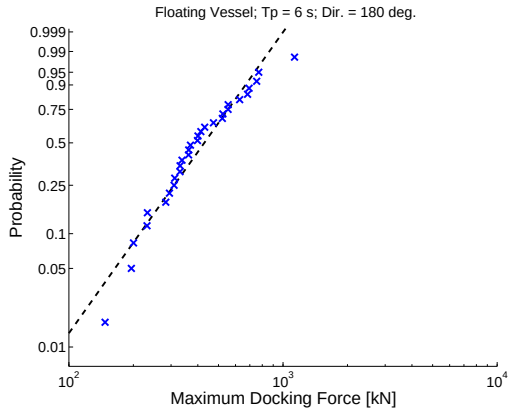
Floating Vessel; Tp = 6 s; Dir. = 180 deg.
Probability
Maximum Docking Force [kN]

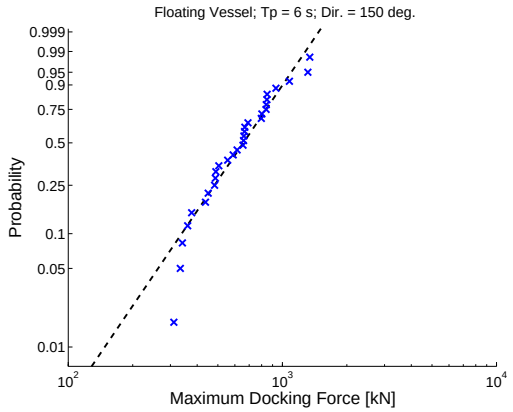
Floating Vessel; Tp = 6 s; Dir. = 150 deg.
Probability
Maximum Docking Force [kN]

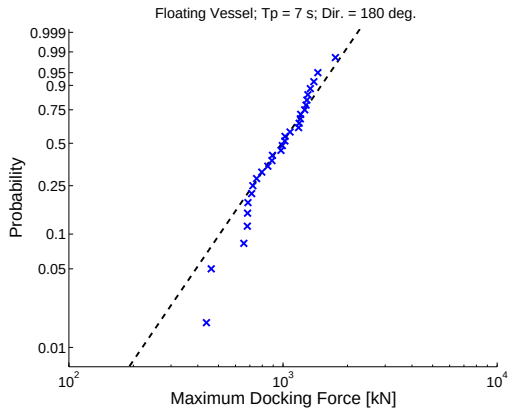
Floating Vessel; Tp = 7 s; Dir. = 180 deg.
Probability
Maximum Docking Force [kN]

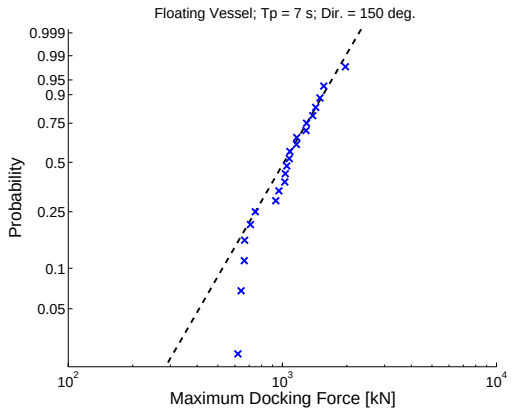
Floating Vessel; Tp = 7 s; Dir. = 150 deg.
Probability
Maximum Docking Force [kN]

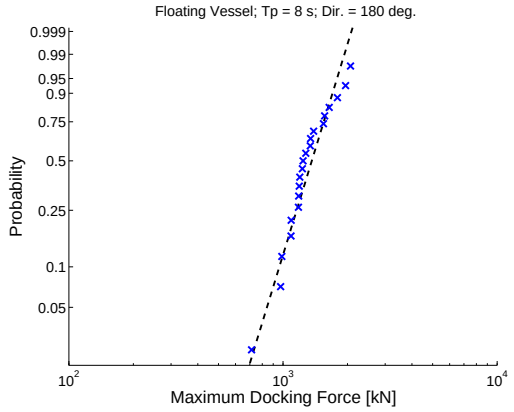
Floating Vessel; Tp = 8 s; Dir. = 180 deg.
Probability
0.999
0.99
0.95
0.9
0.75
0.5
0.25
0.1
0.05
10^2
10^3
10^4
Maximum Docking Force [kN]

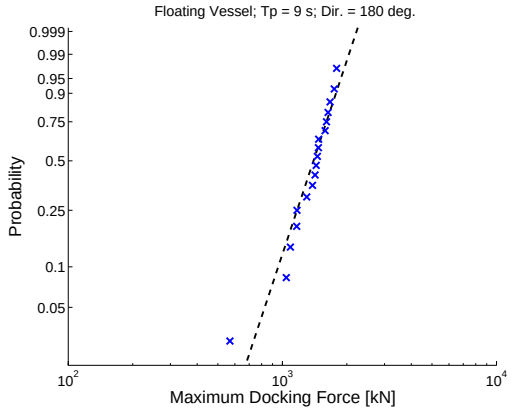
Floating Vessel; Tp = 9 s; Dir. = 180 deg.
Probability
0.999
0.99
0.95
0.9
0.75
0.5
0.25
0.1
0.05
10^2
10^3
10^4
Maximum Docking Force [kN]

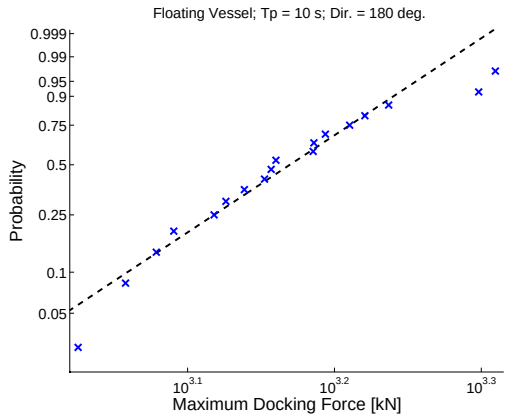
Floating Vessel; Tp = 10 s; Dir. = 180 deg.
Probability
0.999
0.99
0.95
0.9
0.75
0.5
0.25
0.1
0.05
$10^{3.1}$
$10^{3.2}$
$10^{3.3}$
Maximum Docking Force [kN]

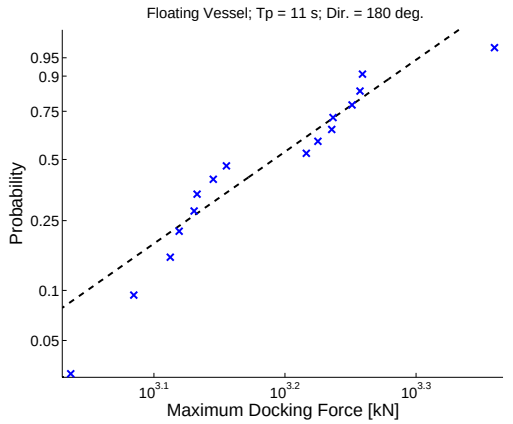
Floating Vessel; Tp = 11 s; Dir. = 180 deg.
Probability
0.95
0.9
0.75
0.5
0.25
0.1
0.05
$10^{3.1}$
$10^{3.2}$
$10^{3.3}$
Maximum Docking Force [kN]

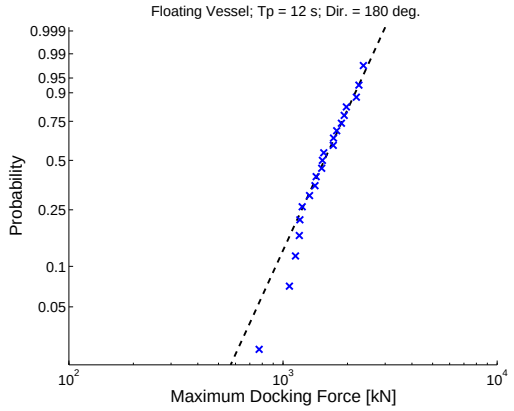
Floating Vessel; Tp = 12 s; Dir. = 180 deg.
Probability
0.999
0.99
0.95
0.9
0.75
0.5
0.25
0.1
0.05
10^2
10^3
10^4
Maximum Docking Force [kN]

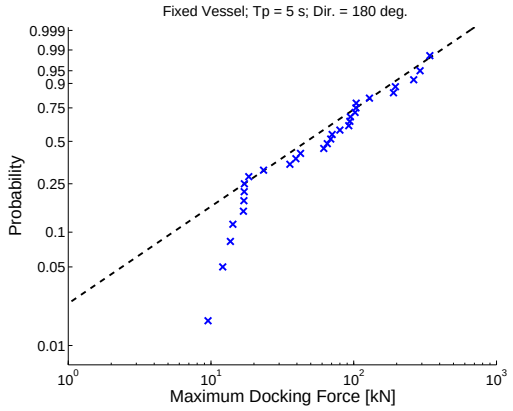
Fixed Vessel; Tp = 5 s; Dir. = 180 deg.
Probability
0.999
0.99
0.95
0.9
0.75
0.5
0.25
0.1
0.05
0.01
10^0
10^1
10^2
10^3
Maximum Docking Force [kN]

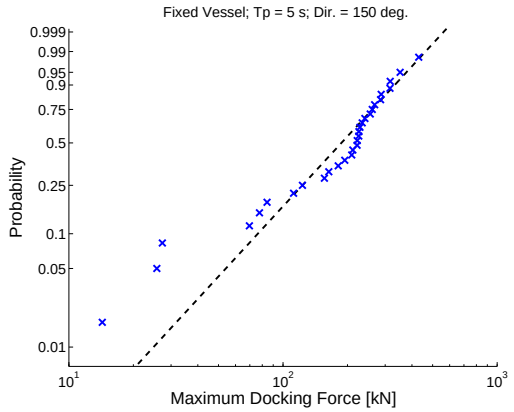
Fixed Vessel; Tp = 5 s; Dir. = 150 deg.
Probability
0.999
0.99
0.95
0.9
0.75
0.5
0.25
0.1
0.05
0.01
10^1
10^2
10^3
Maximum Docking Force [kN]

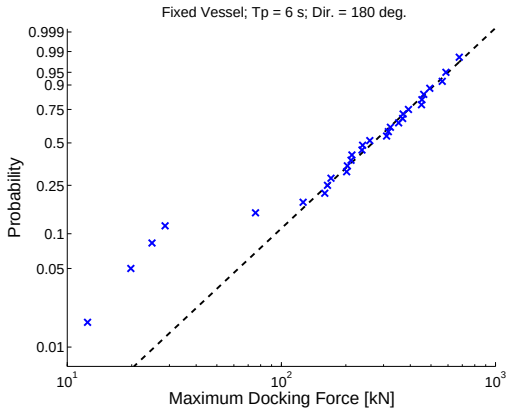
Fixed Vessel; Tp = 6 s; Dir. = 180 deg.
Probability
0.999
0.99
0.95
0.9
0.75
0.5
0.25
0.1
0.05
0.01
10^1
10^2
10^3
Maximum Docking Force [kN]

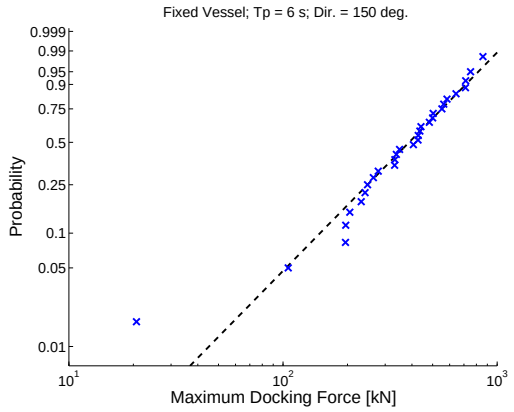
Fixed Vessel; Tp = 6 s; Dir. = 150 deg.
Probability
0.999
0.99
0.95
0.9
0.75
0.5
0.25
0.1
0.05
0.01
10^1
10^2
10^3
Maximum Docking Force [kN]

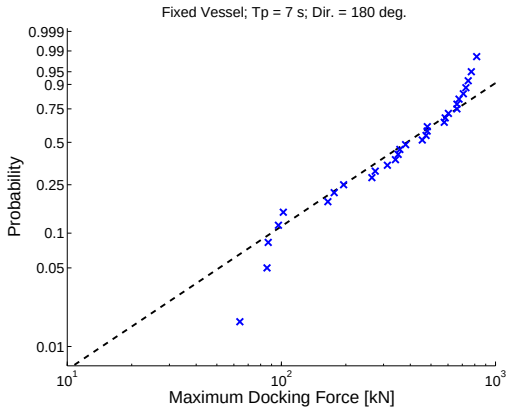
Fixed Vessel; Tp = 7 s; Dir. = 180 deg.
Probability
0.999
0.99
0.95
0.9
0.75
0.5
0.25
0.1
0.05
0.01
10^1
10^2
10^3
Maximum Docking Force [kN]

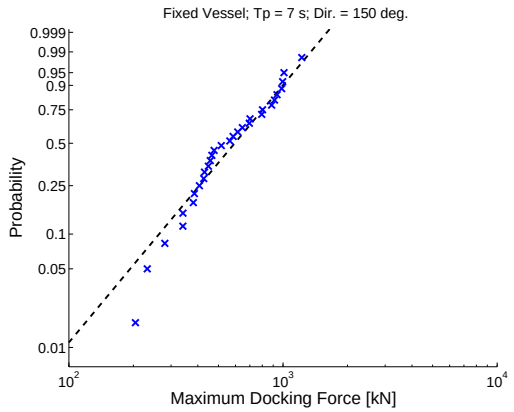
Fixed Vessel; Tp = 7 s; Dir. = 150 deg.
Probability
0.999
0.99
0.95
0.9
0.75
0.5
0.25
0.1
0.05
0.01
10^2
10^3
10^4
Maximum Docking Force [kN]

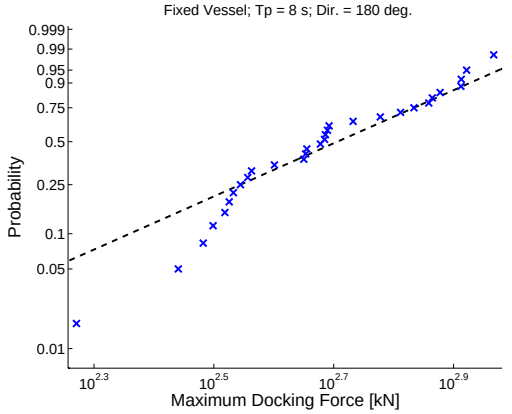
Fixed Vessel; Tp = 8 s; Dir. = 180 deg.
Probability
0.999
0.99
0.95
0.9
0.75
0.5
0.25
0.1
0.05
0.01
$10^{2.3}$
$10^{2.5}$
$10^{2.7}$
$10^{2.9}$
Maximum Docking Force [kN]

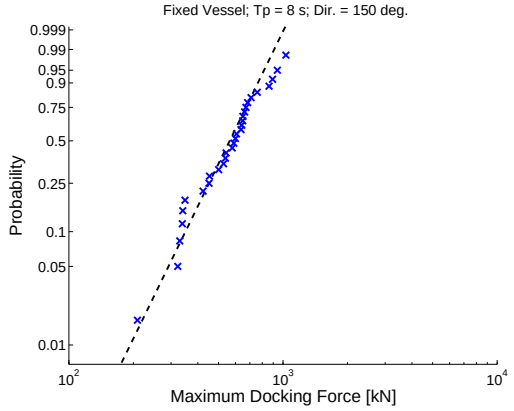
Fixed Vessel; Tp = 8 s; Dir. = 150 deg.
Probability
0.999
0.99
0.95
0.9
0.75
0.5
0.25
0.1
0.05
0.01
10^2
10^3
10^4
Maximum Docking Force [kN]

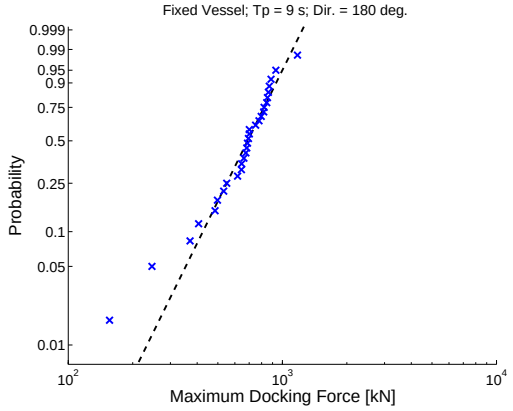
Fixed Vessel; Tp = 9 s; Dir. = 180 deg.
Probability
0.999
0.99
0.95
0.9
0.75
0.5
0.25
0.1
0.05
0.01
10^2
10^3
10^4
Maximum Docking Force [kN]

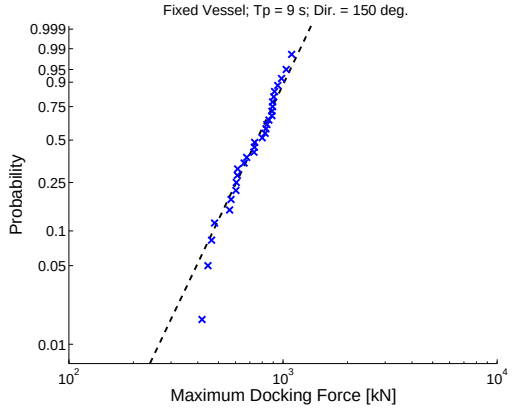
Fixed Vessel; Tp = 9 s; Dir. = 150 deg.
Probability
0.999
0.99
0.95
0.9
0.75
0.5
0.25
0.1
0.05
0.01
10^2
10^3
10^4
Maximum Docking Force [kN]

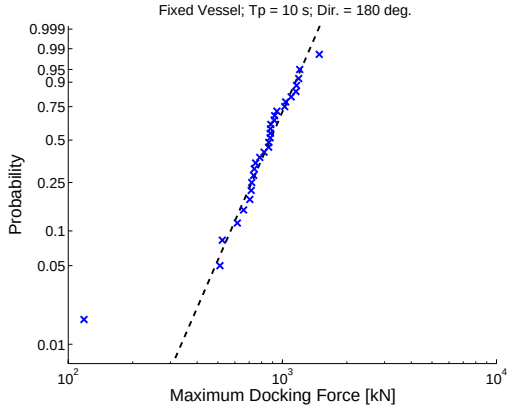
Fixed Vessel; Tp = 10 s; Dir. = 180 deg.
Probability
0.999
0.99
0.95
0.9
0.75
0.5
0.25
0.1
0.05
0.01
10^2
10^3
10^4
Maximum Docking Force [kN]

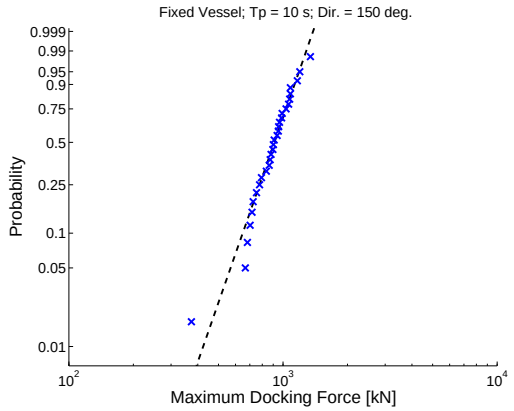
Fixed Vessel; Tp = 10 s; Dir. = 150 deg.
Probability
0.999
0.99
0.95
0.9
0.75
0.5
0.25
0.1
0.05
0.01
10^2
10^3
10^4
Maximum Docking Force [kN]

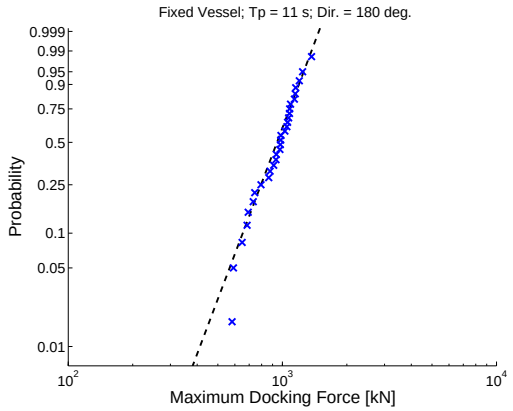
Fixed Vessel; Tp = 11 s; Dir. = 180 deg.
Probability
0.999
0.99
0.95
0.9
0.75
0.5
0.25
0.1
0.05
0.01
10^2
10^3
10^4
Maximum Docking Force [kN]

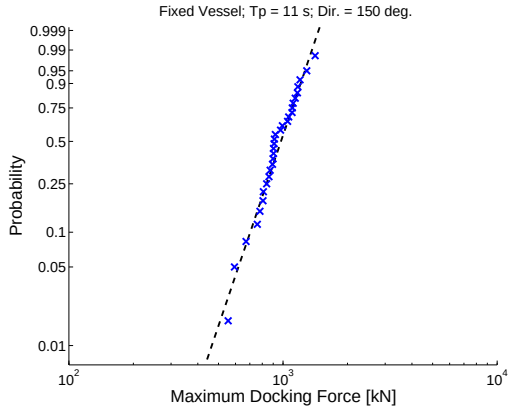
Fixed Vessel; Tp = 11 s; Dir. = 150 deg.
Probability
0.999
0.99
0.95
0.9
0.75
0.5
0.25
0.1
0.05
0.01
10^2
10^3
10^4
Maximum Docking Force [kN]

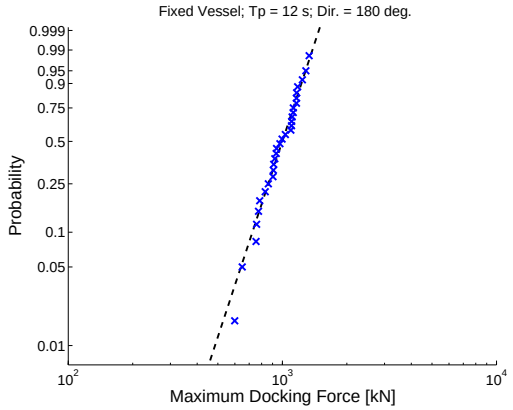
Fixed Vessel; Tp = 12 s; Dir. = 180 deg.
Probability
0.999
0.99
0.95
0.9
0.75
0.5
0.25
0.1
0.05
0.01
10^2
10^3
10^4
Maximum Docking Force [kN]

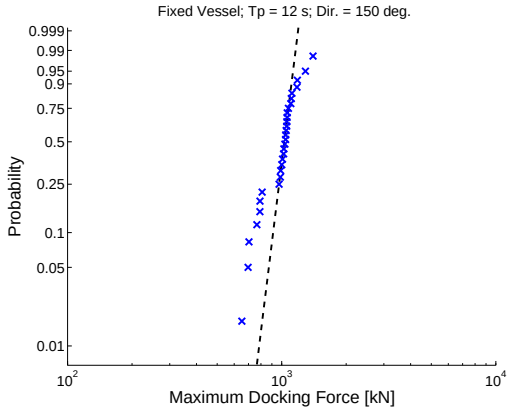
Fixed Vessel; Tp = 12 s; Dir. = 150 deg.
Probability
0.999
0.99
0.95
0.9
0.75
0.5
0.25
0.1
0.05
0.01
10^2
10^3
10^4
Maximum Docking Force [kN]